EFFECT OF STEEL WIRE FIBER ON COMPRESSIVE STRENGTH OF CONCRETE FILLED STEEL TUBULAR COMPOSITE COLUMNS

MD. SAJJAD HOSSAIN SAJIB
(B.Sc. Engg, RUET)

A THESIS SUBMITTED FOR THE DEGREE OF MASTERS OF SCIENCE IN CIVIL ENGINEERING

DEPARTMENT OF CIVIL ENGINEERING
MILITARY INSTITUTE OF SCIENCE & TECHNOLOGY

JULY 2020

EFFECT OF STEEL WIRE FIBER ON COMPRESSIVE STRENGTH OF CONCRETE FILLED STEEL TUBULAR COMPOSITE COLUMNS

Thesis submitted by

Md. Sajjad Hossain Sajib

Student ID: 1013110018

Supervised by

Major Md. Soebur Rahman, PhD, PEng

Instructor Class 'B'

Department of Civil Engineering

Military Institute of Science & Technology

In partial fulfillment of the requirement for the degree of

MASTERS OF SCIENCE IN CIVIL ENGINEERING (STRUCTURE)

CERTIFICATION OF APPROVAL

The thesis titled **"Effects of Steel Wire Fiber on Compressive Strength of Concrete Filled Steel Tubular Composite Columns"**, submitted by Md. Sajjad Hossain Sajib (ID no. 1013110018), Session 2013-2014, has been accepted as satisfactory in partial fulfillment of the requirement for the degree of M.Sc. in Structural Engineering from Department of Civil Engineering, Military Institute of Science & Technology on 20th July 2020.

BOARD OF EXAMINERS

Major Md. Soebur Rahman, PhD, PEng. Instructor, Class-B Department of Civil Engineering MIST, Dhaka.	**Chairman** (Supervisor)
Brig Gen Md Abul Kalam Azad, psc Dean & Head Department of Civil Engineering MIST, Dhaka.	**Member** (Ex-Officio)
Lt. Col. Md. Jahidul Islam, PhD Instructor, Class-A Department of Civil Engineering MIST, Dhaka.	**Member** (Internal)
Dr. Tanvir Mustafy Assistant Professor Department of Civil Engineering MIST, Dhaka.	**Member** (Internal)
Dr. Mahbuba Begum Professor Department of Civil Engineering BUET, Dhaka-1000.	**Member** (External)

DECLARATION

It is hereby declared that, this thesis is my original work of investigation and it has been written by me in its entirely under the supervision of Maj Md. Soebur Rahman, PhD, PEng., Instructor Class 'B', Department of Civil Engineering, Military Institute of Science & Technology. I have duly acknowledged all the specific reference of information which has been used in this thesis. Neither the thesis nor any part of this thesis has been submitted to any other university or other educational establishment for degree or other qualification previously.

Md. Sajjad Hossain Sajib
ID: 1013110018

ACKNOWLEDGEMENT

(In the name of ALLAH, the most gracious and the most Merciful)

The author sincerely expresses his deepest gratitude to the Almighty ALLAH.

First and foremost, the author would like to express thanks and profound gratitude to his supervisor **Major Md. Soebur Rahman, PhD, PEng., Instructor Class 'B', Department of Civil Engineering, MIST.** It has been an honor to be his M.Sc. student. His guidance on the research methods, deep knowledge, motivation, encouragement and patience in all the stages of this research work has been made the task of the author less difficult and made it possible to complete the thesis work.

The author would like to thank his supervisor for his cordial help and guidance in every step of the research. His constant supervision, invaluable suggestion, motivation in difficult times and affectionate encouragement which have been very helpful for the author.

The author would like to thank **Kamrul Islam**, Assistant Professor, MIST for his kind arrangement of all the steel tubular columns from McDonald Steel Ltd. These columns were the key specimens of this experimental study.

The author also wishes to express his deepest gratitude **Dr. Mahbuba Begum**, Professor, Department of Civil Engineering, BUET for her guidance, which were extremely helpful in accomplishing this study.

The author also takes the opportunity to pay his heartfelt thanks to all the staff members of Concrete Laboratory and Strength of Materials Laboratory for their consistent support and painstaking contributions to the research and experimental work.

The author also appreciatively remembers the assistance and encouragement of his friends and well-wishers and everyone related to carry out and complete this study. Finally, the author wishes to express his deep gratitude to his **Wife** for her constant support, encouragement and sacrifice throughout the research work.

ABSTRACT

The concrete filled steel tubular (CFST) column is a composite structure which consists of steel tube and concrete infilled core. This study presents an experimental investigation on the structural behavior and geometric parameters of CFST composite column due to the inclusion of GI fiber under concentric and eccentric loading. Addition of GI fiber in concrete infill is a cost effective way to improve the behavior of CFST column and it is also locally available. The design codes AISC-LRFD (2010), Australian Standard 4100 and Eurocode 4 were also studied and compared these code predicted capacities with the experimental results.

Total twenty-nine (29) square shaped concrete filled steel columns were tested in this study. Among these columns, twelve (12) long column specimen and six (6) stub column specimen were made with 2.5 % of GI wire (weight basis). Three types of concrete strength (20, 30 and 40 MPa), three types of cross sections (100x100, 125x125 and 150x150 mm) and two types of tube thickness (4 and 5 mm) were used. The geometric variables were addition of GI fiber, cross sectional slenderness ratio (B/t), global slenderness ratio (L/B) and loading eccentricity ratio (e/B). The material variable considered as concrete compressive strength ($f_c^{/}$). The experimental capacity and load-deflection curve of concrete filled steel tubular column with or without steel wire fiber were observed. The structural behavior as ductility index (DI) and mid-height deflection were also measured.

From the results, the load carrying capacity was observed to be increased by 10-11% and average deformation capacity is increased by 30% with addition of GI fiber in the concrete. The ductility indexes were also increased by 25-30% which indicates improved ductile behavior of CFST column. Ultimate load capacity was increased by 15% and 10% with the increase of compressive strength for fibered and plain concrete, respectively; whereas, ductility was decreased by 4% and 15%, respectively. Ultimate load capacity, deformation and ductility were increased by 19%, 18% and 1.5%, respectively for decreasing the cross sectional slenderness ratio from 31.25 to 25 of CFST columns with plain concrete. For the fibered concrete, these increment were higher than plain concrete by 21%, 19% and 4%, respectively. Adding GI wire fiber into concrete delayed the local buckling of composite columns. It was observed from the experimental study that failure initiated at the middle and edge of the columns due to buckling of steel section followed by concrete crushing.

Ultimate load carrying capacity matched with the AISC-LRFD (2010), Australian Standard 4100 and Eurocode 4 code predicted capacities with good accuracy (0.98-1.03). AISC-LRFD (2010) takes more conventional approach (Mean 1.01 and standard deviation 0.05) on determining the ultimate load carrying capacity of CFST columns. This experimental study indicates that the addition of GI fiber in core concrete has very significant effect on the strength and behavior of concrete filled steel tubular composite columns.

TABLE OF CONTENTS

LIST OF TABLES

LIST OF FIGURES

LIST OF NOTATIONS

B	Width of the column cross section
D	Depth of the column cross section
L	Height of the column
$f_c^/$	Compressive strength of concrete
f_y	Yield strength of steel
A_s	Cross sectional area of steel section
A_c	Area of concrete
b_i	Effective width of the column cross section
d_i	Effective depth of the column cross section
E_{cy}	Modulus of elasticity of concrete
E_s	Modulus of elasticity of steel
P_n	Compressive strength
I	Moment of inertia of steel section
C_e	Coefficient of effective rigidity
EI_{eff}	Effective stiffness of composite section
P_e	Elastic critical buckling load
RC	Reinforced concrete
CFST	Concrete filled steel tubular column
CFT	Concrete filled tube
HT	Hollow tube
SRC	Steel reinforced concrete
CHS	Circular hollow section
SHS	Square hollow section
RHS	Rectangular hollow section
HST	Hollow steel tube
HPS	High performance steel
B/t	Column cross-sectional slenderness ratio
OPC	Ordinary Portland cement
UTM	Universal testing machine
LVDT	Linear variable differential transducer
ε_y	Yield strain
ε_u	Ultimate strain

DI	Ductility index
ACI	American Concrete Institute
AISC	American Institute of Steel Construction
EC4	Eurocode 4
AS	Australian standard
ξ_s	Steel contribution ratio
P_u	Ultimate load of the tested column
ξ_c	Concrete contribution ratio
α_c	Strength reduction factor
f_{ysr}	Specified minimum yield stress of reinforcing bars
K	Effective length factor
L	Laterally unbraced length of the member
W_c	Weight of concrete per unit volume
p_{no}	Nominal compressive strength of axially loaded composite member
p_e	Elastic critical buckling load
δ_m	Mid-height deflection

CHAPTER 1
INTRODUCTION

1.1 General

Composite column is a type of structural member that uses a combination of structural steel shapes, pipes or tubes with or without reinforcing steel bars and concrete to provide adequate load carrying capacity to sustain either axial compressive loads alone or a combination of axial loads and bending moments. In a composite column both the steel and the concrete sections resist the external loading by interacting together by bond and friction. There are three types of composite column sections used in structural construction. Among these concrete filled steel tubular (CFST) composite columns are widely regarded all over the world due to enhanced strength, stiffness, ductility, and energy dissipation capacity. Moreover, CFST columns significantly reduce the construction time and cost as no formworks are required during construction. In this column, concrete is fully confined by the surrounding steel section which gives confining effect to the concrete core (Figure 1.1).

In current international practice, CFST columns are widely used as the primary lateral resistance systems of both braced and unbraced building structures. There are several countries where CFSTs are also used as bridge piers. However, CFSTs can also be utilized for retrofitting purposes and for strengthening of concrete columns in earthquake zones. Extensive numerical and experimental works were conducted by several researchers (O'Shea and Bridge 2000; Shanmugam and Lakshmi 2001; Uy 2001; Tokgoz and Dundar 2010) on CFST columns with normal and high-strength concrete as well as high-strength steel under concentric and eccentric loading. However, very limited study was conducted to investigate the behavior of CFST columns with the inclusion of GI wire steel fibers. This fiber is low in cost and available in Bangladesh. Previous studies have shown the beneficial effect of different type of fibers such as glass fiber and steel fiber within concrete. Inclusion of fiber within the concrete increases the strength, ductility, energy absorption capacity and impact resistance.

1.2 History of Composite Column

Composite columns have been used for over 100 years, initially to provide fire protection and increase capacity to the steel structure. Until the 1950s; it was normal practice to use a wet mix of low strength concrete and to neglect the construction of the good quality

concrete to the strength of the column. Later, the strength properties were also taken into account while designing concrete encased columns, but it was not until the 1960s that research into concrete filled steel tubes began. Empirical method was developed by stages from earlier design procedure for steel columns, and is not based on fundamental research on composite columns.

Current design rules for composite structures are specified in Architectural Institute of Japan (AIJ 2005), Eurocode 4 (2005), Canadian Standard Association, CSA (2009), AISC-LRFD (2010), Australian Standard (AS4100), ACI 318 (2014) and Egyptian code (2012). Out of this ACI-318, AISC-LRFD (2010), AS4100 and Eurocode 4 - are being used extensively all over the world for the design of CFST columns.

Concrete filled steel tubular column (CFST) has higher efficiency in large energy dissipation, ensuring ductility and retaining higher load. The steel section prevented local buckling due to confining pressure of infill concrete. No additional curing required because the steel encased the concrete in this column. There is a less requirement of extra formwork which reduces construction cost and time. In CFST column, steel confines the concrete and resists bending moment, shear force, column buckling and brittle failure. Limited studies have been done to investigate the behavior of CFST column (buildup steel section) constructed with GI wire fiber. This study aims to perform extensive research on the behavior of CFST with or without GI wire fiber with concentric and eccentric loads.

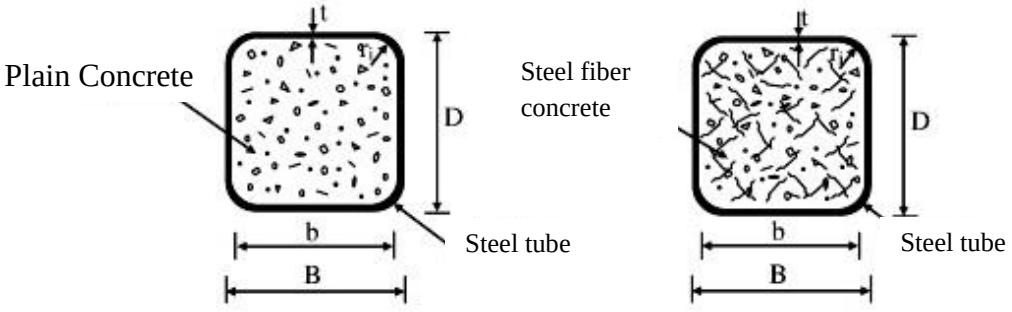

Figure 1.1 Cross-section details of CFST column specimens

1.3 Objectives of the Study

The objectives of this research work are summarized below:

a) To investigate the compressive behavior of CFST columns with GI fiber reinforced concrete and normal strength plain concrete.
b) To investigate the effect of concrete compressive strength ($f_c^{/}$), the geometric parameters such as cross sectional dimension and steel tube thickness on the capacity of CFST columns with and without GI fiber reinforced concrete.
c) To compare the experimental results of the CFST columns with the different code predicted capacities subjected to axial loading.

1.4 Scope of the Study

To achieve the objectives of this study, an extensive experimental study was conducted. Total seventeen (17) numbers of CFST column having length 1000 mm and twelve (12) numbers of CFST column with length 300 and 375 mm were tested experimentally. Out of these, twelve (12) long columns and six (6) stub columns were made with 2.5 % of GI wire (weight basis). These columns were different in cross-sectional sizes (100 mm × 100 mm, 125 mm × 125 mm, 150 mm × 150 mm) with a steel tube thickness of 4 mm and 5 mm. These columns were constructed with three different types of concrete strength 20, 30 and 40 MPa. Yield strength of structural steel of these columns was 345 MPa. These columns were tested for concentric and eccentric axial loading. Knife edge arrangement was placed at the top and bottom of the columns to apply eccentric axial loading. The loads were applied until the specimens failed. Linear variable differential transducer (LVDT) was used to measure the lateral-displacement of CFST columns due to axially applied load. Finally, the experimental results were compared with the code (AISC-LRFD 2010, Eurocode 4 and Australian Standard 4100) predicted capacities.

1.5 Organization of the Thesis

The thesis report is divided into six chapters. An overview of each chapter is as follows.

Chapter one presents the introduction of thesis and related discussion about CFST columns. It also includes objective and methodology of this study.

Chapter two includes a review of literature related to composite columns made with standard steel sections and inclusion of different fiber condition. All past researches are included with many observations and methodology for testing and comparing traditional concrete to composite columns.

Chapter three presents the experimental program and details the CFST column parameters to be examined. It also includes a description about fabrication of the steel section and the placement of the concrete. The mix designs of the three types of concrete used in the study are explained. In this chapter the properties of steel and concrete, the inclusion of a specific percentage (2.5%) of GI wire in CFST columns are shown. The test setup for applying different types of load is also shown here. A relatively new system i.e. the knife edge system which is used for eccentric loading applying on test specimens was introduced in this thesis.

Chapter four contains the result and discussion of the GI fibered and plain concrete CFST columns subjected to concentrically and eccentrically load. The observations were comprised of the failure criteria of the column. The results include lateral deformation by LVDT setup fixed at mid height of the column specimen. The various types of relationship like effect of structural steel percentage; load-versus-deformation relationship is examined for CFST columns. It also includes axial capacity, mode of failure, peak load and corresponding axial shortening etc. for the effect of GI fiber inclusion. All the result and discussion is based on the comparative study between fibered and plain concrete CFST columns.

Chapter five presents the design guidelines and different code equations for prediction of the ultimate capacity of CFST columns. It also shows the result for comparison of the code predicted capacities with the experimental capacities.

Chapter six presents a summary of the test program, conclusion drawn from the results presented in chapter four and recommendations for design of CFST columns and scope of future research.

CHAPTER 2
LITERATURE REVIEW

2.1 General

Concrete filled steel tube (CFST) is a composite structure consists of steel tube and concrete core inside it. It has various cross-sections like circular, square, rectangular and multi-side. Among these types circular, rectangular and square sections are mostly used in construction works. The inclusion of fiber with concrete is being used with the intention to reinforce brittle matrices to enhance their mechanical properties. Concrete is a well-known brittle material which is strong in compression and weak in tension. Fibers increase the flexural strength by diminishing and arresting development of cracks in concrete and improve toughness by furnishing energy dissipating mechanisms. Fibers influence many other properties including shear and compressive strength. The strength and toughness of fiber reinforced concrete is affected by many parameters e.g. properties of the fiber, the matrix, the fiber-matrix interface, size, geometry and volume/weight fraction of fibers.

The history of composite materials started in ancient Egypt over 2000 years ago with mud bricks, reinforced with straw fibers. In early period, straw was used as additives in clay which made bricks stronger against failure. The method of adding these ingredients to bricks were unknown earlier, but the benefits of including them were clearly obvious for the improvement of brick's strength. Adding fiber into plain concrete has been proved to be an effective method of eliminating its inherent brittleness, the fibers bride the crack in the matrix and transfer the applied load to the matrix, thus fiber reinforced concrete has better post crack behavior that plain concrete.

A good number of researches (Tokgoz and Dundar 2010; Lu et al. 2015; Yi-yan et al. 2015; Emon et al. 2016; Ravindran et al. 2016; Muktadir et al. 2017) are found in the recent concrete history on Fiber Reinforced Concrete (FRC). However, limited literature is available on use of GI wire as fiber in concrete with buildup section. Therefore, researches on steel fiber reinforced concrete would provide the necessary guideline for the present research on GI wire fiber reinforced concrete with composite columns.

Different codes are available for evaluating the strength of concrete filled steel tubular column. American Institute of Steel Construction (AISC) and the American Concrete Institute (ACI) provided rules for the design of these structural elements. In the United States of America, a joint Structural Specifications Liaison Committee (SSLC) was

organized in 1978 to evaluate the acceptability of composite column design procedure. Successively, the numbers of versions on AISC-LRFD specifications and ACI-318 were issued in different time. Other specifications or codes that provided the rules for design of composite structure were the Eurocode 4 (2005), the Australian Standard code (AS4100), the Architectural Institute of Japan (AIJ, 1997). Among all the codes Australian Standard 4100, AISC-LRFD and Eurocode 4 are used all over the world. A short note about composite columns is given below.

2.2 Types of Composite Columns

There are three types of composite columns: Fully Enchased Column (FEC), Partially Enchased Column (PEC) and Concrete Filled Steel Tube (CFST). Figure 2.1(a) to 2.1(c) shows the fully encased composite (FEC) columns which are consist of structural steel sections encased by concrete where the structural steel area comprises of at least 4% of the total composite column cross sections. Figure 2.1 (d) and 2.1 (e) shows the partially encased composite (PEC) column which is a type of composite column that generally consists of an H-shaped steel section with concrete between the flanges.

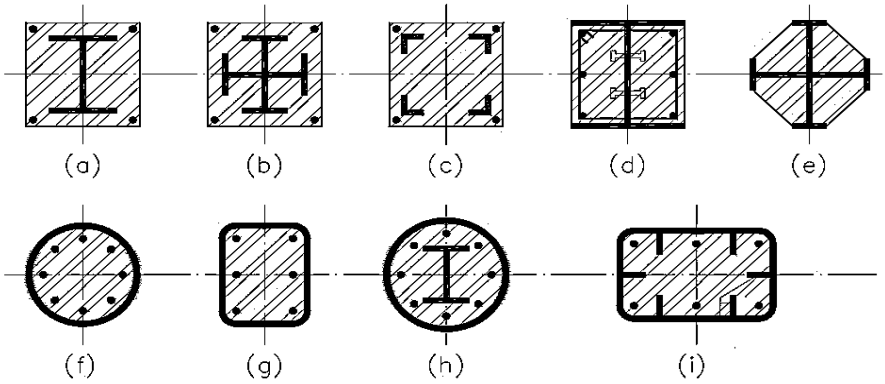

Figure 2.1 Detail X-sections of different composite columns, (i) FEC columns (a)-(c); (ii) PEC columns (d)-(e); (iii) CFST columns (f)-(i) (Eurocode 4-2005)

One of the advantages of this type of column over fully encased columns is that it requires formwork on only two sides of the column. Figure 2.1 (f) to 2.1 (i) shows the concrete filled steel tube (CFST) column. It is a structural system with excellent structural characteristics, which is the result of combining the advantages of a steel and concrete. A CFST column is constructed by filling a hollow rectangular or circular structural steel tube with concrete.

2.3 Concrete Filled Steel Tube (CFST) Column

The CFST column comprises a combination of concrete and steel; utilizing favorable properties of the two constituent materials. CFST column have been widely used in modern structure. This is mainly due to the combination of advantages of both steel and concrete, such as high strength, ductility etc. In this paper research has been done by using Concrete Filled Steel Tube (CFST) incorporating with specific percentage of GI wire fiber.

CFST column is becoming an attractive solution because it provides not only an increase in the load carrying capacity but also economy and rapid construction, and thus additional cost saving. The CFST columns are mainly divided into three types; Plain concrete filled hollow section, Reinforced concrete filled hollow section, CFST with encased steel section. The types are shown in Figure 2.2.

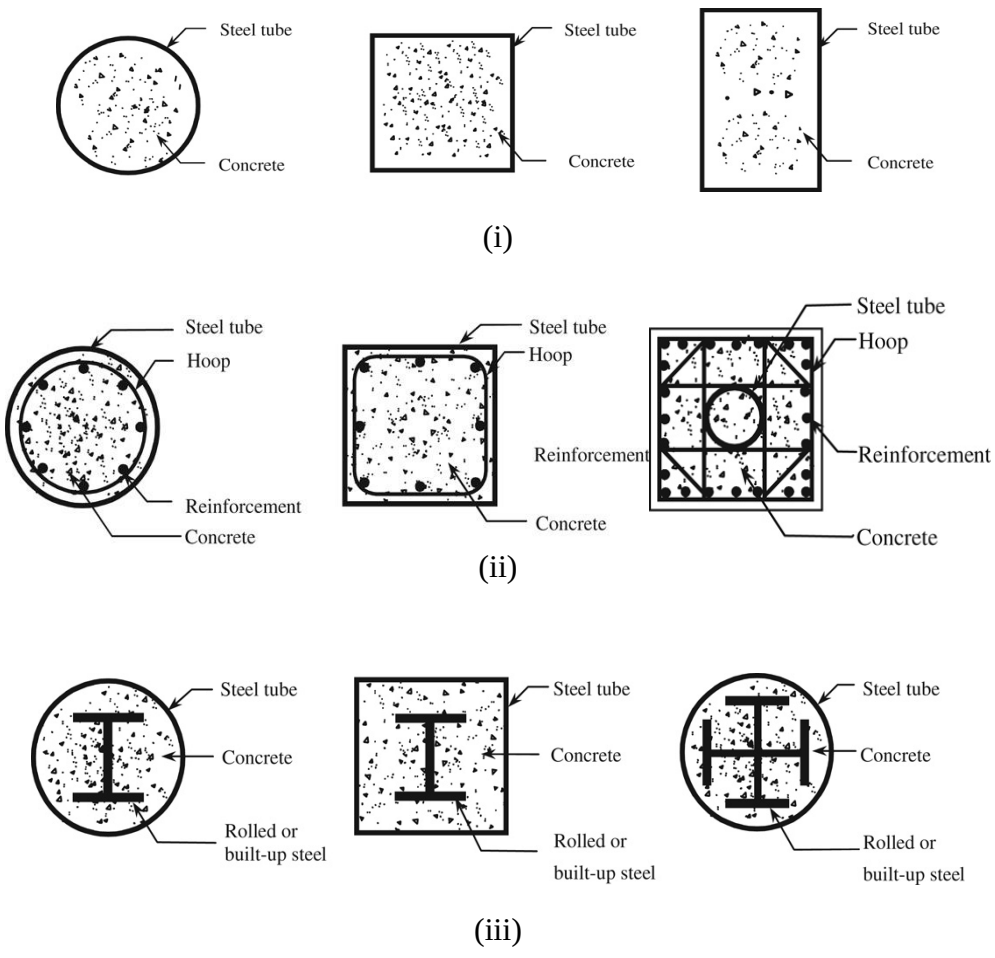

Figure 2.2 Different types of CFST. (i) Plain concrete filled hollow section (ii) Reinforced concrete filled hollow section (iii) CFST with encased steel section (Eurocode 4-2005)

2.4 Advantages of CFST Columns

CFST system has many advantages compared with ordinary steel or reinforced concrete system. As a structural system, a CFST column has a high load bearing capacity, excellent earthquake-resistance, good ductility and its higher stiffness which delays the onset of local buckling. Their use in multi-storied building has been increased in USA, Australia, China, Japan and many other countries in recent year owing to the benefit of increased load carrying capacity for reduced cross section. It has high performance in compressive strength and gives a significant improvement of ductility. This composite system prevents local buckling of member as well as lateral torsional buckling and the strength deterioration after the local buckling is moderated, both due to the restraining effect of concrete. Besides that, the steel tube can function as a permanent formwork as well as reinforcement, thus more economical to be utilized considering the whole life basis and rapid Construction work. The structural properties of the CFST columns increase due to the composite action between the constituent elements. The strength of concrete is increased due to the lateral confining effect provided from the steel tube, and the strength deterioration is not very severe, since the concrete spalding is prevented by the tube and no additional reinforcement is required. These columns give a significant improvement of energy dissipation capacity with greater flexural and tensile strength. The steel tube acts as longitudinal and transverse reinforcement. The steel tube provides confining pressure to the concrete so a triaxial state of stress is created. It is used for aesthetic application and it reduces cross section without varying capacity. Concrete into CFST column heads to higher impact resistance and high fire resistance and the amount of fireproof material can be reduced. This is an effective method of eliminating its inherent brittleness which results high torsional stiffness. Drying, shrinkage and creep of concrete are much smaller than ordinary reinforced concrete. The steel ratio is in the CFST column is much larger than those in the reinforced concrete and concrete encased steel cross section. The steel of the CFST cross section is well plastified under bending since it is located on the outside the section. For these all circumstances, the cost is automatically reduced. The environmental burden can be reduced by omitting the form work, and by reusing steel tubes and high quality concrete as recycled aggregate.

Inclusion of steel fiber in CFST columns has certain advantages over conventional normal weight concrete. CFST itself adds confinement to the concrete and for that reason adding fiber to concrete has its own benefits. Fibered concrete adds resistance to crack

development and propagation. This steel fiber has also been introduced to obtain ductile behavior. In case of CFST columns, the enhanced tensile and flexural strength and higher stiffness of steel fiber reinforced concrete were applied to improve their behavior. The study has conducted to investigate the reinforcing effect of GI fiber on the CFST columns with different concrete strength. GI fiber is relatively low cost and easily available in our country.

2.5 Application of CFST Columns

The application of CFST in tall buildings has been adopted in the form of partial columns in early days, and then their usage as full columns was adopted. This process has been very short, only a decade long. Figure 2.3 shows the statistics of using material for the worlds 100 tallest buildings from 1930 to 2015 Report by Jason Gabel, Council on Tall buildings and Urban Habitat (CTBUH) in 2018. As can be seen from 1960, all-steel construction has continued to decline as a primary structural material, comprising only 11% of the world's 100 tallest buildings in 2015.

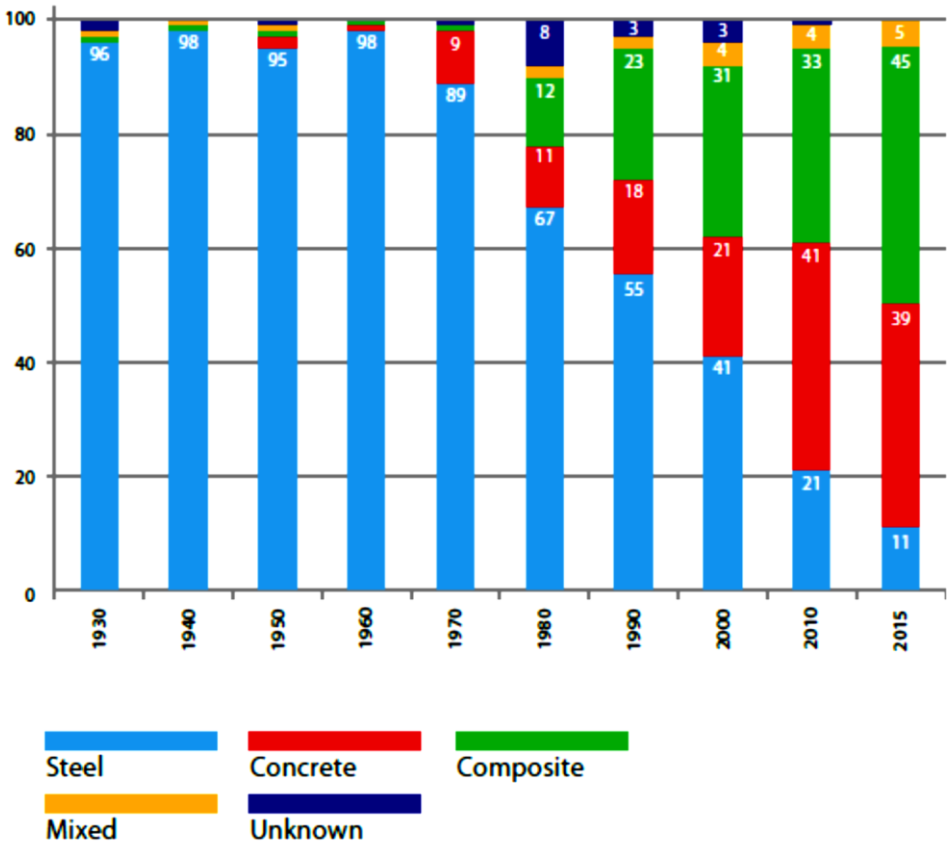

Figure 2.3 World's 100 tallest buildings by construction materials (Jason Gabel, CTBUH, 2018)

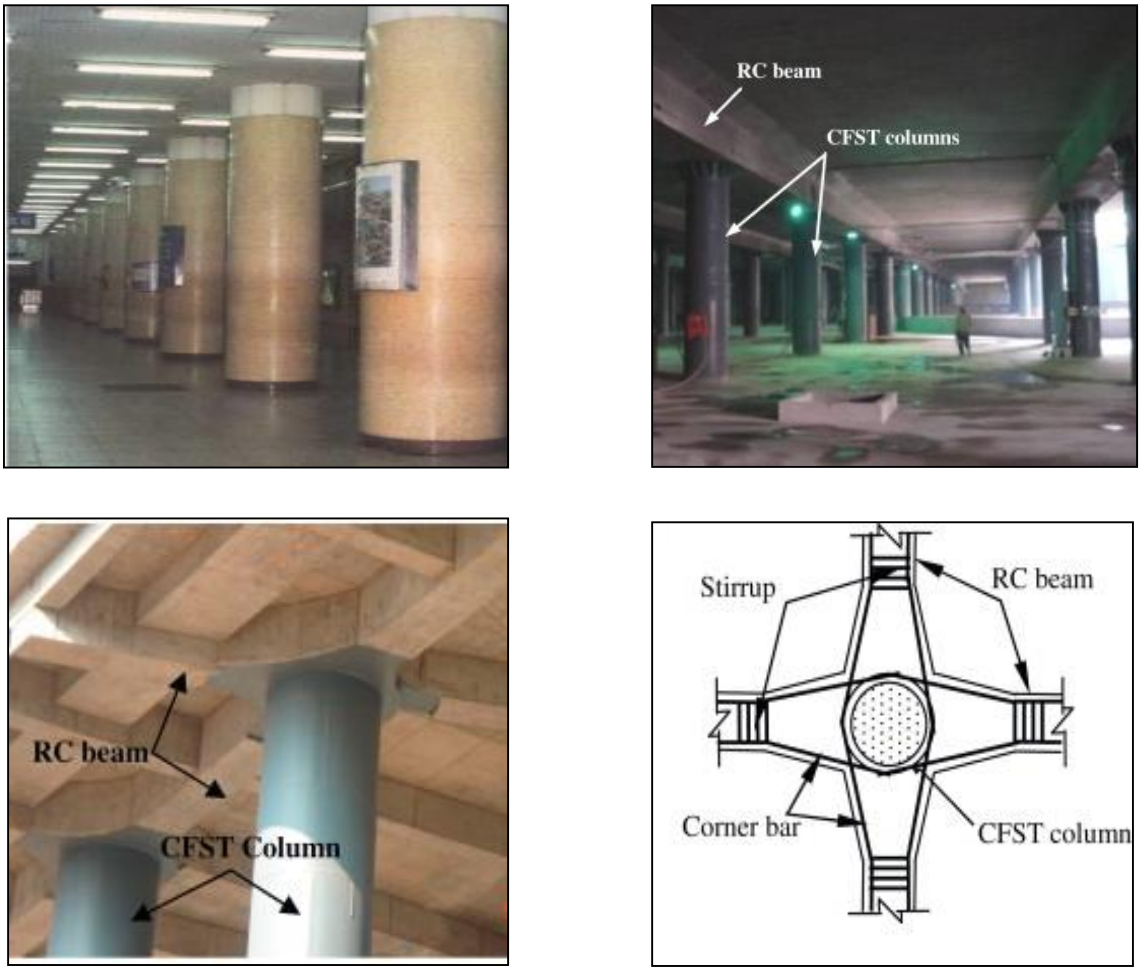

Figure 2.4 Composite steel structure system (Tao and Han, 2006)

Buildings with concrete and composite become the majority of material in construction and the proportions of these two material forms are predicted to increase. Only 3% of buildings which were 200 meters and higher in 2015 were constructed with all-steel material. Without any doubt concrete and composite building construction will be the most popular structural form in the future. The rise of market demand on these materials calls for urgent research. There are a lot of new technology and experiences in design, fabrication, and construction of this building. It can also promote the development of CFST structures in all over the world. Figure 2.4 illustrates a subway having composite structural system. The first engineering adopted CFST structure is the No.1 subway of Beijing (Figure 2.5- a).

Chinese Zhejiang Lishui Suichang Wuxi River bridge 260 meter span on the CFST arch bridge, concrete-filled steel tube arch bridge in Zhejiang Province, the longest single span (Figure 2.5- b). This concrete steel pipe arch bridge construction of the longest single span is long 1.32 kilometers, among which, a big bridge of 372 meters, a tunnel 355 m.

The project is designed on the secondary standard roads. Design speed limit is 60 kilometers per hour. The road is 8.5 meters wide, 10 meters wide subgrade, 12 meters wide bridge, and the construction period is 35 months.

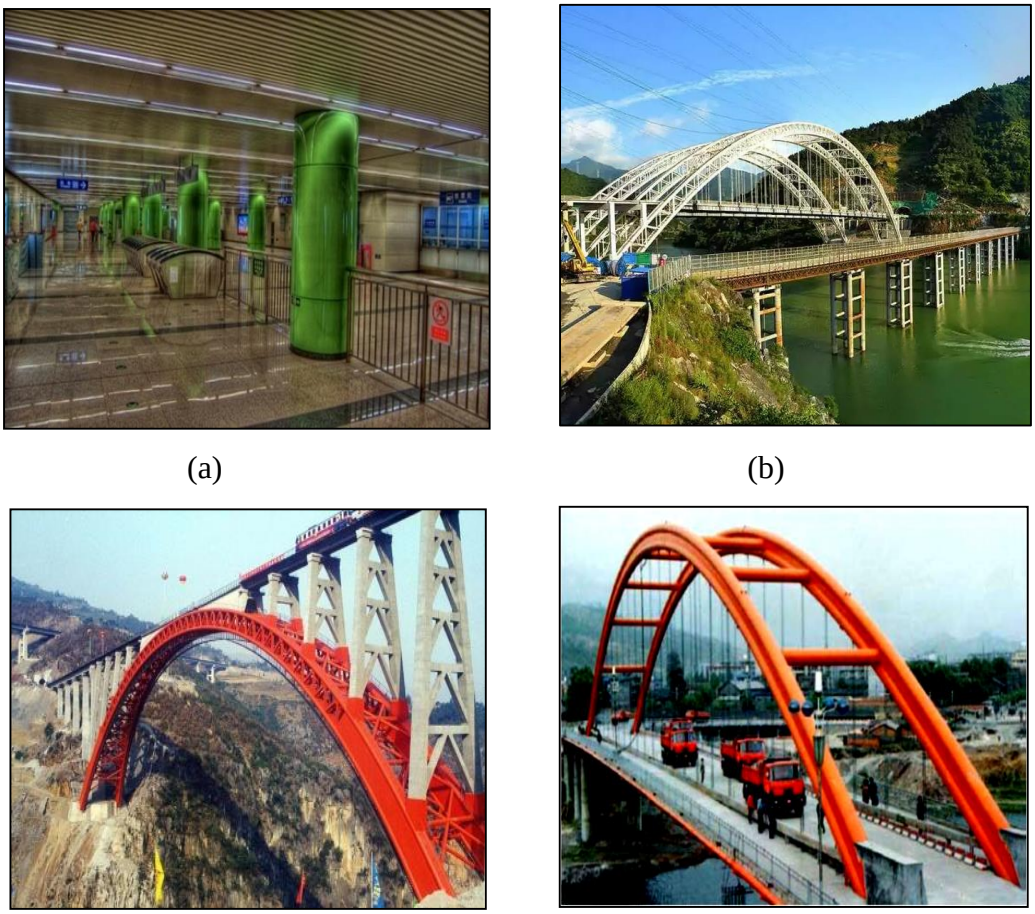

(a) (b)

(c) (d)

Figure 2.5 CFST structures, (a) No.1 subway of Beijing (b) Wuxi River bridge (c) Beipanjiang River Railway Bridge (d) Wanchang Bridge (Han et al, 2014)

Beipanjiang River Railway Bridge is the World's Highest Railway Bridge with 902 feet high, 771 feet span (Figure 2.5- c). The central bearing located on top of each of the foundations consisted of a pair of closely fitted 11.5 foot (3.5 m) diameter concave spherical sections with a radius of 26 feet (8 m). The first CFST Arch Bridge was constructed in china, of the span 115m over the china's Wangchang River (Figure 2.5- d). It offers a good example of the adoption of CFST columns in super tall buildings. The Anthony J. Celebrezze Federal Building (also known as the Federal Office Building, the Celebrezze Building, or the Federal Building for short) is a skyscraper of height 419 feet located in downtown Cleveland, Ohio (Figure 2.6- a).

(a)

(b)

(c)

(d)

(e)

Figure 2.6 High-rise building with CFST (a) Federal Office Building (b) Mori Tower (c) Canton Tower building (c) Benxi steel company (d) SEG plaza building (Source-https://en.wikipedia.org/wiki/)

The building has 32 stories, rises to a height of 419 feet (128 m), 1,007,000 square feet (93,600 m2) of space, and is located at 1240 East 9th Street. It was completed in 1967 and houses U.S. government agency offices. Roppongi Hills Mori Tower is a 54-story mixed-use skyscraper in Tokyo in 2003 (Figure 2.6- b). It is the sixth tallest building in Tokyo at 238 meters (781 ft). The tower has a floor space area of 379,408 square meters (4,083,910 sq ft), making it one of the largest building in the world by this measure.

The Canton Tower building has a unique architectural form and one of the world's tallest structures (Figure 2.6- c). It is one of the most spectacular structures of recent times built using CFST members. With a height of 612m becomes the highest TV tower in the world, surpassing the CN Tower in Toronto with 553m. The entire tower was completed in 2010 and put into operation for the Asian Games that year. The steel ingot work-shop of Benxi steel company built in 1972 was the first industrial building with CFST columns (Figure 2.6- d). The highest tall building which adopted CFST is Shenzhen SEG Plaza building was completed in 2000 (Figure 2.6- e). It is the highest one in China and abroad. The CFST members were used as the external columns of the frame as well inside as concrete shear walls. The diameter of the columns used in the building ranges from 900mm to 1600mm. They were brought to the site in lengths of three stories and concrete was poured from the top of the column. The critical design loads for the SEG Plaza building were seismic and wind loads. Therefore, rigid connections between the steel beams and the concrete filled tubes were used.

2.6 Experimental Investigation on CFST Columns

Experimental researches were carried out on concrete filled steel tubular columns by several researchers to investigate the behavior of columns with fiber with variable properties such as eccentricity, loading conditions, dimension of specimen, concrete strength etc. Experimental studies on concentrically loaded composite columns with circular hollow sections (CHS) in compression had been carried out by Stephen P. Schneider. (1998), O'Shea and Bridge (2000) and Lam and Giakoumelis (2004) to investigate the effect of steel tube shape and wall thickness on ultimate capacity. The results have suggested that CHS offer substantial post-yield stiffness and ductility that are not available in square or rectangular hollow sections. Lam and Giakoumelis (2004) also assessed concrete filled tubes under different loading conditions - on the concrete and steel simultaneously, the concrete alone and the concrete and steel with a greased column. Results indicated that when the concrete and steel were loaded simultaneously, the tube

provided little confinement in comparison to the concrete only loaded specimens; similar findings were also reported by Sakino et al. (2004).

Gibbons and Scott (1996)

The authors found that utilizing high strength concrete results in increased stiffness and hence reduced section sizes for columns designed for slenderness effects and lateral loading. Strength enhancement and improved ductility provided by the confined concrete was confirmed, but it was reported that the concrete infill had little effect on the local buckling strength of the steel tube. Experimental results on the strength, local and post-local buckling behavior were reported. The results have indicated that the width-to-thickness ratio of the steel elements and the constraining factor (the ratio of the component resistances of the composite column) both have a significant influence on the compressive load carrying capacity and ductility of the concrete filled columns.

Schneider (1998)

Experimental studies on the behavior of short composite columns with circular hollow sections (CHS) concentrically loaded in compression have been carried out to investigate the effect of steel tube shape and wall thickness on ultimate capacity. This paper presented an experimental and analytical study on the behavior of short, concrete-filled steel tube columns concentrically loaded in compression to failure. Fourteen specimens were tested to investigate the effect of the steel tube shape and wall thickness on the ultimate strength of the composite column. Ultimate strength results were compared to current specifications governing the design of concrete-filled steel tube columns. Of these 14 CFT specimens, three were circular, five were square, and six were rectangular steel tube shapes. For each tube profile, specimens were arranged in order of increasing wall thickness. The *D/t* ratios in this study ranged from 17 to 50, and the steel to total composite area ratio A_s/A_{total} ranged from 8 to 22%. For the rectangular shapes, *D/t* was listed for the broad face. All steel tubes were cold-formed carbon steel with specified yield strength of 317 MPa. Circular steel tubes offer much more post-yield axial ductility than the square or rectangular tube sections. The square and rectangular tube walls, in most cases, did not offer significant concrete core confinement beyond the yield load of the composite column. Local wall buckling for the circular tubes occurred at an axial ductility of 10 or more, while most local wall buckling of the square and rectangular tubes occurred at a ductility between 2 and 8. For small dimensional concrete-filled steel tube columns, smaller *D/t* ratios provided a significant increase in yield load compared to the

computed AISC-LRFD Specifications. Experimental results suggested that circular tubes offer substantial post-yield strength and stiffness, not available in most square or rectangular cross sections. Also observed by these results was that current design specifications were adequate to predict the yield load under most conditions for a variety of structural shapes. In almost all cases the AISCI/LRFD Specification provides a reasonable, conservative estimate for the axial strength of the concrete-filled steel tube column. In the few cases that the LRFD predicted load under estimated the actual yield load, the predicted load was non conservative by only 5%.

O'Shea and Bridge (2000)

Several design methods have been developed that can be used to conservatively estimate the strength of circular thin-walled concrete filled steel tubes under different loading conditions. The loading conditions examined include axial loading of the steel only, axial loading of the concrete only, and simultaneous loading of the concrete and steel both axially and at small eccentricities. The test specimens were short with a length-to-diameter ratio of 3.5 and a diameter thickness ratio between 60 and 220.The internal concrete had nominal unconfined cylinder strengths of 50, 80, and 120 MPa. The bond (or lack of) between the steel and internal concrete was critical in determining the formation of a local buckle. The strength of unfilled circular steel tubes has been found to be significantly affected by local buckling. Although the buckling strength of square tubes could be improved by providing internal lateral restraint, this was not observed in the circular steel tubes examined. Instead, the predominantly outward buckle remained unaffected by the internal concrete. The degree of confinement offered by a thin-walled circular steel tube to the internal concrete is dependent upon the loading condition. The greatest concrete confinement occurred for axially loaded thin-walled steel tubes with only the concrete loaded and the steel tube used as pure circumferential restraint. Equations had been developed to predict the strength of this type of column and to provide an estimate of the shape of the post ultimate curve.

Han and Yang (2001)

Concrete compaction was identified as playing a key role in the performance of concrete filled tubes. Tests on concrete filled carbon steel tubes were carried out to determine the influence of compaction methods on column capacity. Tests on sixteen concrete filled steel tubes to investigate the influence of concrete compaction methods on the section capacities of concrete filled steel tubes with rectangular sections are reported. The main

objectives of these tests were twofold: firstly, to report a series of tests on composite stub columns under different concrete compaction methods; and secondly, to investigate the influence of concrete compaction on the section capacities and the modulus of elastic of concrete filled steel tubes with rectangular sections. It was found that better compaction of concrete resulted in higher sectional capacities and higher elastic module in concrete filled steel tubes. The tests showed the importance of good concrete compaction for concrete filled steel tubes with rectangular sections. Sixteen specimens were tested under concentric axial load. The aim of the experimental study was to determine not only the maximum load capacity of the specimens, but also to investigate the behavioral pattern up to and beyond ultimate load. The tests confirmed that better compaction resulted in higher section capacities and highlighted the importance of concrete compaction on the performance of composite concrete filled CHS.

Shanmugam and Lakshmi (2001)

A state of the art review reported on steel–concrete composite columns had highlighted the significant research in this area. The majority of research to date had been focused on the capacity, fire resistance, and seismic resistance of carbon steel composite columns, with numerous models proposed for the prediction of structural behavior. Tests were conducted on two 47 ft (14 m) long, 13 in (33 cm) diameter pipe columns, one empty and the other filled with concrete. Rectangular in-filled composite columns of 3 m long were tested under three different loading i.e. axial, uniaxial bending applied about major or minor axis and biaxial bending. Effect of end eccentricity ratios e_x/D and e_y/D up to 0.5 was also studied. It was concluded that concrete increased the load and moment carrying capacity without increasing the size of the column. The effect of confinement of concrete was noticeable in columns of slenderness ratio L/D less than 15. No appreciable difference in load carrying capacity was detected between long and short specimens and between loading on the whole section and on concrete alone. In most columns, the yield strain was reached in the compressive zones at loads varying between 80% and 90% of the failure load. After the failure, the tensile strains reached the yield as the columns underwent large lateral displacements and consequently were subjected to high bending moments. It was concluded that the failure mode of all columns was an overall buckling mode, with no sign of local buckling of the steel section.

Uy (2001)

An investigation into the use of high strength material in composite columns was reported. However, as the strength of the steel is increased the buckling characteristics became more dominant with slenderness limits for both local and global buckling becoming more significant. To arrest the problems associated with buckling of high strength steel and concrete filling encasement could be utilized as it has the effect of changing the buckling mode, which increased the strength and stiffness of the member. An experimental program undertaken for both encased and concrete filled composite columns, which were designed to be stocky in nature and thus fail by strength alone was described in this paper. The columns were designed to consider the strength in axial compression and were fabricated from high strength steel plate. In addition to the encased and concrete filled columns, non-encased columns and hollow columns were also fabricated and tested to act as calibration specimens. A model for the axial strength was suggested and this is shown to compare well with the test results.

Lam and Giakoumelis (2004)

An experimental investigation on behavior of circular concrete-filled steel tubes (CFT) with various concrete strengths under axial load was performed. The effects of steel tube thickness, the bond strength between the concrete and the steel tube, and the confinement of concrete were examined. Measured column strengths were compared with the values predicted by Eurocode 4, Australian Standards and American Codes. Fifteen specimens were tested with 30, 60 and 100 N/mm^2 concrete strength, with a D/t ratio from 22.9 to 30.5. All the columns were 114 mm in diameter and 300 mm in length under axial load. The effect due to concrete shrinkage was critical for high-strength concrete and negligible for normal strength concrete. All three codes predicted capacities were lower than that measured during the experiments. Eurocode 4 gave the best estimation for both CFT with normal and high-strength concrete. The results showed that for high-strength CFT columns, the peak load was achieved for small shortening (3.0 mm), whereas for normal concrete the ultimate load was gained with large displacement. As the concrete strength increased the effects of the bond of the concrete and the steel tube became more critical. For normal concrete strength, the reduction on the axial capacity of the column due to bonding was negligible. For high-strength concrete, the variation between non-greased and greased was 17%. Eurocode 4 provided a good prediction of the axial strength of concrete filled steel tube columns. Based on the largest difference between the

experimental and calculated value on the axial capacity was 17%. The predicted axial strengths using ACI and AS were 35% lower than the results obtained from experiments. A coefficient was proposed for the ACI/AS equations to take into account the effect of concrete confinement on the axial load capacity of CFTs. The results had suggested that CHS offer substantial post-yield stiffness and ductility that are not available in square or rectangular hollow sections. The results also assessed concrete filled tubes under different loading conditions-on the concrete and steel simultaneously, the concrete alone and the concrete and steel with a greased column. Results indicated that when the concrete and steel were loaded simultaneously, the tube provided little confinement in comparison to the plain concrete loaded specimens.

Sakino et al. (2004)

One hundred and fourteen (114) specimens were tested experimentally with concentric loading. The columns specimens included both hollow and concrete filled tube. The shapes of the columns were being both circular and square. The tensile strengths of the tubes were 400, 600 and 800 MPa. The concrete strengths were 20, 40 and 80 MPa. Another variable parameter in the specimens was the size of the columns. The columns were classified according to their sizes. The circular steel tubes were cold formed and square steel sections were made joining two channel sections together. The objectives of test included investigation of the confining effect of steel tube on the concrete strength and restraining effect of the concrete filled on local buckling phenomenon of the steel section. For measuring the longitudinal strain four transducers were used. The authors reported that for circular columns the experimental load carrying capacity was greater than the squash load owning to the confining effect. The author established load versus deformation graphs and concluded that with increasing B/t or D/t ratio the capacity obtained from the equation is less than from experimental capacity due to local buckling in the steel section. The author developed different analytic models to estimate the ultimate load carrying capacity of CFT short columns. The authors also derived different equations to calculate the capacity of the square columns taking consideration of the strength reduction due to local buckling.

Fujimoto et al. (2004)

The effect of higher material strengths on the flexural behavior and created mathematical models of the steel tube and filled concrete was investigated. In this study, the effect of the section shape, diameter (width)-to-thickness ratio and the combination of strengths of

the steel tube and filled concrete were included. The Authors tested sixty-five (65) specimens of concrete filled tube for eccentric loading. The shapes of column being both circular and square. The tensile strengths of the tubes were 400 MPa, 590 MPa and 780 MPa. The concrete strengths were 20, 40 and 80 MPa. The other variable parameters in the specimens were the size and thickness of the column. The circular tubes were cold formed from a flat plate by press bending and seam welding and square tubes were fabricated by welding together two pieces of channel section. The objectives of this research were to investigate the effect of higher material strengths on the flexural behavior and to create mathematical models of the steel tube and filled concrete. The Authors concluded that for circular and square columns the experimental load is less than the squash load. The researchers recommended the use of high strength filling concrete which generally caused a reduction in the ductility of a circular CFT column. However, the ductility behavior improved by confining the concrete within a high strength steel tube having a small diameter-to-thickness ratio. They observed that an increase in bending strength due to the confinement effect cannot be expected in square CFT columns. Moreover, the effect of local buckling must be considered when evaluating the bending strength in square CFT columns with large width-to-thickness ratios. Furthermore, the authors noted that the fiber analysis reproduced the flexural behavior of eccentrically loaded CFT columns within a reasonable level of accuracy and the ultimate strength obtained in these tests are also estimated to be accurate. According to this study the use of fiber improved the lateral confinement of infilled concrete.

Tao et al. (2007)

An experimental study on the structural behavior of concrete-filled stiffened thin wall tubular columns was presented. The test results showed that the local buckling of the tube was effectively delayed by the stiffeners. The plate buckling initially occurred when the maximum load had almost reached for stiffened columns. The stiffening was achieved by welding longitudinal stiffeners on the inner surfaces of the steel tubes. A total of 18 specimens, including six stiffened columns and 12 unstiffened columns, were tested to failure. In the case of the unstiffened specimens, half of them were filled with normal concrete (NC), and the rest of them filled with steel fiber reinforced concrete. Companion tests were also undertaken on 12 unstiffened concrete-filled steel tubular (CFST) columns, with or without steel fibers in the infill concrete. The test results showed that the local buckling of the tubes was effectively delayed by the stiffeners. The plate buckling

initially occurred when the maximum load had almost reached for stiffened specimens, thus they had higher serviceability benefits compared to those of unstiffened ones. Some of the existing design codes were used to predict the load-carrying capacities of the tested composite columns.

Lam and Gardner (2008)

The authors performed this experimental study to assess the compressive response of stainless steel concrete filled tubular columns. Two cross-section types were investigated square hollow sections (SHS) and circular hollow sections (CHS). Tests were performed on four different section sizes - SHS 100 x 100 x 5, SHS 100 x 100 x 2, CHS 114 x 6 and CHS 104 x 2. This paper presented the behavior and design of axially loaded concrete filled stainless steel circular and square hollow sections. For each section size, four stub column tests were carried out on a empty stainless steel tube and three concrete filled specimens with nominal concrete strengths of 30, 60 and 100 MPa. The column strengths and load-axial shortening curves were evaluated. The study was limited to cross-section capacity and had not been validated at member level. Comparisons of the tests results together with other available results from the literature had been made with existing design methods for composite carbon steel sections - Eurocode 4 and ACI. Tests were also conducted on the constituent materials - tensile tests on coupons extracted from the stainless steel tubes and cube and cylinder tests on the concrete. It was found that existing design guidance for carbon steel might generally be safely applied to concrete filled stainless steel tubes, though it tended to be over-conservative. A continuous strength method was proposed and it is found to provide the most accurate and consistent prediction of the axial capacity of the composite concrete filled stainless steel hollow sections due largely to the more precise assessment of the contribution of the stainless steel tube to the composite resistance.

Dundar and Tokgoz (2010)

An experimental study was conducted on steel tubular column in-filled with plain and steel fiber reinforced concrete. The main variable parameters in this study were the cross section, slenderness, concrete strength and load eccentricity. In the study, a theoretical method for the prediction of ultimate strength capacity and load deflection curve of concrete filled tube column with fiber was proposed. A total of 16 nos of CFST column specimens were constructed with plain and steel fiber concrete. All specimens were tested as pinned conditions at both ends under short-term axial load and biaxial bending. The

eight specimens were designed with different mixtures of plain concrete. Besides this, another eight specimens were constructed with almost the same previous concrete mixtures by adding 0.75% volume fraction of steel fibers to determine the steel fiber effects. Each set had 60 x 60 x 5mm, 70 x 70 x 5mm, 80 x 80 x 4mm and 100 x 100 x 4mm cross section, and length of 1250 mm. The result of this study indicated that the use of the proposed stress-strain relations for the materials gives reasonable accuracy in predicting the behavior of bi-axially loaded steel tube columns in-filled with plain and steel fiber reinforced concrete.

Ghannam et al. (2011)

Twelve (12) specimens experimentally under concentric load were tested. The columns were lightweight and normal concrete were used to fill the steel tube columns. The shapes of the columns were circular and square. The concrete strengths were 10 MPa and 33.4 MPa. The tensile strength of the steel sections was 320 MPa and 360 MPa for rectangular and 350 MPa and 355 MPa for circular columns. The columns were of different size, shapes, lengths and slenderness ratios. The purpose of the research was to investigate behavior and compare between normal and lightweight concrete filled tube under axial loading. The author reported that sections filled with lightweight aggregate concrete failed due to local buckling and sections filled with normal concrete failed due to overall buckling. Moreover, bare steel sections failed due to excessive yielding and bulging (local buckling) at both top and bottom ends of the column specimens before reaching the plastic load. However, the researchers concluded lightweight aggregate concrete is better than normal aggregate concrete due to its low specific gravity and thermal conductivity.

Emon et al. (2014)

The authors summarized that inclusion of fiber within the concrete increases the strength, ductility, energy absorption capacity and impact resistance. In this study rectangular reinforced concrete beams, with seven separate mix-proportions, including one control mix (without any GI wire) and six mixes (with different fraction of GI wire) with brick chips as coarse aggregate were designed in accordance with ACI provisions. Each beam was 150 mm (6 in.) wide, 200 mm (8 in.) deep, with an effective depth to the steel centroid of 169 mm (6.76 in.) and d_0 = 31 mm (1.24 in.). The effective span length for the test beams was 1.35 m (54 in.). The beams were reinforced with longitudinal reinforcement at the bottom and two binder rods were placed at the top. Minimum and maximum ACI permitted reinforcement ratios for the beams were found to be 0.0028 and

0.015, respectively. Two 10 mm dia bars were provided at bottom, which furnished 36% of the maximum reinforcement ratio. To avoid premature shear failure of the beams during loading and handling and to ensure a flexural failure, 8 mm dia two-leg vertical stirrups were provided with 150 mm (6 in.) center to center spacing throughout the span. According to this study, fiber content of 2–2.5% (approx. 0.6–0.75% vol. fractions) by weight was suitable for use in conventional concrete mixes with burnt clay brick chips as coarse aggregate. No additional admixture or special attention was necessary for concrete mix but fiber addition might impart significant performance enhancement which was, in the long run, ensured a durable structure. Increased wire volume might lead to decrease workability and difficulty in concrete placement, especially for large concrete members. In such cases, utilization of admixture might be necessary.

Yang et al. (2015)

The connection between beam and concrete filled elliptical steel tubular column and its failure mode was investigated. Of all the specimens, five different joint assemblies had been considered. Each type of assembly comprised one specimen with an elliptical hollow section (EHS) column and another specimen with an EHS column filled with concrete, to explore the enhancement of concrete infill on the structural behavior of these joints. All EHS columns were manufactured from Grade S355 steel with minimum yield strength of 355 MPa. Only one stiffener plate was adopted for each joint. For minor axis connection, a through plate, function in gas both fin plate and stiffener, was adopted to ensure the continuous stiffness of the joint. A number of experiments were conducted to investigate the rotational behavior of simple bolted beam to elliptical column connections. Based on the experimental results, the typical failure mode of the connections with hollow columns was found to be inward local buckling of the column surface near the upper portion of the joints, though stiffeners were arranged in either the major or minor axis direction in some cases. However, the inward deformation was eliminated by the core concrete. Instead, shear failure of the bolts governed the ultimate rotation capacity of the joints with concrete infill. According to the moment versus rotation responses of beam to elliptical column connections, friction was in control in the initial stage with the friction force existing between fin plates, beams and bolts. In this section, the rotation of the connection was quite low but the slope of the moment rotation curves was nearly constant, with the column, beam and bolts working well together. Then, slippage occurred when the load applied was bigger than the friction force, and the moment climbed slowly

with the increase of rotation. Afterwards, the bolts, the bolt holes in the fin plates and the beam webs acted together in resisting the load until the joints failed in one of the modes described previously. For all of the joint assemblies, connections with concrete-filled columns had much higher moment capacity than their unfilled counterparts. Based on this experimental result, the typical failure mode of the connection with hollow columns was found to be inward local buckling of the column surface near the upper portion of the joints. The enhancement in moment ranged from1.91 to 5.19. Additionally, a minor axis through plate connection was found to have higher stiffness and better moment capacity. Hence this joint type was recommended form in or axis beam to elliptical column connections.

Lu et al. (2015)

A detail study was carried out to explore the effect of steel fiber on the behavior of concrete filled steel tube columns with different concrete and thickness of steel tube. The author presented an experimental work for short steel tube columns filled with plain concrete and steel fiber reinforced concrete under axial load. The study aimed to explore the effect of steel fiber on the behavior of concrete-filled steel tube (CFST) columns with different concrete strengths and thicknesses of steel tube. Thirty-six specimens were tested with steel fiber volume percentages of 0%, 0.6%,0.9% and 1.2%, thicknesses of steel tube of 3, 4 and 5 mm and concrete strengths from 50 to 70 MPa. The failure modes, ultimate loads and axial load-axial shortening relationships were presented. Experimental results showed that steel fiber failed to change the failure mode of CFST columns, but delayed the local buckling of steel tube through bridging the plastic cracks near the sliding plane and improving the shear-frictional resistance of concrete. This beneficial effect from steel fibers also led to significant improvement of the ductility and the energy dissipation capacity of CFST columns. Compared with thicker steel tube, adding steel fibers to concrete was a more effective and economical method in enhancing the ductility of CFST columns. The results also indicated that the presence of steel fibers had no obvious effect on the ultimate load of CFST columns. Design formulas for the load capacity and ductility of CFST columns were proposed, and the predictions agreed well with the experimental results from this study and the literature. This study concluded that, adding steel fiber into concrete core has little effect on the failure mode and exhibited slightly higher ultimate load compared to plain concrete tube column. But it led to substantial enhancement of ductility and energy dissipation capacity.

Yi-yan et al. (2015)

An experimental study was presented on the compressive behavior of steel fiber reinforced concrete-filled steel tube columns. Specimens were tested to investigate the effects of the concrete strength, the thickness of steel tube and the steel fiber volume fraction on the ultimate strength and the ductility. The experimental results indicated that the addition of steel fibers in concrete could significantly improve the ductility and the energy dissipation capacity of the concrete-filled steel tube columns and delayed the local buckling of the steel tube, but had no obvious effect on the failure mode. It had also been found that the addition of steel fibers was a more effective method than using thicker steel tube in enhancing the ductility, and more advantageous in the case of higher strength concrete. An analytical model to estimate the load capacity was proposed for steel tube columns filled with both plain concrete and steel fiber reinforced concrete. The predicted results were in good agreement with the experimental ones obtained in this work and literatures.

Petrus et al. (2016)

Twenty-six (26) specimens of slender concrete filled steel tube columns under eccentric loading were tested in this study. The shape of the column being square. The variables in the specimens were size, thickness, eccentricity and height of stiffener. Axial loading was applied through the V-shaped edges at each specimen so that the load eccentricity could be controlled precisely. The objective of the research was to investigate the axial load capacity and bending capacity of eccentrically loaded concrete filled tube with stiffeners in variable height. The authors observed that non-filled slender tubes failed by local buckling and the concrete filled tube columns failed due to global buckling. The failure mode improved with the increasing stiffener height. It was also observed that long square concrete filled tube with longitudinal stiffeners and height of 25 mm is best in axial load carrying capacity and bending capacity than other tab stiffener. The strength increased significantly when extended tab stiffeners were used with it. The mid deflection increased with increasing eccentricity and columns with extended tab stiffeners had the lowest deflection. It was also reported that with the increasing eccentricity the effect of stiffeners decreased.

Wang et al (2017)

Total fourteen (14) specimens experimentally tested under axial compression. In this experiment twelve (12) specimens were tested with concrete filled steel double tube stub

columns and two (2) specimens were tested with thin-walled concrete filled stiffened tube counterparts. The objective of the research was to investigate the behavior of concrete-filled stiffened double-tube (CFSDT) stub columns under axial compression. The concrete strengths were 42.1 MPa, 69.8 MPa and tensile strength of steel was 230 MPa. The author reported that the stiffened columns have high strength and good deformation capacity. The author also noted that in finite element models, the inner steel tube can provide strong confinement to its concrete core. It was also reported that the strength obtained from experimental and numerical investigation was very close to the code predicted capacity.

Islam (2019)

This paper presented an experimental investigation on the behavior of CFST columns regarding three parameters: concrete compressive strength, cross sectional slenderness ratio and global slenderness ratio. Total nine CFST columns with square cross section were tested under concentric loading. The tested columns were filled by concrete with compressive strength of 27 MPa to 44 MPa, cross-sectional slenderness ratio of 25 to 42 and global slenderness ratio of 3 to 10. The influence of these parameters on the failure mode, load-strain response, ultimate load and performance indexes of the square CFST column was discussed. Finally, the design approaches adopted in (Eurocode 4, AISC-LRFD 2010, ACI 2014 and Wang et al. 2016) were reviewed and applied to calculate the ultimate strength of the tests columns. Subsequently, the predicted values were compared with the experimental results obtained from the experiments.

Based on the results, it was determined that concrete compressive strength, cross sectional slenderness ratio and global slenderness ratio have significant effect on the fundamental behavior of CFST column. Increasing the concrete compressive strength improved the ultimate capacity and concrete contribution ratio of the column but decreased the peak strain because of its less ductile behavior. On the other hand, columns with higher global slenderness ratio showed lower ultimate capacity and less ductile behavior with global buckling failure. However, columns with lower cross sectional slenderness ratio exhibited better column performance for its higher steel contribution and columns with higher cross sectional slenderness ratio showed outward local buckling failure. Moreover, all the codes somewhat overestimated the capacities except AISC-LRFD (2010). AISC-LRFD (2010) presented best prediction with a mean of 0.99 and Standard deviation of 0.04. EC4 and ACI (2014) predicted higher capacity than the experimental results about 8% and 2%

respectively; whilst Wang et al. (2016) predicted highest 12% higher capacity of all the methods analyzed. In general, all the codes showed good agreement with the experimental results.

Ali (2019)

This experimental investigation was done on the behavior of eccentrically loaded CFST columns regarding four parameters: concrete compressive strength (f_c'): 27 Mpa to 44 Mpa; cross sectional slenderness ratio (B/t): 25 to 41.6; global slenderness ratio (L/B): 3 to 10 and load eccentricity ratio (e/B): 0 to 0.45. Total eleven CFST columns with square cross section were tested under uniaxial eccentric compression. The influences of these parameters on the failure mode, load-strain response, peak load, ultimate moment, mid-height deflection and performance indexes of the square CFST column were discussed. Finally, the design approaches adopted in (Eurocode 4 and AISC-LRFD 2010) were reviewed and applied to calculate the ultimate strength and moment of the tests columns. Subsequently, the predicted values were compared with the experimental results obtained from the experiments.

Based on the results, it was observed that concrete compressive strength (f_c'), cross sectional slenderness ratio (B/t), global slenderness ratio (L/B) and load eccentricity ratio (e/B) have significant effects on the load and deformation behavior of eccentrically loaded CFST columns. Stiffness and ultimate capacity of the tested column decreased with the increase of cross-sectional width to tube thickness ratio and load eccentricity ratio, whilst they increased with the increase of concrete compressive strength and the decrease of global slenderness ratio of the specimen. On the other hand, Axial strain at peak load and ductility index of the tested specimen decreased with the increase of concrete compressive strength, B/t ratio and L/B ratio but increased with the increase of e/B ratio of the specimen. However, Ultimate bending moment of the tested column increased with the increase of (f_c'**)** and (e/B) ratio but decreased with the increase of B/t ratio and L/B ratio of the specimen. Eurocode 4 (2005) somewhat overestimated the ultimate axial strengths but underestimated the ultimate bending moments of the tested square CFST columns in built-up steel sections, whilst AISC-LFRD (2010) presented the best and safe prediction for both of them. EC4 (2005) predicted higher capacity than the experimental results about 6%. Overall, both codes exhibited decent covenant with the experimental results.

2.7 Design Codes

From the past researches, different formulas were proposed to calculate the axial capacity of the CFST columns. Some of them accounted for the increase in the infilled concrete strength. The American Institute of Steel Construction AISC-LRFD (2010) formula is based on the structural steel, while the exclusively used for composite elements design, Eurocode-4 (2005) combine both these approaches. Australian Standard 4100 uses the concept of reinforced concrete design in their formulation without any consideration to the concrete confinement effects. In this chapter, the design approaches adopted in different codes (AISC-LRFD 2010, Eurocode 4 and Australian Standard 4100) are reviewed and applied to calculate the ultimate strength of the tests columns. The experimental results obtained from the experiments are compared with the predicted values from different codes simultaneously.

2.7.1 AISC-LRFD (2010) Code

The AISC-LRFD (2010) defines a composite column as a steel column fabricated from rolled or built-up steel shapes and encased in structural concrete or fabricated from steel pipe or tube and filled with structural concrete. In this specification, the design method for composite columns is based on the ultimate capacity of the materials part of the cross-section and takes into account the inelastic material properties with the required design loads as factored service loads. It contains the latest design approach of structural steel based on the ultimate strength concept. The nominal strength of a composite cross section is calculated from the ultimate resistance to load and reduction capacity factors related to material properties and characteristics of member failure are applied to the nominal strength of the cross-section.

Composite columns are consisting of three different type of sections; (a) compact sections, (b) non compact sections and (c) slender sections. When the slenderness ratios are sufficiently small, the member can attain its full plastic moment is called Compact section. When the slenderness ratios are larger, the compression may buckle locally before gaining full plastic moment is called non-compact section. Slender section may be defined as the slenderness ratios are sufficiently large, local buckling will occur before the yield stress of the material is reached. For the plastic stress distribution method, the nominal strength shall be computed assuming steel components have reached a stress of f_y in either tension or compression and concrete components in compression due to axial force and/or flexure have reached a stress of $0.85f_c^{/}$. For circular hollow steel section

filled with concrete, a stress of 0.95 $f_c^{/}$ is permitted to be used for concrete components in compression due to axial force and/or flexure to account for the effects of concrete confinement. Based on these characteristics, all the tested sections in this study are compact.

For compact CFST sections,

$P_{no} = P_p$ (2.1)

where

P_{no} = Nominal compressive strength of axially loaded composite column

$P_p = f_y A_s + C_2 f_c^{/} (A_c + A_{sr} (E_s/E_c))$ (2.2)

or $P_p = f_y A_s + C_2 f_c^{/} A_c$

C_2 = 0.85 for rectangular sections

The effective stiffness of the composite section, EI_{eff}, for all section shall be:

$EI_{eff} = E_s I_s + E_s I_{sr} + C_3 E_c I_c$ (2.3)

Where, C_3 = coefficient for calculation of effective rigidity of filled composite compression member.

$C_3 = 0.6 + 2 \left[\frac{As}{As+Ac}\right] \leq 0.9$ (2.4)

The available compressive strength need not be less than specified for the bare steel member

$$P_e = EI_{eff} \frac{\pi^2}{(KL)^2} \quad (2.5)$$

A_c = Area of concrete, in^2 (mm^2)

A_s = Area of the steel section, in^2 (mm^2)

E_c = Elasticity modulus concrete = $W_c^{1.5}\sqrt{f_c^{/}}$ ksi (0.043 $W_c^{1.5}\sqrt{f_c^{/}}$ MPa)

EI_{eff} = Effective stiffness of composite section, kip-in^2 (N-mm^2)

E_s = Modulus of elasticity of steel = 29,000 ksi

f_y = Specified minimum yield stress of steel section, MPa

f_{ysr} = Specified minimum yield stress of reinforcing bars, MPa

I_c = Moment of inertia of the concrete section about the elastic neutral axis of the composite section, in^4 (mm^4)

I_s = Moment of inertia of steel shape about the elastic neutral axis of the composite section, in^4 (mm^4)

I_{sr} = Moment of inertia of reinforcing bars about the elastic neutral axis of the composite section, in^4 (mm^4)

K = Effective length factor

L = Laterally unbraced length of the member, in (mm)

f_c' = Specified compressive strength of concrete, MPa

W_c = Weight of concrete per unit volume ($90 \leq W_c \leq 155$ lbs/ft^3 or $1500 \leq W_c \leq 2500$ kg/m^3)

The design compressive strength, P_n of doubly symmetric axially loaded concrete filled composite members shall be determined for the limit state of flexural buckling based on member slenderness as follows:

When $P_{no}/P_e \leq 2.25$

$$P_n = P_{no}\,[0.658^{Pno/Pe}] \tag{2.6}$$

When $P_{no}/P_e > 2.2$

$$P_n = 0.877[P_e] \tag{2.7}$$

P_e = Elastic critical buckling load (kN)

2.7.2 Eurocode 4 (2005)

In Eurocode 4 (2005), to calculate the axial capacity of concrete filled steel tube columns, the general method and the simplified method. In the general method, the second order effects and imperfections of the compression members are taken into consideration apparently. This method may be used for members with symmetrical sections, but they are also applicable to non-prismatic axial members. Consequently, appropriate software for numerical computation is essential for the application of the general method. In the simplified method, the European buckling curves for steel columns are utilized. The element's imperfections are implicitly taken into account. Unlike the general method, the simplified one is limited to prismatic composite axial members with symmetrical sections. Both methods are based on the following assumptions:

a) Flat sections stay flat while the column is deforming due to loading,

b) Till failure, the existence of full interaction between the concrete and steel surfaces is maintained.

In this research, only the simplified method is applied due to its applicability to the tested specimens and the calculation simplicity.

The plastic resistance to compression $N_{pl,Rd}$ of a composite cross-section should be calculated by adding the plastic resistance of its components:

$$N_{pl,Rd} = A_a f_{yd} + A_c f_{cd} \tag{2.8}$$

For members in axial compression, the design value of the normal force N_{Ed} should satisfy:

$$\frac{N_{Ed}}{\chi N_{plRd}} \leq 1.0 \quad (2.9)$$

Where: $N_{pl,Rd}$ is the plastic resistance of the composite section.

χ is the reduction factor for the relevant buckling mode.

$$\chi = \frac{1}{\Phi\sqrt{(\Phi^2 - \lambda^{-2})}}$$

$$\Phi = 0.5(1 + \alpha\,(\lambda - 0.2) + \lambda_2) \quad (2.10)$$

For concrete filled tubes of circular cross-section, account is taken of increase in strength of concrete caused by confinement provided that the relative slenderness λ does not exceed 0.5 and e/d < 0.1, where e is the eccentricity of loading given by M_{Ed}/ N_{Ed} and d is the external diameter of the column.

The plastic resistance to compression is calculated from the following expression:

$$N_{pl,Rd} = f_y d + A_c f_{cd}\,(1 + \eta_c\, t/d\, f_y/f_{ck}) \quad (2.11)$$

Where: t is the wall thickness of the steel tube, for members with e = 0 the values $\eta_a = \eta_{ao}$ and $\eta_c = \eta_{co}$ are given by the following expressions:

$$\eta_{ao} = 0.25\,(3 + 2\lambda) \text{ (but 1.0)} \quad (2.12)$$

$$\eta_{co} = 4.9 - 18.5\lambda_2 + 17\lambda_2 \text{ (but 0)} \quad (2.13)$$

For high strength concrete with f_{ck} > 50 MPa, the effective compressive strength of concrete accordance with EC2 (EN 1992-1-1, 2004) is determined by multiplying the characteristic strength by a reduction factor η as given below.

$$\eta = 1.0 - (f_{ck} - 50)/200 \quad (2.14)$$

The relative slenderness λ for the plane of bending being considered is given by:

$$\lambda = \sqrt{\left(\frac{Np1RK}{Ncr}\right)} \quad (2.15)$$

Ncr is the elastic critical normal force for the relevant buckling mode, calculated with the effective flexural stiffness $(EI)_{eff.}$

Where, K_e is a correction factor that should be taken as 0.6.

I_a, and I_c are the second moments of area of the structural steel section, the un-cracked concrete section for the bending plane being considered.

2.7.3 Australian Standard (AS4100) Code

In AS4100 code, the formula for calculating the ultimate load in the limit states design format with load factors and capacity reduction factors. This code didn't take the concrete confinement into consideration. The limiting thickness of steel tube to prevent local buckling is based on achieving yield stress in a hollow steel tube under monotonic axial loading which is not a necessary requirement for an in-filled composite column. The strength of a composite column is computed as for reinforced concrete members. The expression for equivalent stiffness includes a creep factor, and cracked concrete stiffness is considered. Minimum eccentricities are specified to cover construction tolerances. The following sections briefly introduce the concerned strength provisions for the concrete filled steel tubular columns as recommended in these codes.

Concrete stresses and steel stresses can be determined using the stress-strain relationships for the concrete (non-linear) and the steel (linear-elastic plastic) respectively using the value of the axial strain ε_a. The axial force N resulting from the application of an axial strain ε_a to both the concrete and the steel is given by

$$N = \sigma_c A_c + \sigma_s A_s \tag{2.16}$$

The concrete stress σ_c is a non-linear function of the strain ε_a where

$$\sigma_c = f(\varepsilon_a) \tag{2.17}$$

The steel stress σ_s is a simple linear function of the strain ε_a where the steel is either elastic with an elastic modulus E_s of 200,000 MPa, or plastic with a yield stress of f_{sy}. To determine the ultimate strength N_{uo} in axial compression, the strain ε_a can be increased until the axial force N given by Eq. (1) reaches a maximum. This process is indicated where the axial force behavior for the composite reinforced concrete section is compared with the corresponding stresses in the steel and concrete that make up the composite section. The strain corresponding to the ultimate strength N_{uo} in axial compression is defined as ε_{uo}.

When the yield strain ε_{sy} of the steel is less than the strain ε_o (= 0.0022) at the maximum strength of $0.85f_c'$ for the concrete (i.e. the steel yields before the concrete has reached its maximum strength), the ultimate strength N_{uo} in axial compression is simply given by,

$$N_{uo} = 0.85f_c' A_c + f_{sy} A_s \tag{2.18}$$

This will be the case for 400Y grade rebar having a yield stress f_{sy} = 400 MPa with a yield strain ε_{sy} = 0.002 which is less than the strain ε_o (= 0.0022) at the maximum strength of $0.85f_c'$ for the concrete. The ultimate strength N_{uo} in axial compression is reached at a

strain ε_{uo} = 0.0022. This is reflected in clause 10.6.3 of AS3600-1994 where N_{uo} can be calculated assuming a uniform concrete compressive stress of $0.85f_c^{/}$ and a maximum strain in the steel and concrete of 0.002 (which is approximately equal to 0.0022).

About 10 - 15% of the concrete segment is reduced to account for the uncertainties of this code. In other words, the compression composite members are considered as regular reinforced concrete in this code. To account for local buckling of the structural steel tube, a limiting thickness is specified and, not to be exceeded. The magnitude of this thickness is based on the achievement of yield stress in the empty steel tube when subjected to axial monotonic loading. Moreover, these formulas do not differentiate between different cross-sectional shapes.

2.8 Conclusions

From the past researches described in this chapter, it can be summarized that extensive experimental investigation were carried out on load bearing capacity and mode of failure of CFST columns. Maximum numbers of experiments were done by CFST columns built with hot rolled section. Limited experiment has been carried out on evaluating different type of eccentricity, different steel section, percentage of steel fiber, length variations, capacity and failure behavior of fibered CFST columns with buildup section simultaneously. But there was no study on the behavior and capacity of the CFST columns of buildup section infilled with concrete and addition of GI wire fiber. Experimental study on compressive behavior of CFST columns with GI fiber, different steel percentages and concrete strength are required. Moreover, different types of variations including eccentricity, strength, thickness, specimen dimension also requisite for predicting accurately the behavior of CFST columns with and without GI fiber under various combinations of geometric and materials properties. Three design code predicted capacities were also calculated and compared with the experimental capacities of the individual CFST column specimens.

CHAPTER 3
EXPERIMENTAL INVESTIGATION

3.1 General

In this study, an experimental research was carried out to investigate the effect of GI wire fiber in CFST columns. The main variables considered in the test program were percentage (%) of GI fiber, concrete compressive strength, size of columns, structural steel tube thickness and loading conditions. These columns were constructed with built-up section of the steel. The peak loads, failure behavior, comparison of ultimate capacity of fibered and plain CFST columns were examined for concentric and eccentric axial compressive load. These tests were performed in the Solid Mechanics Laboratory of Bangladesh University of Engineering and Technology (BUET) and Military Institute of Science & Technology (MIST) jointly. The description of the test specimen, inclusion of GI fiber, test setup, loading condition and results obtained are presented in the following sections.

3.2 Description of Test Specimens

Total twenty-nine (29) square shaped CFST columns were tested in this study. Out of these, seventeen (17) long columns were 1000 mm in length. Others five (5) and seven (7) stub columns were 375 mm and 300 mm in length, respectively. These columns were constructed with three different sizes (100 x 100 mm, 125 x 125 mm and 150 x150 mm). Among these, twelve (12) long and six (6) stub columns were constructed with 2.5 % of GI wire (weight basis). From the long columns, eleven (11) were tested under concentric axial load and (06) columns under eccentric axial loading. Thickness of structural steel shape in CFST columns were 4 and 5 mm. All the columns are constructed with concrete compressive strength ($f_c^{/}$) of 20, 30 and 40 MPa. All the stub columns were tested under concentric axial loading. Figure 3.1 shows the detail the elevation and cross section of a typical square CFST column. Two types of loading were used to investigate the capacity of plain and GI wire fibered concrete. Detail geometric and material properties of these columns are shown in Table 3.1, Table 3.2 and Table 3.3, respectively.

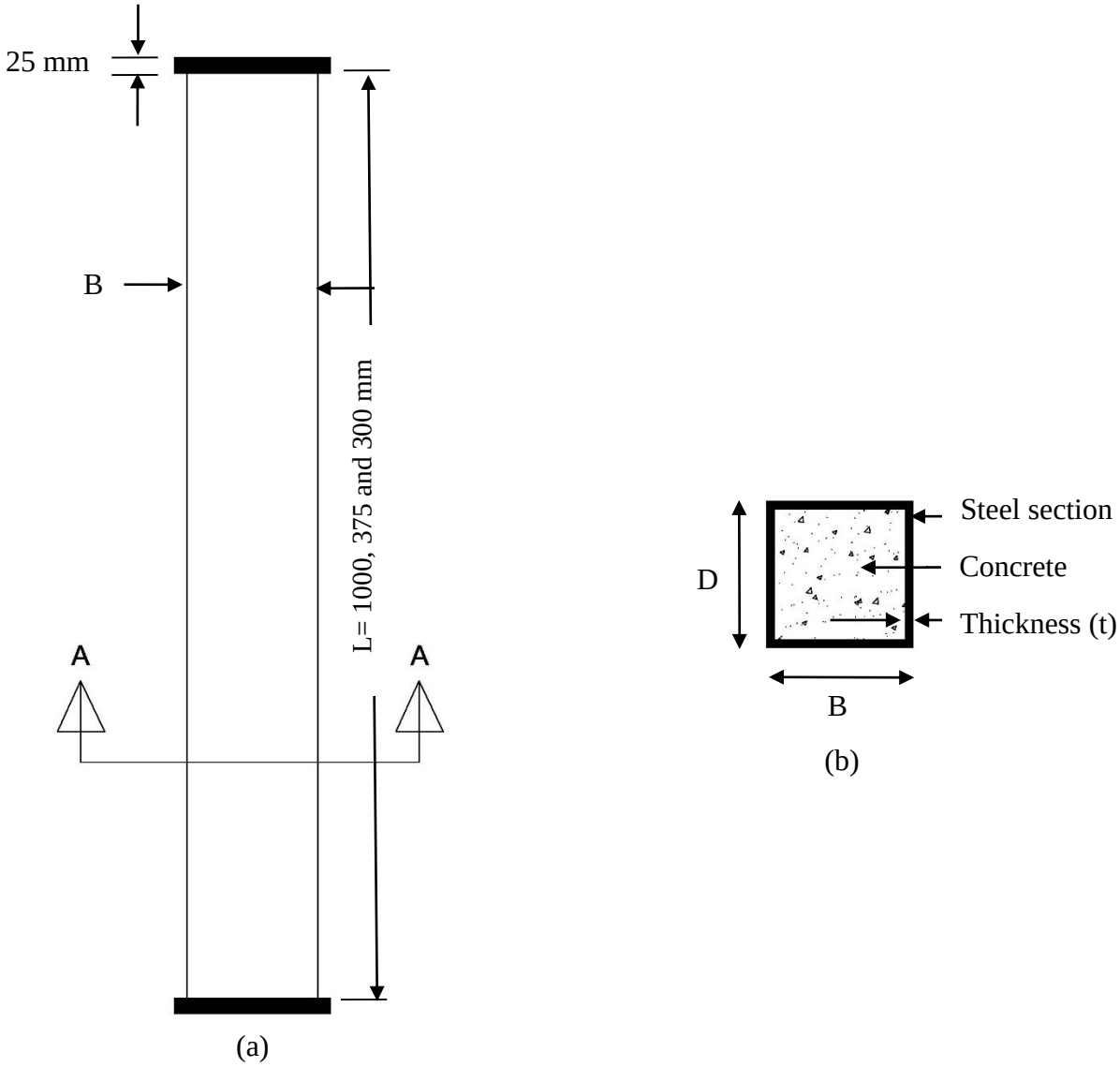

Figure 3.1 Geometry of CFST columns (a) Elevation (b) Section A-A

Table 3.1 Geometric Properties of Test Specimens (Long column)

Ser	Specimen Designation	Steel Section (B x D)	Thickness (t)	Cross section slenderness	Global slenderness	Steel Percentage
		(mm× mm)	(mm)	B/t	L/B	(%)
1	SST-100-20-5-2.5	100 x 100	5	20	10	20
2	SST-100-30-5-2.5	100 x 100	5	20	10	20
3	SST-125-20-5-2.5	125 x 125	5	25	8	16
4	SST-125-30-4-2.5	125 x 125	4	31.25	8	12.8
5	SST-125-30-5-2.5	125 x 125	5	25	8	16
6	SST-150-20-4-2.5	150 x 150	4	37.5	6.67	10.67
7	SST-150-30-4-2.5	150 x 150	4	37.5	6.67	10.67
8	SST-150-40-4-2.5	150 x 150	4	37.5	6.67	10.67
9	SSTE-125-40-5-2.5	125 x 125	5	25	8	16
10	SSTE-125-40-4-2.5	125 x 125	4	31.25	8	12.8
11	SSTE-150-40-4-2.5	150 x 150	4	37.5	6.67	10.67
12	SSTE-150-20-4-2.5	150 x 150	4	37.5	6.67	10.67
13	SSTE-100-30-5-0	100 x 100	5	20	10	20
14	SSTE-125-40-4-0	125 x 125	4	31.25	8	12.8
15	SST-100-30-5-0	100 x 100	5	20	10	20
16	SST-125-20-4-0	125 x 125	4	31.25	8	12.8
17	SST-125-40-4-0	125 x 125	4	31.25	8	12.8

Table 3.2 Material Properties of Test Specimens (Long column)

Ser	Specimen Designation	Concrete compressive strength $f_c^{/}$	Steel yield strength f_y	Percentage of fiber (%)
		(MPa)	(MPa)	%
1	SST-100-20-5-2.5	38	345	2.5
2	SST-100-30-5-2.5	47	345	2.5
3	SST-125-20-5-2.5	38	345	2.5
4	SST-125-30-4-2.5	47	345	2.5
5	SST-125-30-5-2.5	47	345	2.5
6	SST-150-20-4-2.5	38	345	2.5
7	SST-150-30-4-2.5	47	345	2.5
8	SST-150-40-4-2.5	53	345	2.5
9	SSTE-125-40-5-2.5	53	345	2.5
10	SSTE-125-40-4-2.5	53	345	2.5
11	SSTE-150-40-4-2.5	53	345	2.5
12	SSTE-150-20-4-2.5	38	345	2.5
13	SSTE-100-30-5-0	35	345	0
14	SSTE-125-40-4-0	44	345	0
15	SST-100-30-5-0	35	345	0
16	SST-125-20-4-0	27	345	0
17	SST-125-40-4-0	44	345	0

Table 3.3 Geometric Properties of Test Specimens (Stub columns)

Ser	Specimen Designation	Size (B x D)	Length (L)	Thickness (t)	Percentage of fiber (%)
		(mm)	(mm)	(mm)	
1	SC-100-20-4-2.5	100x100	300	4	2.5
2	SC-100-20-5-2.5	100x100	300	5	2.5
3	SC-100-30-5-2.5	100x100	300	5	2.5
4	SC-100-40-5-2.5	100x100	300	5	2.5
5	SC-125-20-4-2.5	125x125	375	4	2.5
6	SC-125-20-5-2.5	125x125	375	5	2.5
7	SC-100-20-4-0	100x100	300	4	0
8	SC-100-30-4-0	100x100	300	4	0
9	SC-100-30-5-0	100x100	300	5	0
10	SC-125-20-5-0	125x125	375	5	0
11	SC-125-20-4-0	125x125	375	4	0
12	SC -125-30-5-0	125x125	375	5	0

3.3 Explanation of Columns Designation

In this study, the tested parameters were the inclusion of GI fiber (%), concrete strength ($f_c^{/}$), thickness of steel tube (t), cross section (B x D), percentage of steel fiber and eccentricity ratio (e/B). The CFST columns were numbered as SST-100-30-4-0. The 'SST' means square steel tubular column; 'SC' means stub column; '100' is for size of the steel tube whether 100, 125 or 150 mm. Then '30' stands for concrete strength either 20, 30 or 40 MPa; '4' means thickness of steel tube either 4 or 5 mm. The last one is for percentage of fiber; 0 means the normal concrete and 2.5 means concrete with 2.5% of fiber content (weight basis). On Table 3.2 also shows the width to cross sectional slenderness ratio (B/t) and the global slenderness ratio (L/B) i.e. the length to width ratio. All specimens were designed to examine the behavior of CFST columns under concentric and eccentric loads.

3.4 Fabrication of CFST Columns

The composite column consists of two parts. The square shaped steel tube section and the concrete. Two U channels were welded to construct CFST steel tube columns. The steel sections were fabricated by McDonald Steel Ltd, Dhaka. Figure 3.2 shows the sequences for the construction CFST columns. Then fillet welding was done to join U channel and steel plate continuously. The thickness of the steel tube was measured by screw gauge at

four places and the average value was considered. The width was measured by slide calipers. After fabricating the box column, a 25 mm thick steel plate was welded at each end by continuous welding. The concrete then poured in the box column. When the concrete was hard then another side of the columns was welded by continuous welding again. Finally, these columns were prepared for testing. End plates were used with each specimen to apply uniform distributed load during experimental test.

(a)

(b)

(c)

(d)

Figure 3.2 CFST column sample making (a) 3-D view of column tube (b) Welding of end plate (c) Final sample after construction (d) Sample stack

3.5 Specification of GI Wire for Fibred Concrete

Generally, GI wire is used to fixing stirrup with main longitudinal or horizontal reinforcement in construction works. There are many types of GI wire ranges from #8 (Φ = 3.264 mm) to #26 (Φ = 0.4049 mm) available in Bangladesh. In this study, GI wire was used to improve the strength of concrete filled steel tube with low cost consideration for construction. From the past research, it was proved that adding steel fiber could improve

the properties of concrete such as tensile strength, impact resistance durability, toughness, and fire resistance. In this study, locally used # 21 (Φ = 0.7230 mm) GI wire was used, those were available in market. There were some specifications to use this type of fiber in concrete. These specifications consist of length, diameter, aspect ratio etc. According to ACI 544.3R, the length of steel wire fiber to be used in fiber reinforced concrete generally varies between 0.5 inch (12.7 mm) to 2.5 inch (63.5 mm) and the common fiber diameter are in the range of 0.017 inch (0.45 mm) to 0.04 inch (1.0 mm). For this experiment, the length of GI wire 1.5 inch (38.10 mm) of diameter 0.723 mm was taken as average value. The making procedure of GI fiber sample is shown in Figure 3.3. It was an austenitic chromium-nickel-manganese stainless steel which was developed to conserve nickel.

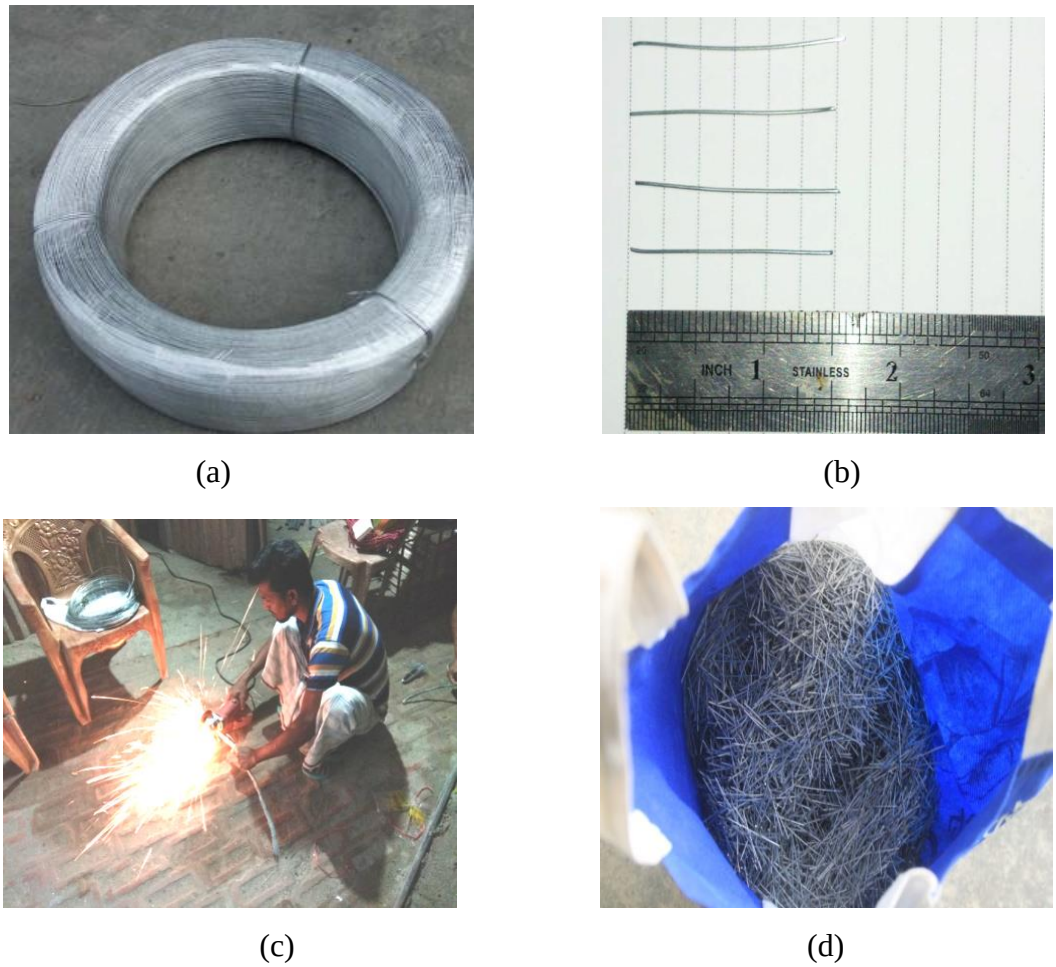

(a) (b)

(c) (d)

Figure 3.3 (a) GI wire coil (b) Cutting length @ 1.5″ (c) GI wire cutting (d) Cutting stack of GI wire

3.6 Preparation of Concrete

Three different concrete strength grades of 20 MPa, 30 MPa and 40 MPa were considered in this experimental study. The concrete was made with locally available materials. The mixtures were made with Portland limestone cement of brand- Seven Ring Gold Cement (CEM-I/BDS EN 197-1:2003, 52.5 N), fine aggregate (sand) of F.M. - 2.5, ½ inch (10 mm) coarse aggregate (stone chips) and ¾ inch (20 mm) downgrade size of crushed stone. The mix designs according to ACI guideline (ACI 211.1-91) for plain and fiber reinforced concrete are shown in Table 3.4. The GI fiber was added to the mix at ratio of 2.5% (weight basis) of the total weight of cement and all aggregates. Coarse aggregates were being fully saturated before mixing. All the raw materials were weighted and batched as per the Table 3.4. An electrically operated mechanical mixer of revolving type drum was used for mixing the concrete. The purpose of mechanical mixing was to produce an intimate mixture of cement, water, fine and coarse aggregate of uniform consistency throughout each batch. To determine concrete strength, compressive strength test of total fifty-four (54) number of concrete cylinders was performed.

Table 3.4 Concrete mix design

Concrete Strength	Cement (OPC) **(1)**	Fine aggregate **(2)**	Coarse aggregate **(3)**		Total weight **(1+2+3)**	2.5% of GI wire (by weight)	Water	w/c ratio
			¾" Black stone	½" Black stone				
	Kg/m^3	Kg/m^3	Kg/m^3	Kg/m^3	Kg/m^3	Kg/m^3	Kg/m^3	
20 MPa (M20)	320	712	825	353	2210	55.25	176	0.55
30 MPa (M30)	385	732	719	308	2144	53.60	181	0.47
40 MPa (M40)	435	695	698	300	2128	53.20	183	0.42

3.7 Properties of the Steel Tube

The concrete filled steel tube consists of buildup steel section and concrete. To determine steel section's property, the coupon test was performed. All the plates used in sections were cut from the same steel plate. The yield strength of the steel plates was determined through coupon test of structural steel. The tensile test of the steel plates was performed according to ASTM D638-02a (2003) in the Solid Mechanics laboratory of Military Institute of Science & Technology (MIST) shown in Figure 3.4. The result of the coupon test is given in Table 3.5. All the steel columns were constructed with built up sections. According to

the specification, all the sections were found to be compact section. The mean value of yield stress (f_y) and ultimate stress (f_u) was found 341 MPa and 494 MPa, respectively from the tensile coupon test.

(a)

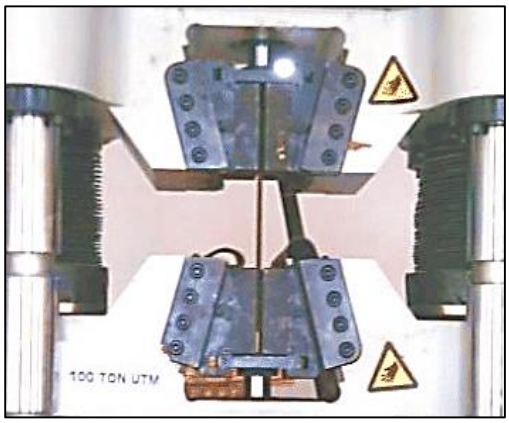

(b)

Figure 3.4 (a) Steel coupon before test (b) Tensile test on UTM

Table 3.5 Tensile properties of steel tube coupon sample

Coupon no.	Yield stress (f_y)	Ultimate stress (f_u)	Elastic modulus (E_s)	Yield Strain (ε_y)	Ultimate Strain (ε_u)
	(MPa)	(MPa)	(GPa)	(με)	(με)
CN 1	341	503	196	2150	27167
CN 2	340	461	192	2148	25167
CN 3	348	519	204	2146	33159
CN 4	352	533	207	2149	28416

3.8 Compressive Test of Concrete Cylinder

Total fifty-four (54) concrete cylinders (4″ x 8″) were prepared for determining the compressive strength. There were three different strength of concrete cylinder of 20, 30 and 40 MPa with and without incorporating 2.5% of GI fiber. After twenty-four hours of casting, all cylinders were removed from molds and kept in the water. Three concrete cylinders from each mix were brought out from the water after 7 days. The other six concrete cylinders were brought out after 28 days. The samples making and samples after test were shown in Figure 3.5.

All cylinders were capped with a high strength capping compound prior to testing to ensure uniform bearing in the testing machine. Cylinders were tested in the concrete Materials Laboratory at MIST. Average compressive strength of these cylinders (M20, M30 and M40) after 7 days and 28 days were found (Table 3.6).

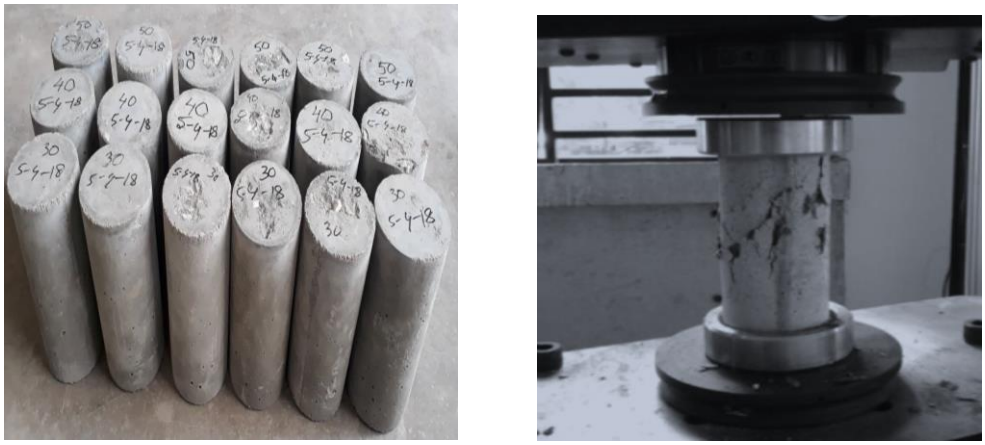

(a) (b)

Figure 3.5 (a) Concrete cylinder making (b) cylinder for 28-day test

Table 3.6: Compressive Strength of cylinder with and without 2.5% GI fiber

Concrete strength	7 days strength		28 days strength			
	without G.I. Wire (MPa)	with G.I. Wire (MPa)	without G.I. Wire (MPa)	% of strength increase	with G.I. Wire (MPa)	% of strength increase
20 MPa	12	15	27	-	38	-
30 MPa	23	29	35	30%	47	24%
40 MPa	27	35	44	63%	53	39%

3.9 Preparation of CFST Columns

All concrete was produced in the batching facility of the concrete laboratory at the Military Institute of Science & Technology (MIST). The main concern during the mix design were strength and workmanship. Total seventeen (17) of long column and twelve (12) stub columns were casted at Military Institute of Science & Technology. Mix design was completed according to the ACI standard (ACI 211.1-91). The slump values of 75 mm to 100 mm. The empty steel tube kept vertical with one sided welded joint plate for placing concrete. The tube was placed on a smooth plain surface. Concrete was poured into the steel tube from top. The concrete was compacted by an electrical needle vibrator. The concrete was poured into three layers. Each layer was vibrated individually. Such type of compaction need to prevent honeycomb, ensure more impermeable and dense concrete. All the process is presented in Figure 3.6.

(a)

(b)

(c)

(d)

(e)

(f)

Figure 3.6 (a) Concrete mixer (b) Concrete batch (c) Concrete casting and vibration (d) CFST column after casting (e) Designation of sample (f) Sample stack

3.10 Testing Setup and Data Acquisition System

This experimental investigation was carried out in BUET and MIST jointly. The apparatus used to test the seventeen (17) long and twelve (12) stub CFST columns, comprised an Instron 2000 kN Universal Testing System (UTS) machine, steel knife-edges each of 82

mm thickness with a maximum rotation of 10° to provide pin-ended conditions in the intended axis of buckling and fixed conditions in the other cross-sectional axis, Linear Variable Differential Transducer (LVDT) at mid-height to measure lateral deflections of the columns at ultimate load under eccentric load as shown in Figure 3.7.

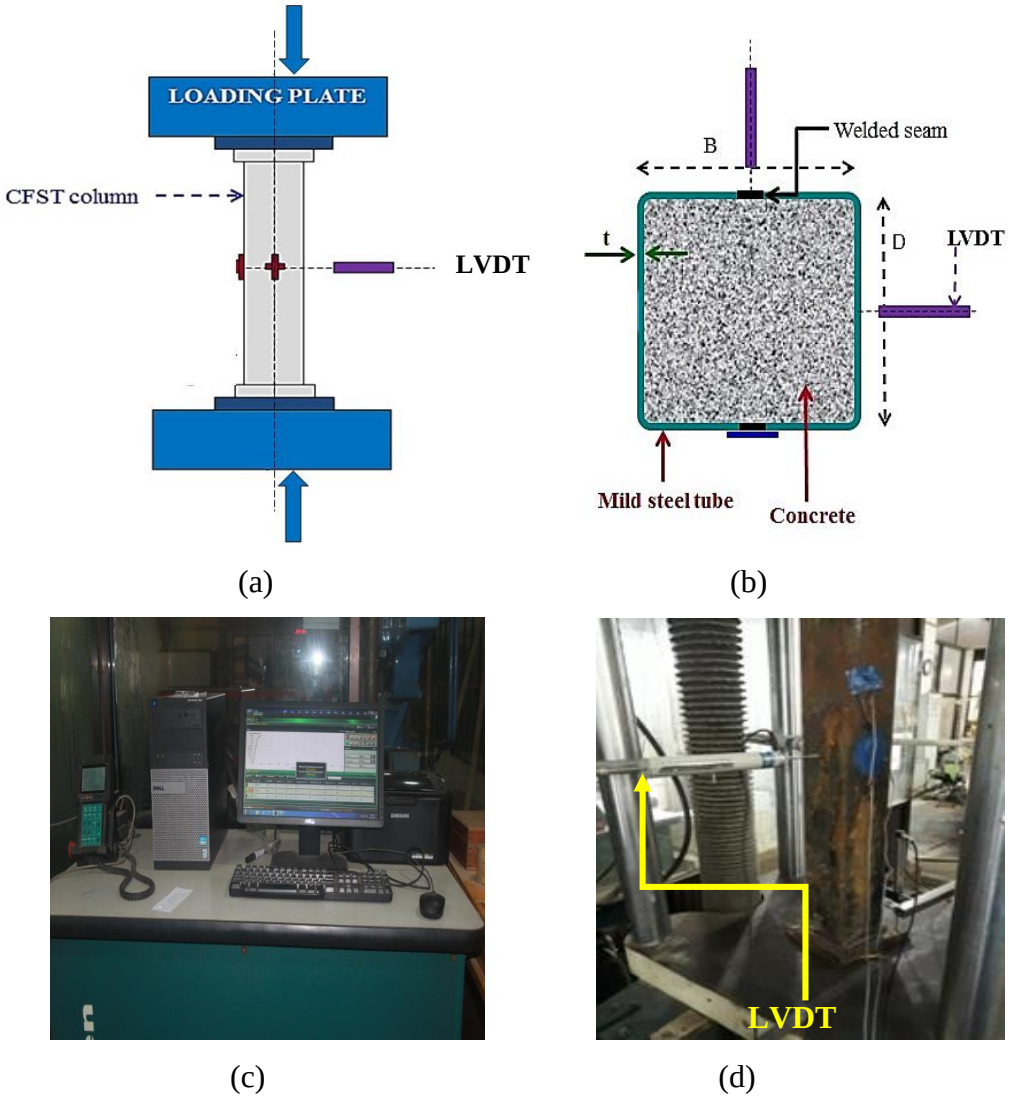

Figure 3.7 (a) Elevation of UTM setup (b) Cross section of the specimen (c) Data acquisition system (d) Location of LVDT and Strain gauge

On of the opposite sides, the two LVDTs were fixed. This setup was also consisting of HORIZON data acquisition equipment and data recording software. The UTS instruments were frequently calibrated and verified according to a regular schedule. Real-time graphs of the key data were displayed during loading to assist in controlling the tests. The set-up is shown in Figure 3.8. The end plates of the testing apparatus were fixed flat and parallel. Two LVDTs were used to determine the end shortening of the columns between the end-

plates of the testing machine. After securing the column in the rig, fixing the end-plates and attaching the measuring equipment, the hydraulic loading machine was set to displacement control at a rate of 0.2 mm/min for columns of 1 m.

The test specimens were then loaded using the hydraulic jacks. Testing continued beyond the attainment of ultimate load and was stopped when the column had undergone at least 50 mm of lateral deflection at mid- height, thus enabling a considerable portion of the unloading behavior of the specimens to be captured. Laboratory safety regulations do not permit personnel near the UTS while it is operating, so a stationary digital camera with a zoom lens was placed at the safe periphery of the test area and was used to take photographs of the specimens during the tests.

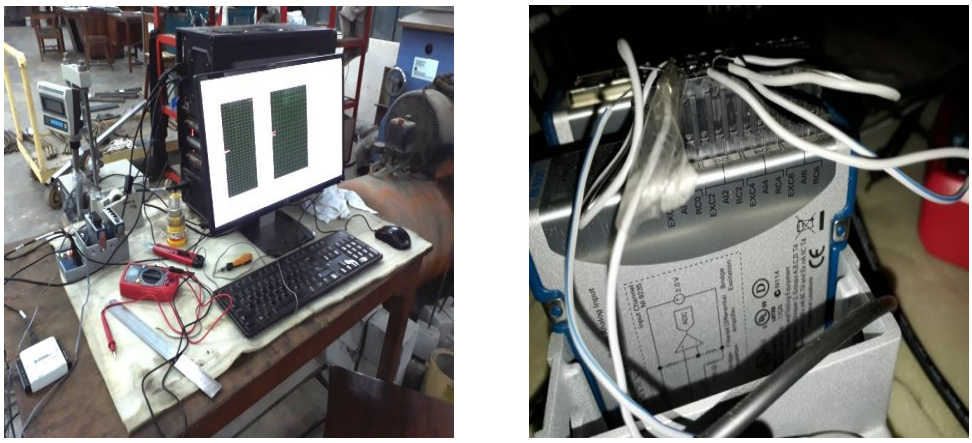

(a) (b)

Figure 3.8 (a) Computerized Data logging system (b) Digital data logger

3.10.1 Setup and instrumentation of concentrically loaded CFST column

Total eleven (11) long columns and twelve (12) stub were tested for concentrically axial load. In every column, plates are welded at the both top and bottom side of the column as shown in Figure 3.9. The columns were tested in Solid Mechanics laboratory of BUET. The column was so placed in the UTS to provide uniform bearing and a fixed end condition. First, the specimen was centered underneath the UTS actuator. Second, the column was aligned vertically. Third, the column height was so adjusted to facilitate the concentric loading. Before starting loading, a sufficient gap between column top and machine had provided. Considering all types of effects including failure of columns, a uniform stroke rate of 0.2 mm/ min was used throughout the loading in columns.

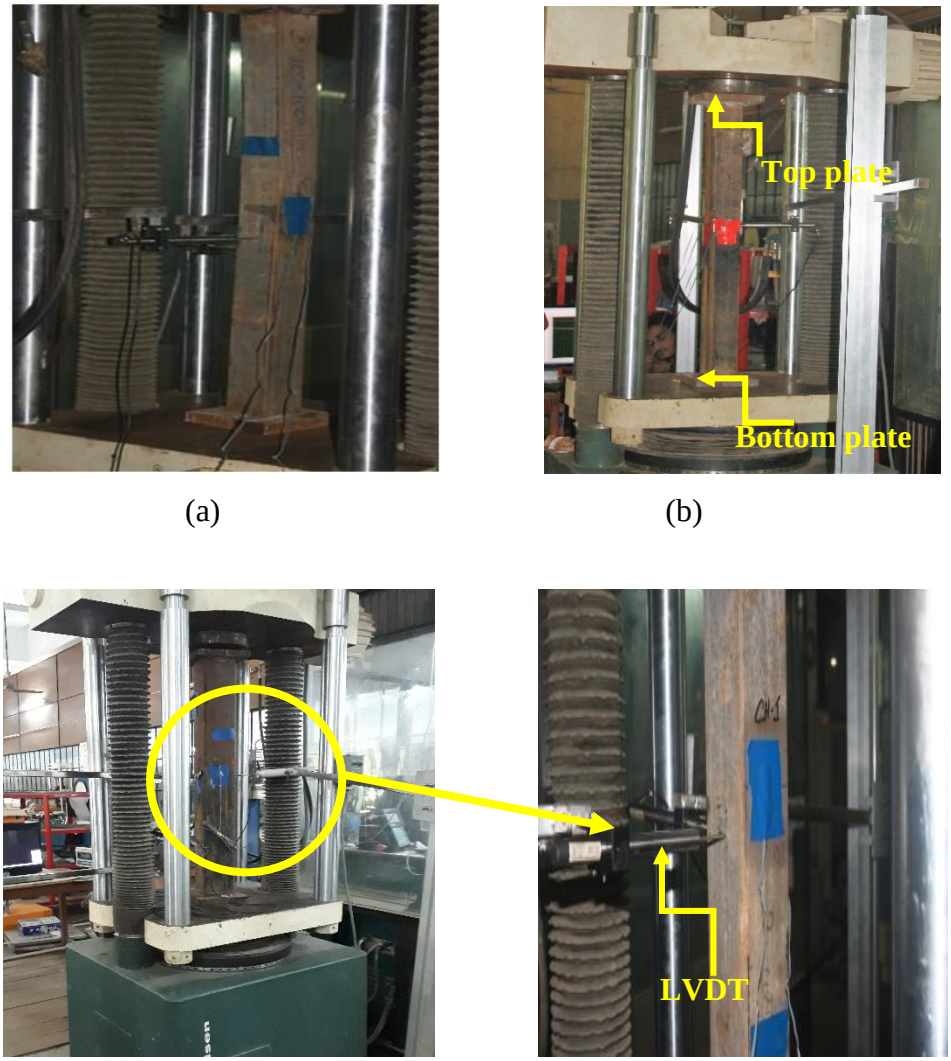

(a) (b)

(c) (d)

Figure 3.9 (a) Setup of concentrically loaded column (b) Location of top and bottom plate (c) and (d) Location of LVDT

3.10.2 Setup and instrumentation of eccentrically loaded CFST column

Total six (6) long columns were tested for eccentrically axial load in this experiment. A special arrangement was used to apply eccentric load on the test specimen. The setup is called Knife edge joint arrangement. The details of this setup and working procedure is described in below section.

3.10.2.1 Knife edge arrangement

Knife edge arrangement is a comparatively new addition to apply eccentric load on the test specimen (Figure 3.10). This setup creates a line load across the line from center of the specimen to the required distance i.e. concerned eccentricity. The picture of the setup and application on the specimen is shown Figure 3.11, Figure 3.12 and Figure 3.13. Considering all types of effects including failure of columns, a uniform stroke rate of 0.2 mm/ min was used throughout the loading in columns.

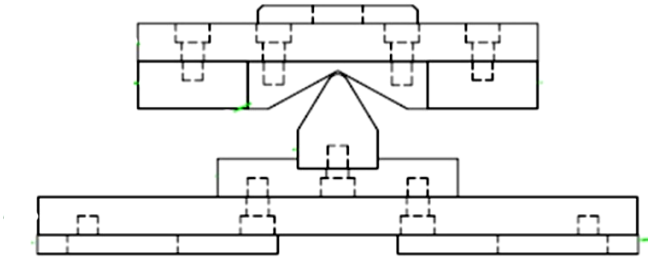

(a)

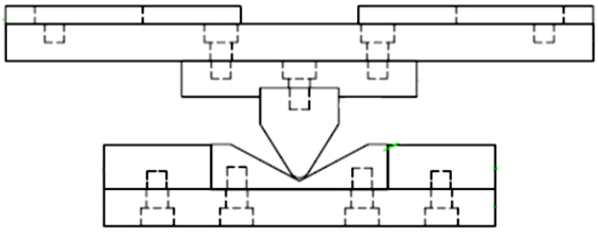

(b)

Figure 3.10 (a) Assemblage of top (b) bottom knife edge

Figure 3.11 Assemblage of knife edge

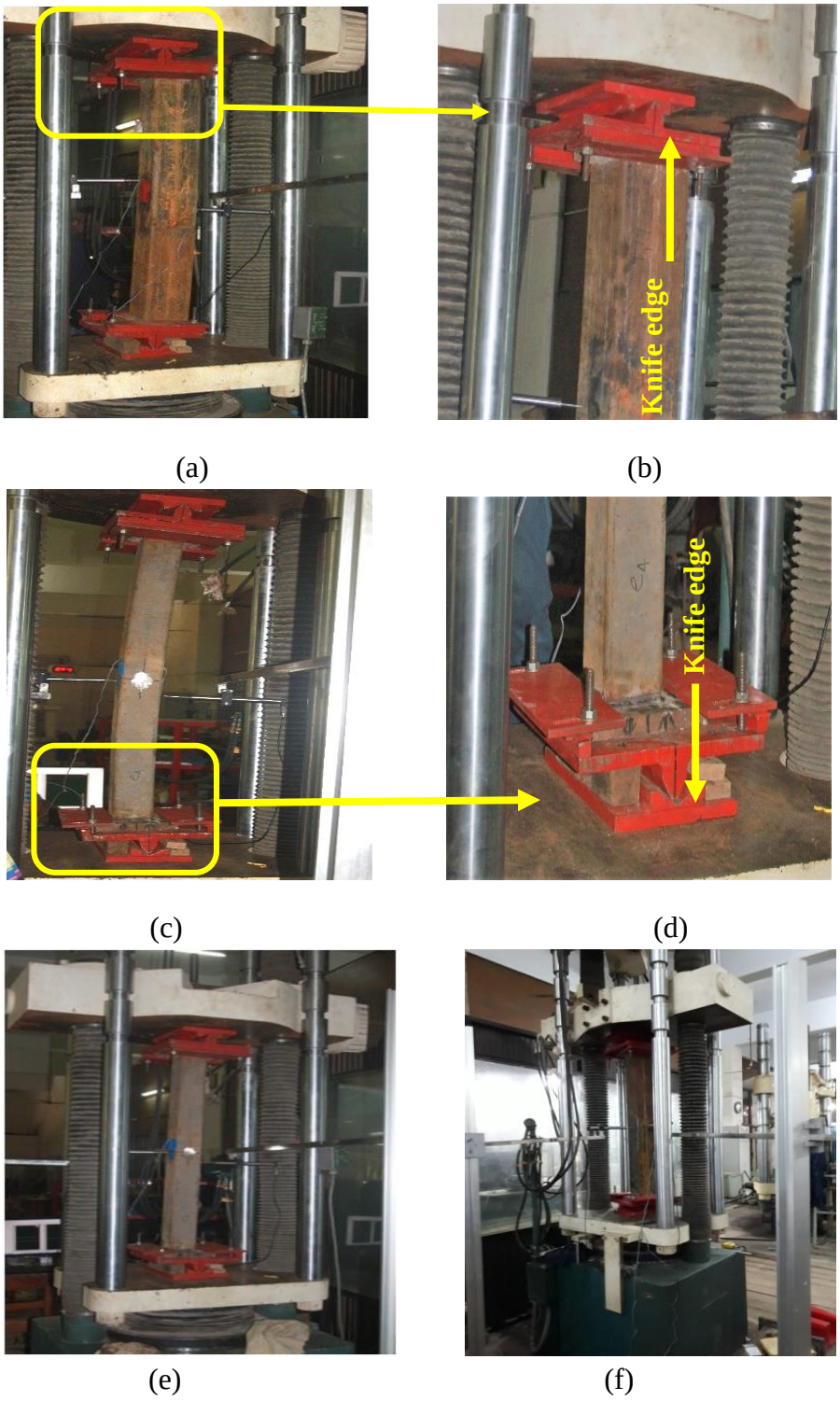

Figure 3.12 (a-d) Knife edge joint top and bottom connection
(e) and (f) Setup of eccectrically loaded columns

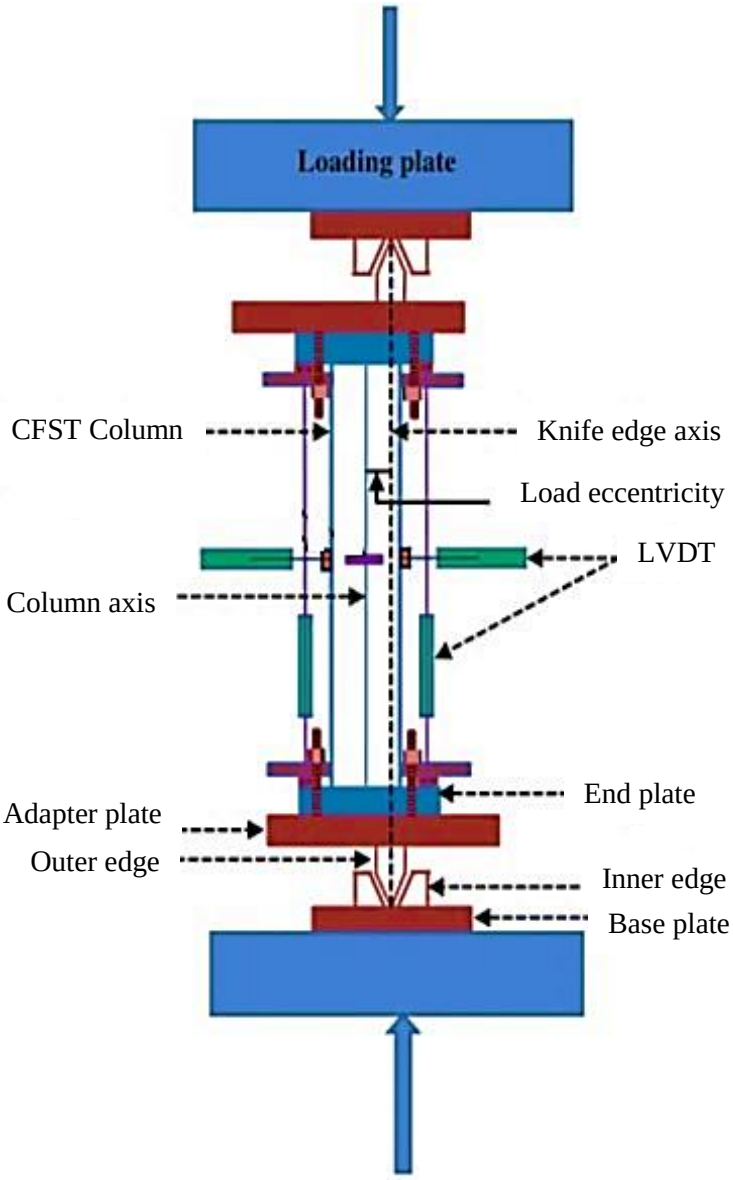

Figure 3.13 Arrangement of knife edge joint with test specimen in UTM

3.11 Setup and Instrumentation of Concentrically Loaded Stub Column

Total twelve (12) stub columns were tested under concentrically axial load. In every column, plates are welded at the both top and bottom side of the column as shown in Figure 3.13. The column was so placed in the UTM to provide uniform bearing and a fixed end condition. First, the specimen was centered underneath the UTM actuator. Second, the column was aligned vertically. Third, the column height was so adjusted to facilitate the concentric loading. Before starting loading, the same process was followed to provide stroke of load throughout the loading period with considering all type of effect. Here no LVDT was used; the ultimate load carrying capacity and axial deformation was calculated from the UTM reading.

(a) (b)

Figure 3.14 (a) Setup of concentrically loaded stub columns (b) sample stuck after test

3.12 Conclusions

In this chapter, the whole experimental system, properties of test specimens and concrete, process of inclusion of GI wire, preperation of concrete and the testing process was desribed. The columns were tested both concentrically and eccentrically to measure the bearing capacity, observe the failure modes and then finally compared the experimental capacity with the code predicted capacity.

CHAPTER 4
TEST RESULT AND DISCUSSION

4.1 General

The investigational program has been carried out to explore the effect of addition of GI wire fiber on compressive strength, ductility index, lateral deflection and failure modes of concrete filled steel tubular columns under concentric and eccentric axial compression loading in this study. The effect of fiber content on the loading eccentricity, cross sectional dimension of the column and wall thickness of the CFST columns was also examined. The fiber influenced the overall structural behavior, failure pattern and ultimate load carrying capacity of concrete filled steel tubular column. Axial load, axial deformation and mid-height deflection was obtained both for the long and stub columns. The ductility index was also determined to observe the performance and behavior of CFST columns due to inclusion of GI wire fiber. All the results obtained from the experimental investigation were prepared and presented to highlight the effect of GI wire fiber on the individual parameters of CFST columns.

4.2 Experimental Result

The experimental capacity and the failure mode for long and stub concrete filled steel tubular columns contained with and without GI fiber that were loaded both concentrically and eccentrically, found from the experiment. The columns failed in this test mainly due to buckling of steel plate followed by infilled concrete crushing and yield of steel tube. In some cases, failure occurred at the welding joint. For concentric load, the columns were failed with global and local buckling both at middle and end section, with some columns of welding failure. For eccentric loading, the columns were generally failed with global failure. Shear bands were also observed to develop along the height of the concrete-filled stub columns.

Experimental capacity of total seventeen (17) long columns and twelve (12) stub columns were listed in Table 4.1 and 4.2, respectively. Among these columns, total twelve (12) long columns and six (6) stub columns were made with GI wire fiber. Eleven (11) long columns and twelve (12) stub columns were tested under concentric loading. Six (6) long columns were tested under eccentric loading.

Table 4.1: Experimental capacity of long columns

Ser	Column designation	Cross section slenderness	Global slenderness	Eccentricity ratio	Experimental capacity
		(B/t)	(L/B)	(e/B)	(kN)
1	SST-100-20-5-2.5	20	10	0	890
2	SST-100-30-5-2.5	20	10	0	951
3	SST-125-20-5-2.5	25	8	0	1209
4	SST-125-30-4-2.5	31.25	8	0	1082
5	SST-125-30-5-2.5	25	8	0	1310
6	SST-150-20-4-2.5	37.5	6.67	0	1290
7	SST-150-30-4-2.5	37.5	6.67	0	1359
8	SST-150-40-4-2.5	37.5	6.67	0	1481
9	SSTE-125-40-5-2.5	25	8	0.3	857
10	SSTE-125-40-4-2.5	31.25	8	0.3	734
11	SSTE-150-40-4-2.5	37.5	6.67	0.3	893
12	SSTE-150-20-4-2.5	37.5	6.67	0.3	710
13	SSTE-100-30-5-0	20	10	0.3	602
14	SSTE-125-40-4-0	31.25	8	0.3	614
15	SST-100-30-5-0	20	10	0	865
16	SST-125-20-4-0	31.25	8	0	1009
17	SST-125-40-4-0	31.25	8	0	1058

Table 4.2: Experimental capacity of stub columns

Ser	Column designation	Cross section slenderness	Global slenderness	Eccentricity ratio	Experimental capacity
		(B/t)	(L/B)	(e/B)	(kN)
1	SC-100-20-5-2.5	20	3	0	960
2	SC-100-30-5-2.5	20	3	0	1051
3	SC-100-40-5-2.5	20	3	0	1152
4	SC-125-20-4-2.5	31.25	3	0	1071
5	SC-125-20-5-2.5	25	3	0	1392
6	SC-125-30-5-2.5	25	3	0	1523
7	SC-100-20-4-0	25	3	0	727
8	SC-100-30-4-0	25	3	0	785
9	SC-100-30-5-0	20	3	0	945
10	SC-125-20-5-0	25	3	0	1276
11	SC-125-20-4-0	31.25	3	0	1005
12	SC-125-30-5-0	25	3	0	1360

4.3 Load Versus Axial Deformation Relationship

The CFST columns were tested to measure the effect due to the variable parameters i.e. addition of GI fiber, cross sectional slenderness ratio, global slenderness, concrete strength and loading eccentricity under different loading condition with plain concrete and fibered concrete. Experimental results from the research work of Islam (2019) and Ali (2019) conducted in the Department of Civil Engineering, BUET (Annexure-A), were considered for comparing the results in this study. The effects on experimental load and deformation capacity of the columns are described in the following sections.

4.3.1 Effect of GI wire fiber on peak load and deformation capacity

Eight (8) CFST columns consisted of four groups were considered to observe the effect of addition of GI wire fiber. Group 1 consisted of columns of 100 x 100 mm size with 30 MPa concrete and 5 mm tube thickness infilled with and without fiber. Group 2 also consisted of 30 MPa concrete and 5 mm tube thickness infilled with and without fiber (Annexure-A) having 125 x 125 mm size. These above two groups are for long columns. Similarly, Group 3 and Group 4 simulated with the same properties of CFST stub columns. The axial load capacity and deformation of plain and fibred concrete of CFST columns were presented in Table 4.3. Figure 4.1(a) shows the effect of GI wire on axial load and deformation for Group 1 and Group 2 of long columns. Similar result and behavior was observed and showed in Figure 4.1(b) for Group 3 and Group 4. From the result, the load carrying capacity is increased by 10-12% and average deformation capacity is increased about 29-36% for addition of GI fiber in the concrete. This behavior was also verified for the stub column and found similar result.

Table 4.3 Effect of GI wire fiber on peak load and deformation capacity

Group	Column designation	Peak load P_{Exp} (kN)	Load variation (%)	Deformation at peak load (mm)	Deformation variation (%)
Gr-1	SST-100-30-5-0	865	-	8.5	-
	SST-100-30-5-2.5	951	+10%	11	+29%
Gr-2	C6 (125-30-5-0) (Islam 2019)	1169	-	12	-
	SST-125-30-5-2.5	1310	+11%	15.5	+30%
Gr-3	SC-100-30-5-0	945	-	4.5	-
	SC-100-30-5-2.5	1051	+12%	6	+33%
Gr-4	SC-125-30-5-0	1360	-	5.5	-
	SC-125-30-5-2.5	1523	+12%	7.5	+36%

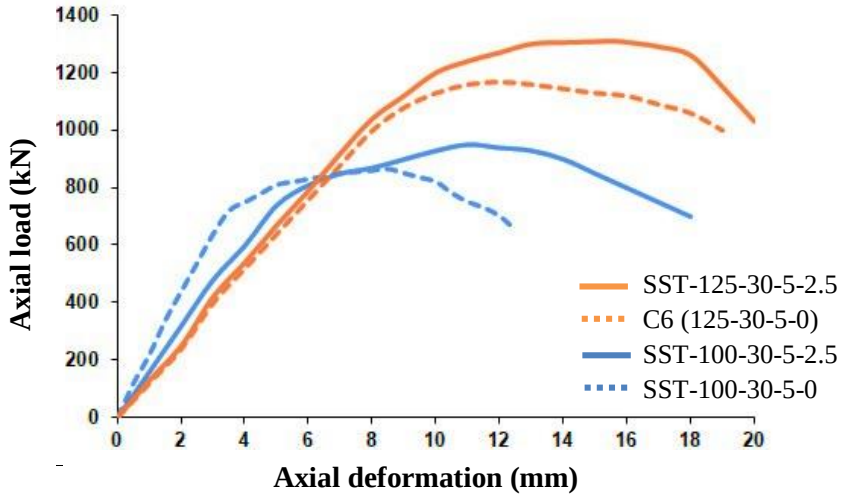

(a)

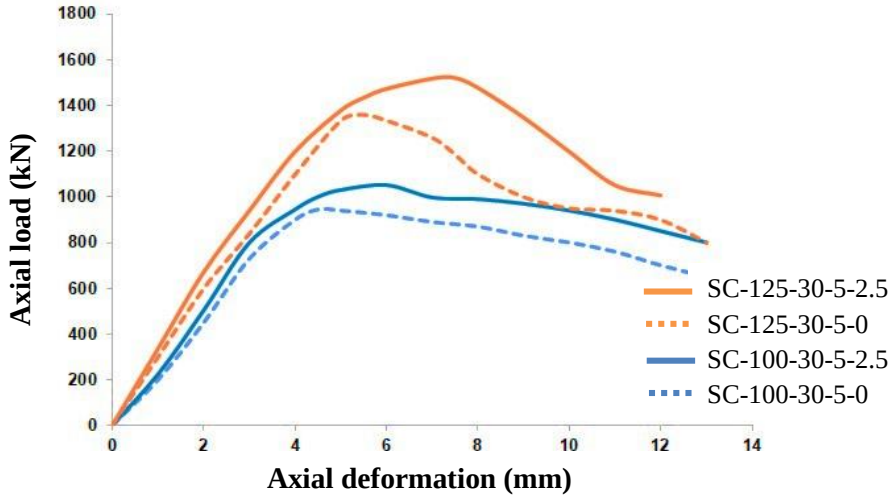

(b)

Figure 4.1 Effect of GI wire fiber on axial load vs axial deformation of (a) long columns (b) stub columns both fibered and plain concrete

From the Figure 4.1, it was observed the due addition of GI fiber increase ultimate load carrying capacity for both long and stub columns and due to transformation of load through the fibers even after the crack developments increases the deformation capacity significantly.

4.3.2 Effect of global slenderness ratio of CFST (L/B)

CFST columns were tested for three different sizes; 100 mm × 100 mm, 125 mm × 125 mm and 150 mm × 150 mm. Eight (8) CFST columns consisted of four groups were considered to observe the effect of GI wire fiber on global slenderness ratio (L/B) as shown in Table 4.4. Group 5 and Group 7 consisted of fibered concrete of long and short column, respectively having concrete of 30 MPa and 5 mm tube thickness. Group 6 and Group 8

consisted of plain concrete of long and short column, respectively having concrete of 20 MPa and 4 mm tube thickness. The increment in cross sectional dimension results in additional flexural resistances to the columns of both for fibered and plain concrete listed in Table 4.4.

Table 4.4 Effect of global slenderness ratio on peak load and deformation capacity

Group	Column designation	L/B	Peak load P_{Exp}	Load variation	Deformation at peak load	Deformation variation
			(kN)	(%)	(mm)	(%)
Gr-5	SST-100-30-5-2.5	10	951	-	11	-
	SST-125-30-5-2.5	8	1310	+38%	14	+27%
Gr-6	C1 (100-20-4-0) (Islam 2019)	10	697	-	8	-
	SST-125-20-4-0	8	1009	+32%	9.75	+22%
Gr-7	SC-100-30-5-2.5	3	1051	-	6	-
	SC-125-30-5-2.5	3	1523	+45%	7.75	+29%
Gr-8	SC-100-20-4-0	3	727	-	5	-
	SC-125-20-4-0	3	1005	+38%	6.5	+25%

From the Table 4.4, load carrying capacity increased by 38% and deformation capacity increased by 27% for decreasing the global slenderness ratio from 10 to 8 for fibered long column of Group 5 shown in Figure 4.2(a). Similarly, the columns of plain concrete i.e. Group 6, the load increment by 32% and deformation capacity increment by 22% shown in Figure 4.2(b). From the Figure 4.2 (a), it was observed that SST-100-30-5-2.5, the linear portion of the Axial load vs. axial deformation curve is steeper than column SST-125-30-5-2.5. For long column, lower dimensions show graph with steeper slope for both fiber and plain CFST columns. Considering the stub columns, the higher dimension shows the steeper slope in load-deformation graph. Increase in size of stub columns for Group 7 and Group 8 also results increment of load carrying capacity and axial deformation capacity by 45 % and 29% for fibered concrete. For the plain concrete, the values were 38% and 25%, respectively (Figure 4.3). Addition of the fiber to the CFST columns, load carrying capacity and axial deformation capacity was increased greater than plain concrete with respect to decrement of global slenderness ratio. As the column gets slender, the axial deformation increases accompanied by a decrease in global slenderness ratio. Moreover, the larger dimension allows more fiber which results to carry more axial load with respect to smaller dimension of CFST columns.

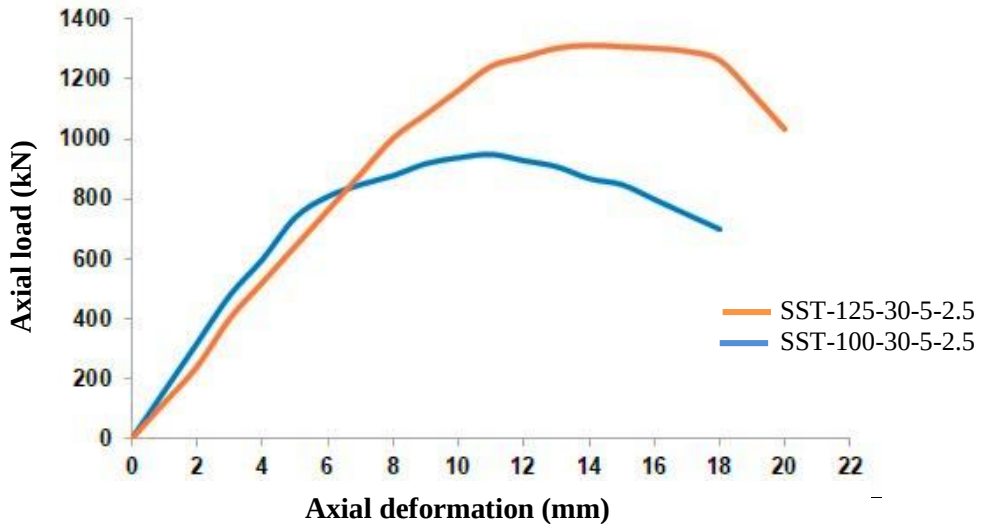

(a)

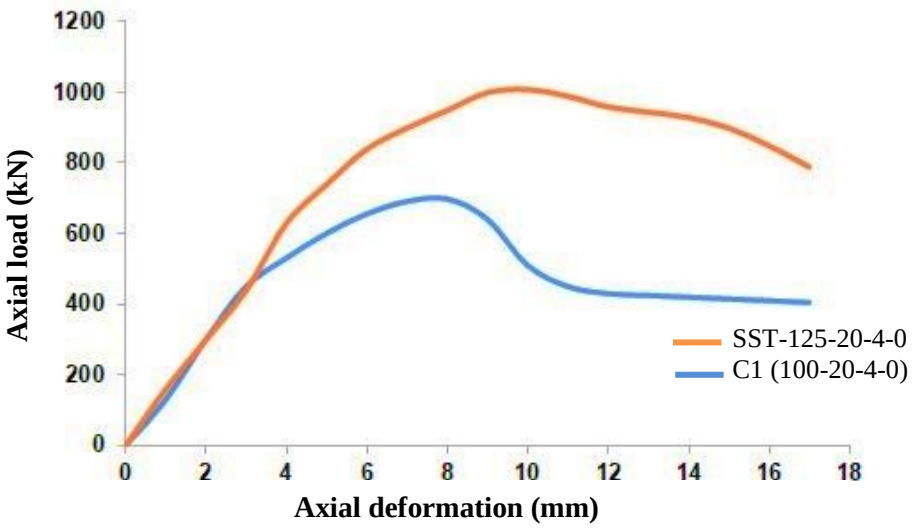

(b)

Figure 4.2 Effect of global slenderness ratio on axial load vs axial deformation of long columns (a) with fiber (b) without fiber

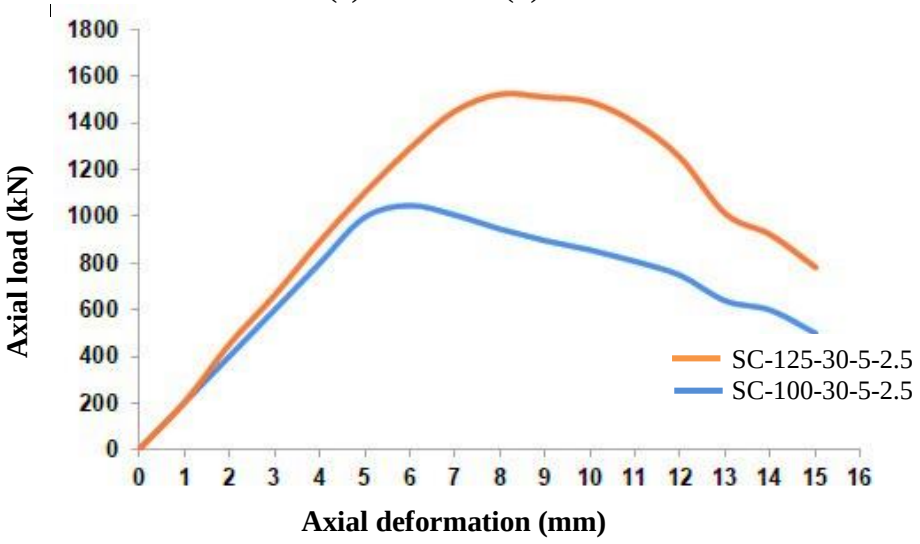

(a)

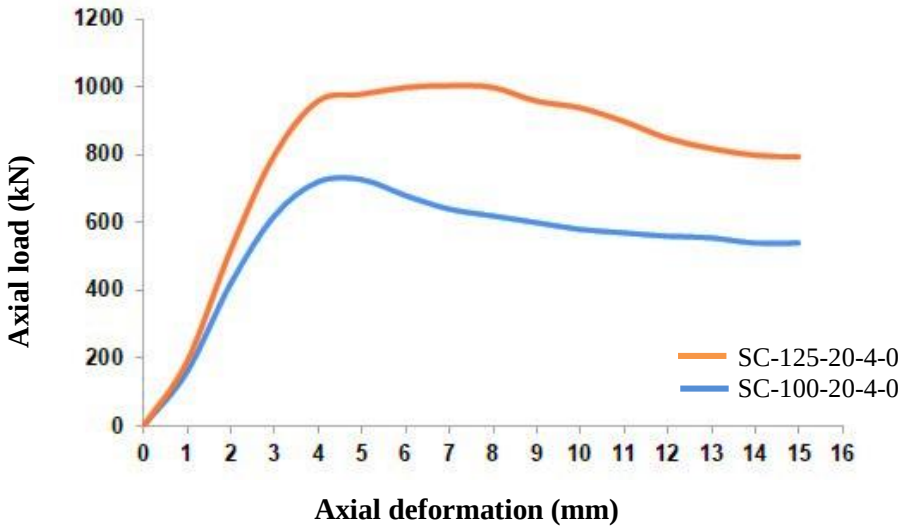

(b)

Figure 4.3 Effect of global slenderness ratio on axial load vs axial deformation of stub columns (a) with fiber (b) without fiber

4.3.3 Effect of loading eccentricity (e/D)

Eight (8) column divided into four groups (Group 9 to Group 12) were considered to observe the effects of GI wire fiber on eccentricity ratio (as shown in Table 4.5). To observe the behavior of the CFST column with plain and fiber concrete, each group having two columns were tested pertaining same material and geometric properties, only difference being the load eccentricity value (e/D). The values of eccentricity were 0 mm, 45 mm, 37.5 mm and 30 mm for the CFST columns of 150 mm, 125 mm and 100 mm, respectively. Group 9 and Group 10 are of 150 mm, Group 11 is of 100 mm and Group 12 is of 150 mm column (Annexure-A) as shown in Table 4.5. The load was applied eccentrically about the major axis of the steel section of the columns.

Table 4.5 Effect of loading eccentricity on peak load and deformation capacity

Group	Column designation	e/D	Peak load P_{Exp}	Load variation	Deformation at peak load	Deformation variation
			(kN)	(%)	(mm)	(%)
Gr-9	SST-150-40-4-2.5	0	1481	-	13.5	-
	SSTE-150-40-4-2.5	0.3	893	-39%	9.75	-27%
Gr-10	SST-150-20-4-2.5	0	1290	-	13	-
	SSTE-150-20-4-2.5	0.3	710	-42%	10	-23%
Gr-11	SST-100-30-5-0	0	865	-	8.5	-
	SSTE-100-30-5-0	0.3	602	-30%	6	-30%
Gr-12	E9 (150-40-5-0) (Ali 2019)	0	1474	-	11	-
	E10 (150-40-5-0) (Ali 2019)	0.3	968	-35%	7.5	-32%

It was observed that for Group 9 and Group 10 of having 2.5% of fiber where the load eccentricity of 45 mm has decreased of load carrying capacity and deformation capacity on average 40% and 25%, respectively. The eccentricity value of Group 11 and Group 12 with plain concrete, load carrying capacity and deformation capacity was decreased about 35% and 31% (on average), respectively. Increase in eccentric load, additional secondary moment also increases in the column reducing the load carrying capacity to a great extent and it affects in larger scale in large dimension of columns compared to small dimension. The columns with larger eccentricity ratio also found earlier steel yielding than the columns having smaller eccentricity ratio value. This is due to the load is rapidly transferred to the adjacent steel tube wall of columns having large eccentricity ratio value. Figures 4.4 (a) and 4.4 (b) show the effect of the load eccentricity ratio on the axial load versus axial deformation curve for the fibered and plain CFST columns, respectively. The decrement of axial capacity and deformation in fibered CFST columns is lesser than that occurs in the plain CFST columns.

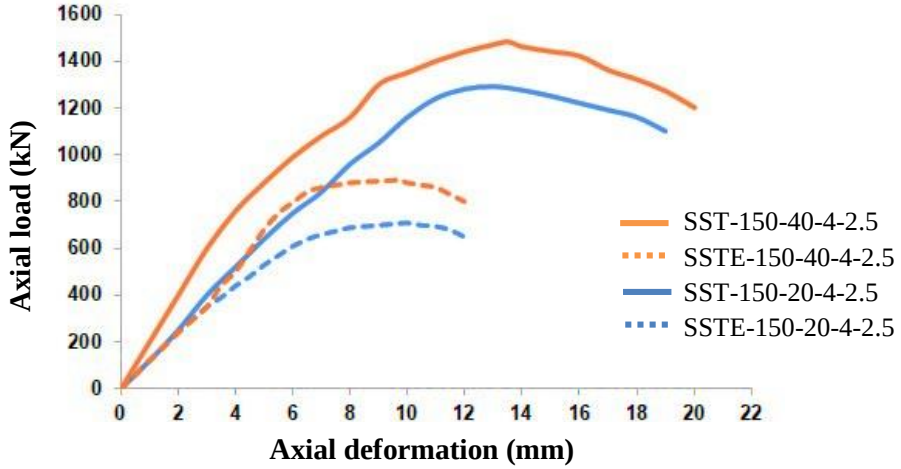

(a)

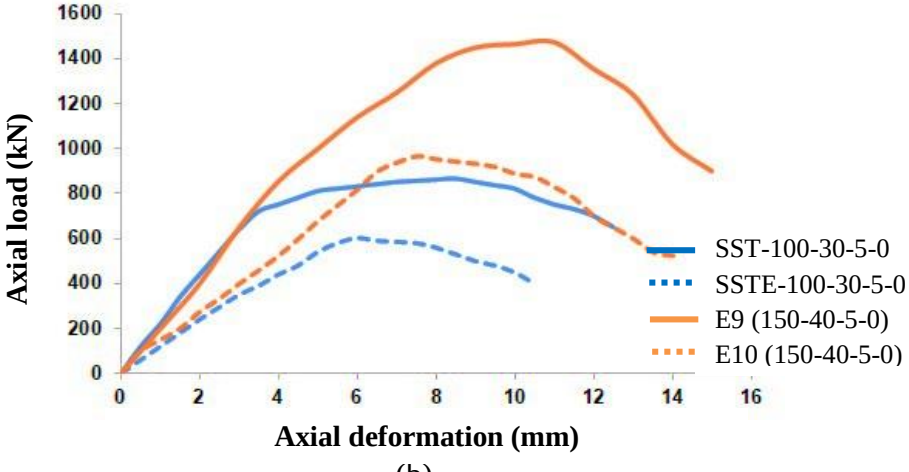

(b)

Figure 4.4 Effect of load eccentricity on axial load vs axial deformation of long columns (a) with fiber (b) without fiber

4.3.4 Effect of concrete compressive strength ($f_c^{/}$)

Total twelve columns consisted of four groups; Group 13 and Group 14 for long columns and Group 15 and Group 16 for stub columns as shown in Table 4.6. Within each group the strength of concrete was varied from 20 MPa, 30 MPa and 40 MPa. Group 13 and Group 15 were for fibered long columns and stub columns, respectively. Similarly, Group 14 and Group 16 were for plain long columns and stub columns, respectively. These columns were tested with three types of concrete strengths to evaluate the performance of CFST columns with and without fiber.

Table 4.6 Effect of concrete strength on peak load and deformation capacity

Group	Column designation	Peak load P_{Exp} (kN)	Load variation (%)	Deformation at peak load (mm)	Deformation variation (%)
Gr-13	SST-150-20-4-2.5	1290	-	13	-
	SST-150-30-4-2.5	1359	10%	14.5	11%
	SST-150-40-4-2.5	1481	19%	15.5	19%
Gr-14	C1 (100-20-4-0) (Islam 2019)	697	-	6	-
	C2 (100-30-4-0) (Islam 2019)	729	5%	6.5	8%
	C3 (100-40-4-0) (Islam 2019)	804	15%	7	17%
Gr-15	SC-100-20-5-2.5	960	-	4	-
	SC-100-30-5-2.5	1051	10%	4.5	12%
	SC-100-40-5-2.5	1152	20%	4.75	19%
Gr-16	SC-100-20-4-0	727	-	5	-
	SC-100-30-4-0	785	8%	5.5	10%
	C8 (100-40-4-0) (Islam 2019)	810	11%	5.75	15%

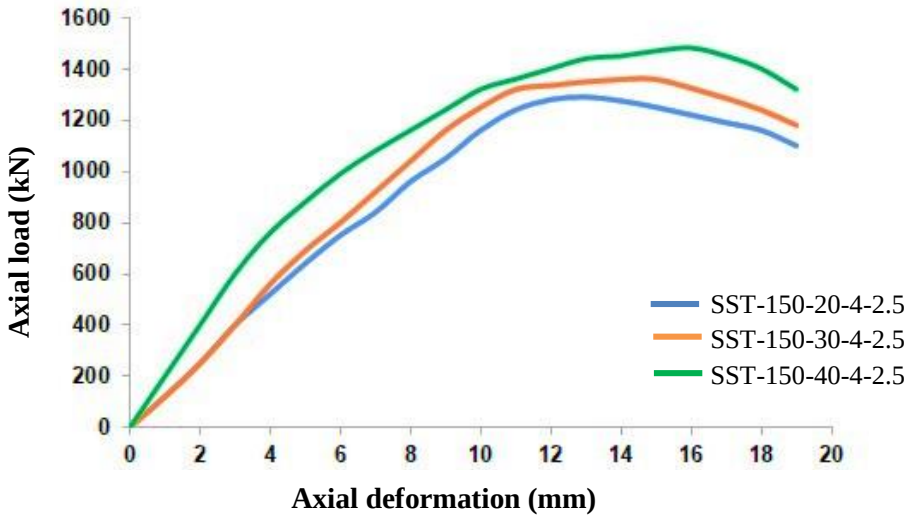

(a)

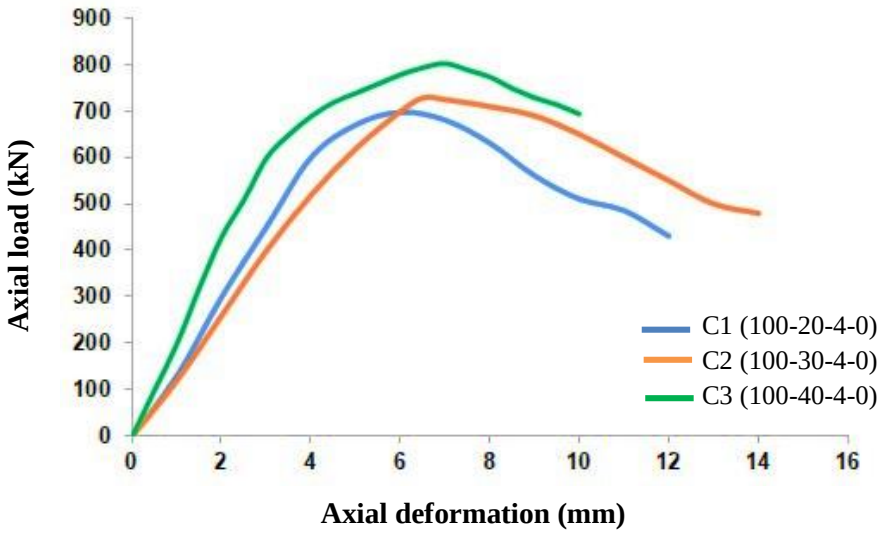

(b)

Figure 4.5 Effect of concrete compressive strength on axial load vs axial deformation of long columns (a) with fiber (b) without fiber

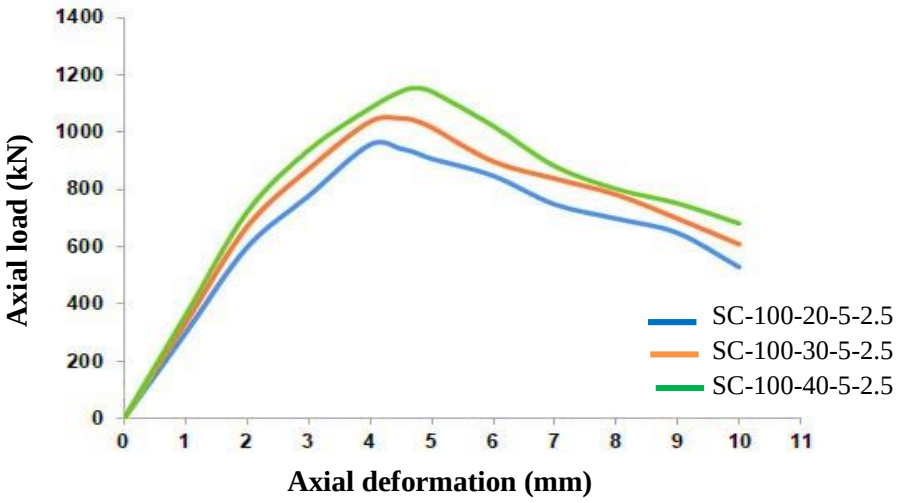

(a)

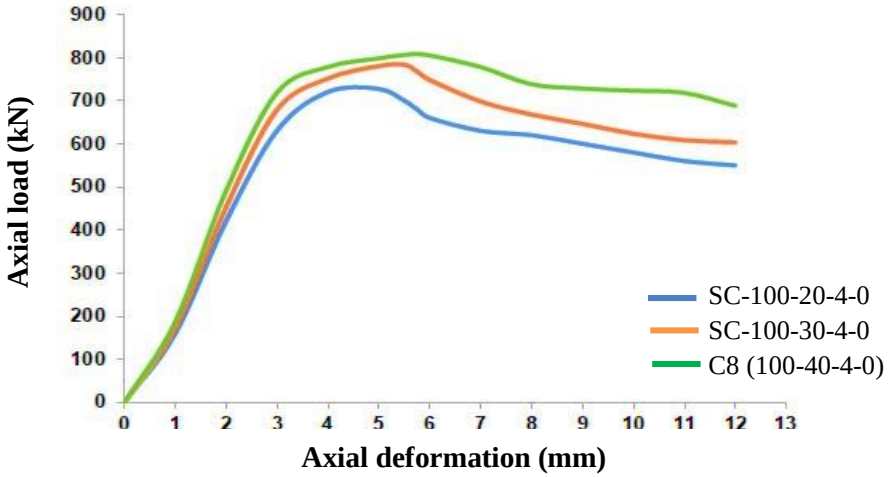

(b)

Figure 4.6 Effect of concrete compressive strength on axial load vs axial deformation of stub columns (a) with fiber (b) without fiber

Load carrying capacity of the columns increased significantly with the increase of concrete strength. Figure 4.5 (a) and Figure 4.5 (b) represents the set of long columns with fibered and plain concrete; Figure 4.6 (a) and Figure 4.6 (b) represents the set of stub columns with fibered and plain concrete, respectively. It was observed from these Figures that ultimate axial load and deformation of CFST column is greatly affected by the strength of concrete. The axial load versus axial deformation responses of CFST columns with higher strength concrete show steeper slopes at the ascending portions of the curves both for fibered and plain concrete. From the experiment, it was observed that the load carrying capacity increased by 10 % and 19% when concrete strength increased from 20 MPa to 30 MPa and 20 MPa to 40 MPa, respectively for the long columns with fiber. On the other hand, the carrying capacity also increased but at a lower rate by 5 % and 15% when concrete strength was increased from 20 MPa to 30 MPa and 20 MPa to 40 MPa, respectively due to absence of fiber. Similarly, for the stub column with fiber, the load carrying capacity increased by 12 % and 20%; by 8 % and 11% for plain concrete if concrete strength was increased from 20 MPa to 30 MPa and 20 MPa to 40 MPa, respectively. It was observed that load carrying capacity increased with the increment in concrete strength is relatively more in fibered concrete due to the more internal bonding strength which gains higher strength to the CFST columns.

4.3.5 Effect of cross sectional slenderness ratio (B/t)

Eight (8) column divided into four groups (Group 17 to Group 20) were considered to observe the effects of GI wire fiber on cross sectional slenderness ratio (B/t) as shown in Table 4.7. To observe the behavior of the CFST column with plain and fiber concrete, each group having two columns were tested consisting B/t ratio of 31.25 and 25 for both long and stub columns. The fibered concrete of Group 17 of long column and Group 19 for stub columns. Other two group; Group 18 and Group 20 of plain concrete for long and stub columns, respectively. Behavior of CFST was examined with two different steel thicknesses to determine the effect of variable thickness on the performance of CSFT columns.

Table 4.7 Effect of sectional slenderness ratio on peak load and deformation capacity

Group	Column designation	B/t	Peak load P_{Exp}	Load variation	Deformation at peak load	Deformation variation
			(kN)	(%)	(mm)	(%)
Gr-17	SST-125-30-4-2.5	31.25	1082	-	13	-
	SST-125-30-5-2.5	25	1310	21%	15.5	20%
Gr-18	C5 (125-30-4-0) (Islam 2019)	31.25	1011	-	10	-
	C6 (125-30-5-0) (Islam 2019)	25	1169	16%	12	18%
Gr-19	SC-125-20-4-2.5	31.25	1071	-	6	-
	SC-125-20-5-2.5	25	1392	30%	7.75	29%
Gr-20	SC-125-20-4-0	31.25	1005	-	7	-
	SC-125-20-5-0	25	1276	27%	9	28%

It was observed from the Table 4.7 that with the decrease of cross sectional slenderness ratio from 31.25 mm to 25 mm, load carrying capacity increased by 21% and 16% for the column of fibered and plain concrete, respectively. This behavior also be verified for the stub columns; by 30% and 27% increase, respectively. The deformation capacity was also increased by 20% and 18% for the long column of fibered and plain concrete; 40% and 33% for the stub column, respectively. Figure 4.7 and 4.8 shows that the ultimate axial load and deformation of CFST column is affected by the cross sectional slenderness ratio. The axial load versus axial deformation responses of CFST columns with lower show steeper slopes at the ascending portions of the curves. In each result, the concrete with fiber shows the higher axial capacity and deformation capacity than plain CFST when thickness increases. Increase in steel thickness has less possibility of local buckling failure to occur. Increasing in steel thickness, the ductility of the columns also increased. This additional ductility due to the fiber can be attributed to the additional stiffness provided by the steel section. Similar enhancement in ductility is also noticed in case of stub columns.

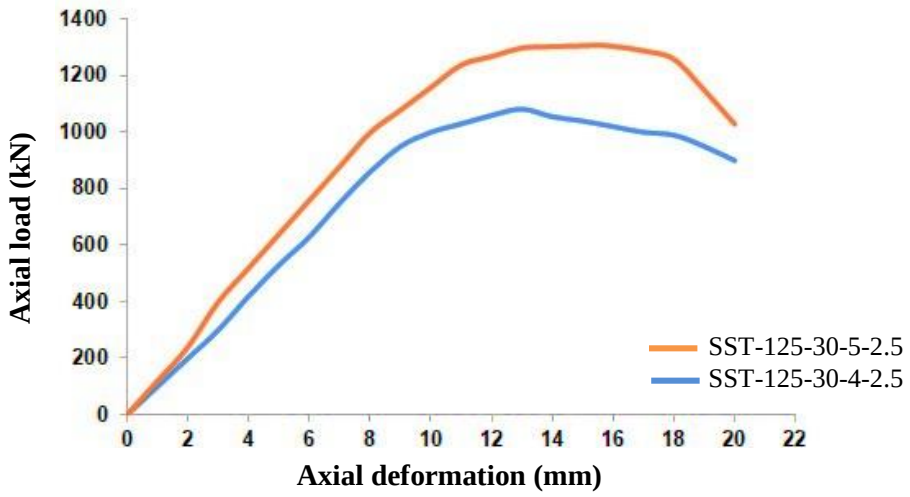

(a)

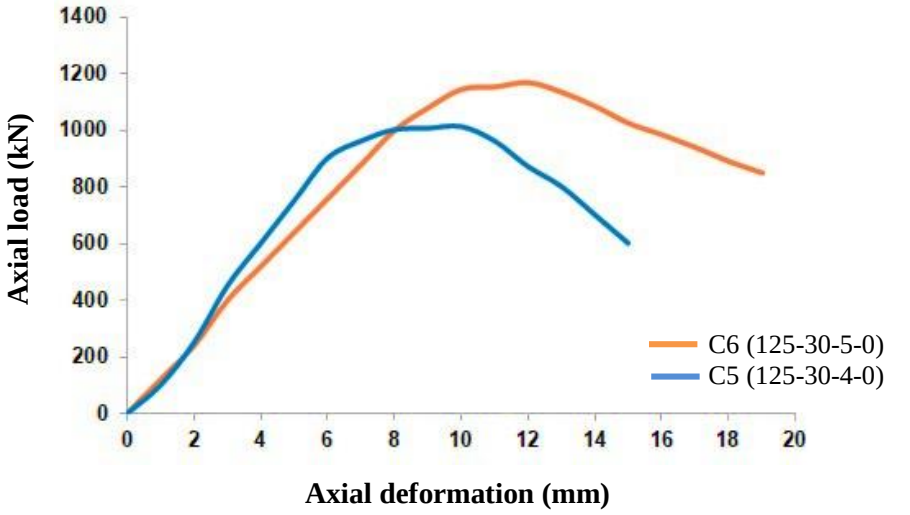

(b)

Figure 4.7 Effect of cross sectional slenderness ratio on axial load vs axial deformation of long columns (a) with fiber (b) without fiber

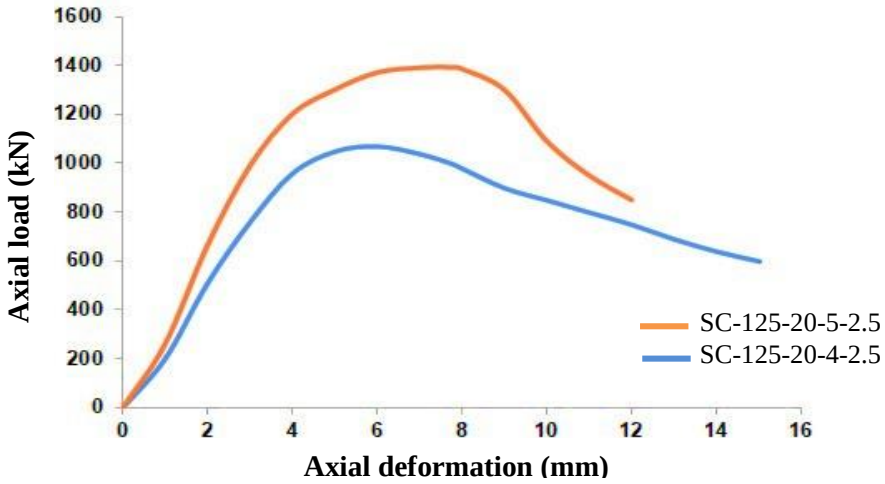

(a)

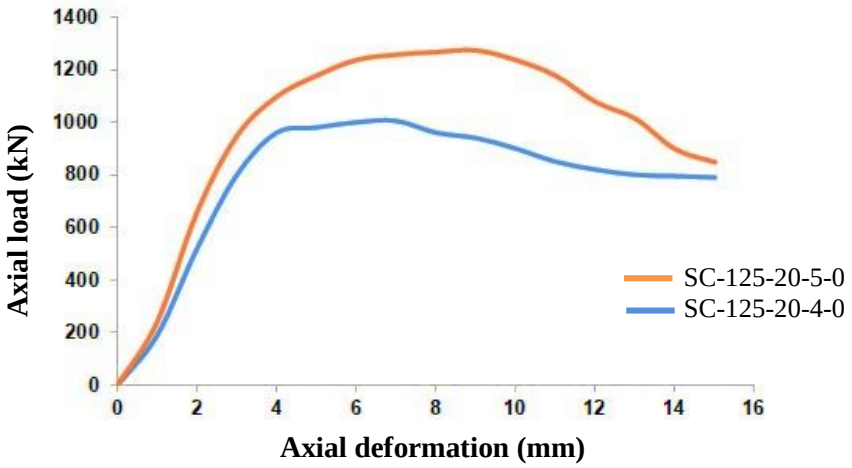

(b)

Figure 4.8 Effect of cross sectional slenderness ratio on axial load vs axial deformation of stub columns (a) with fiber (b) without fiber

4.4 Ductility Index (DI)

Ductility is a measure the ability of a structure to undergo significant deformation beyond the elastic limit while maintaining a reasonable load carrying capacity until rupture or failure. According to modern seismic codes of practice, like Eurocode 4 (2005), it is very common to design ductile structures to drastically reduce the design seismic force, leading to a more economical design. The influence of other extreme events, like blast, impact, cyclone and fire, on structures can also be mitigated if the structures are ductile. Currently, the design of ductile structures is to a large extent based on prescriptive detailing provisions.

Ductility indexing is defined as the ratio of axial shortening at ultimate strength and post peak shortening corresponding to 85% of the ultimate strength according to Ren et al. (2018) as shown in Figure 4.9. The ductility index of the test specimens is shown in Table 4.8 to 4.12 according to the variable to observe the effect of GI fiber in CFST columns.

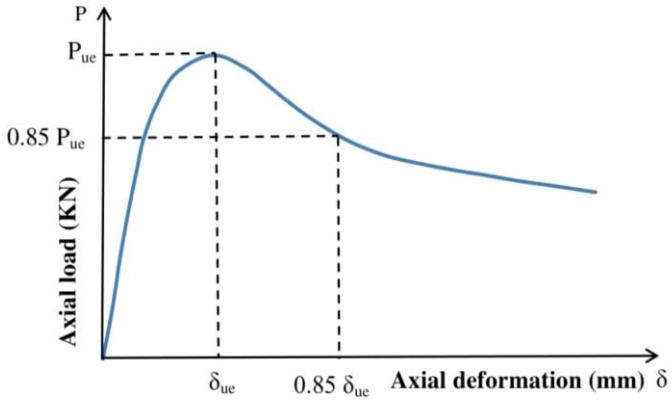

Figure 4.9 Definition of ductility index (Ren et al. 2018)

4.4.1 Effect of addition of fiber

From the Table 4.8 and Figure 4.10, described the effect of the addition of fiber with respect to the plain concrete for ductility index. The ductility index of Group 21 and Group 22 of columns were determined and presented in Table 4.8. The DI was increased due to the addition of fiber to the fibred concrete with respect to the plain concrete in both groups. The ductility was increased because the internal fiber resists the propagation of crack developed in the concrete beyond the elastic limit with increase of load carrying capacity also. From result, the ultimate capacities were increased and the ductility was increased about 25% for Group 21 and 32% for Group 22 due to GI wire. Moreover, it was found that specimens having higher L/B ratio showed lower ductility index, since plasticity and confinement of a specimen decrease with the increase of the length of specimen.

Table 4.8 Effect of addition of fiber on ductility index

Group	Column designation	P_{Exp}	$0.85P_{Exp}$	Global slenderness	Ductility index	% of variation
		(kN)	(kN)	L/B	DI	% of DI
Gr-21	SST-100-30-5-0	865	735	10	1.12	-
	SST-100-30-5-2.5	951	808	10	1.42	+25%
Gr-22	SST-125-30-5-0	1180	1003	8	1.66	-
	SST-125-30-5-2.5	1310	1114	8	2.19	+32%

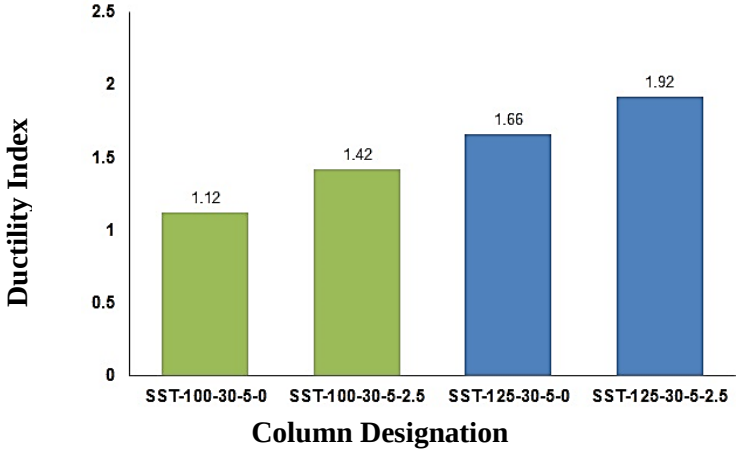

Figure 4.10 Effect of percentage of fiber on ductility index

4.4.2 Effect of global slenderness (L/B)

Four (4) column divided into two groups (Group 23 to Group 24) were considered to calculate the ductility index and derive the effects of GI wire fiber on global slenderness ratio (L/B) as shown in Table 4.9. Group 23 consisted of fibered column and Group 24 of plain concrete. From the Figure 4.10, it was observed that test specimens having higher L/B

showed lower DI due to plasticity and confinement of a specimen decreases with the increase of the size of the specimen. It seems that the composite action between the steel tube and the concrete core decreases with increasing global slenderness ratio. Increased size allows more steel and concrete which results more ductile property to undergo larger deformation of the specimen. The decrease rate of DI is less when the fibered CFST column compared to the plain concrete. If slenderness ratio increased from 8 to 10, the DI of CFST columns was found decreased by 15% for fibered and 20% for the plain concrete.

Table 4.9 Effect of global slenderness on ductility index

Group	Column designation	P_{Exp}	$0.85P_{Exp}$	Slenderness ratio	Global slenderness	Ductility index	% of variation
		(kN)	(kN)	B/t	L/B	DI	% of DI
Gr-23	SST-125-30-5-2.5	1310	1114	25	8	1.69	-
	SST-100-30-5-2.5	951	773	20	10	1.42	-16%
Gr-24	SST-125-20-4-0	1009	858	31.25	8	1.73	-
	SST-100-20-4-0	697	598	25	10	1.38	-20%

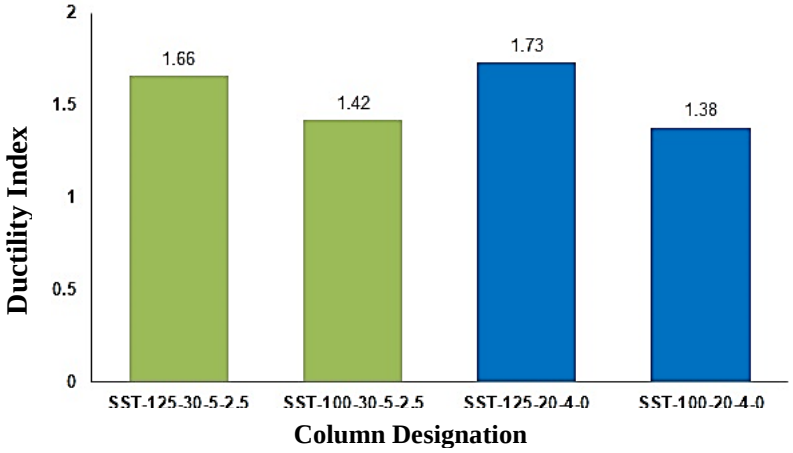

Figure 4.11 Effect of fiber on global slenderness by ductility index

4.4.3 Effect of loading eccentricity (e/B)

The ductility index (DI) affected by the loading eccentricity (e/B) of CFST columns. Four (4) column divided into two groups (Group 25 to Group 26) were considered to calculate the ductility index and derive the effects of GI wire fiber on loading eccentricity as shown in Table 4.10. From the Table 4.10 and Figure 4.12, DI was increased for the eccentric loading applied on the test specimens. If the load eccentricity applied on the plain concrete, the DI increased by about 18% whilst on the fibered concrete it was 34%. Addition of fiber

gives concrete the additional ductility. The ductility of the concrete increased due to the additional resistance from the side which was not directly under loading and the peripheral steel tube of the test specimen. The non-directly concrete are considered as continues lever arm to the steel tube, whilst non-directly loaded concrete and adjacent steel tube could provide extra resistance to the partially loaded concrete with higher eccentricity (e/B) ratio.

Table 4.10 Effect of loading eccentricity on ductility index

Group	Column Designation	P_{Exp}	$0.85P_{Exp}$	Load Eccentricity	Ductility index	% of variation
		(kN)	(kN)	e/B	DI	% of DI
Gr-25	C3 (100-40-4-0) (Islam 2019)	804	687	0	1.31	-
	SSTE-100-40-4-0	488	415	0.3	1.55	+18%
Gr-26	SST-150-40-4-2.5	1481	1259	0	1.13	-
	SSTE-150-40-4-2.5	893	759	0.3	1.51	+34%

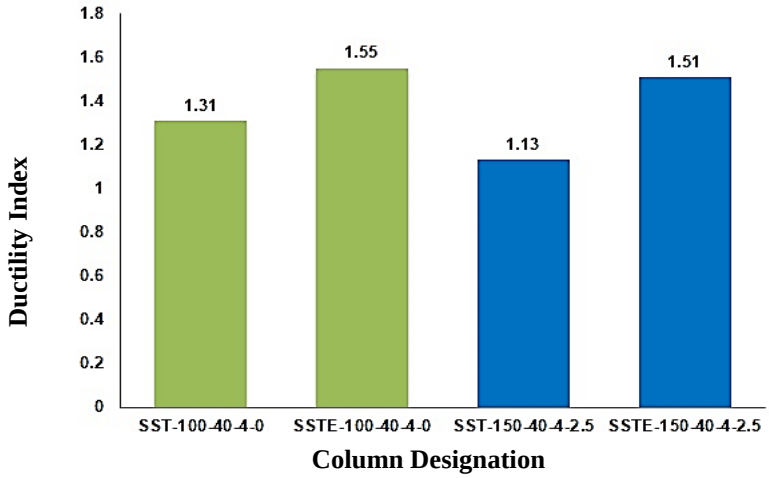

Figure 4.12 Effect of fiber on loading eccentricity by ductility index

4.4.4 Effect of concrete compressive strength ($f_c^{/}$)

The DI influenced by the concrete compressive strength showed in the Figure 4.13 and the Table 4.11. Four (4) column consisted of two groups (Group 27 to Group 28) were considered to calculate the ductility index and observe the effects of GI wire fiber on concrete compressive strength 20, 30 and 40 MPa as shown in Table 4.11. The results appeared from the table and figure that increasing the concrete compressive strength causes a reduction of DI. The DI reduced by 3-4% for the fibered concrete and 11-19% for plain concrete. Increasing the concrete compressive strength decreased the performance of the columns because of losing the ductile behavior of higher strength concrete. The ductility of

the CFST columns with GI wire fiber decreased at a lower rate because it generated remarkable resistance to crack development and propagation. The higher strength concrete had the low DI due to the brittleness of the infilled concrete. The concrete strength of columns of lower slenderness ratio having higher reduction of DI.

Table 4.11 Effect of concrete compressive strength on ductility index

Group	Column designation	P_{Exp}	$0.85P_{Exp}$	Slenderness ratio	Ductility index	% of variation
		(kN)	(kN)	B/t	DI	% of DI
Gr-27	SST-150-20-4-2.5	1290	1097	37.5	1.51	-
	SST-150-30-4-2.5	1359	1155	37.5	1.47	-3%
	SST-150-40-4-2.5	1481	1259	37.5	1.45	-4%
Gr-28	SST-100-20-4-0	697	598	25	1.78	-
	SST-100-30-4-0	729	624	25	1.57	-11%
	C3 (100-40-4-0) (Islam 2019)	804	687	25	1.43	-19%

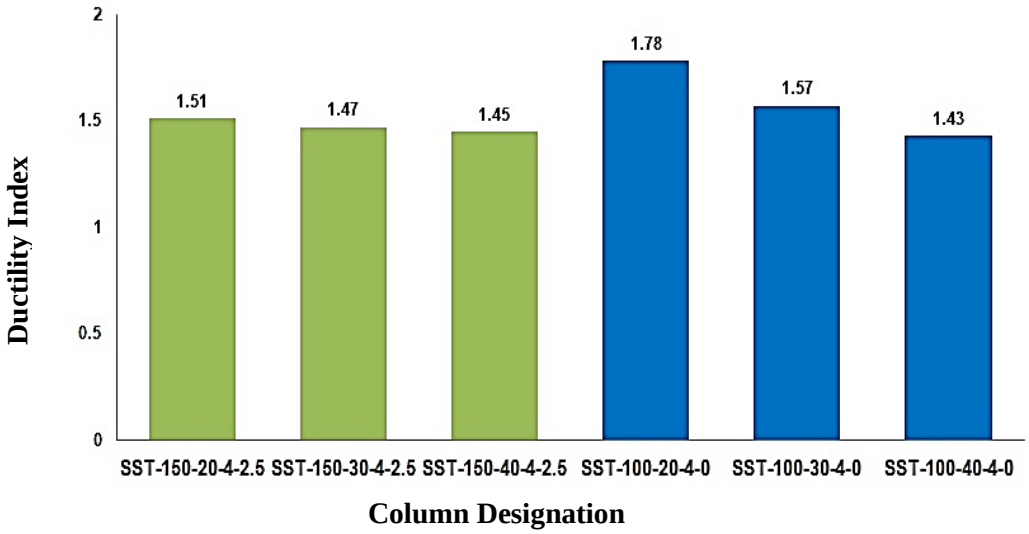

Figure 4.13 Effect of ultimate strength of columns on ductility index

4.4.5 Effect of cross sectional slenderness ratio (B/t)

From the Table 4.12 and the Figure 4.14, it is illustrated that the effect of cross sectional slenderness ratio which varies from 25 to 31.25 on the ductility index of CFST columns. Four (4) column consisted of two groups (Group 29 to Group 30) were considered to calculate the ductility index and observe the effects of GI wire fiber on B/t ratio as shown in Table 4.12. The columns with larger B/t ratio are usually less ductile. In spite of this, a steel tube with a smaller B/t ratio is more effective to exhibits the extra resistance to concrete. Ductility index of the specimens increases at 1.5% and 4% for the fibred concrete and plain concrete for the decrease of slenderness ratio of 31.25 to 25. The increment of DI

in fibered concrete is larger than plain concrete due to the extra ductile property for addition of GI fiber into it. The ductility index increase with the decrease of the cross sectional slenderness ratio of the specimens. This may happen due to regular decrease of ultimate load of high steel contributed specimens.

Table 4.12 Effect of cross sectional slenderness ratio on ductility index

Group	Column designation	P_{Exp}	$0.85P_{Exp}$	Slenderness ratio	Ductility index	% of variation
		(kN)	(kN)	B/t	DI	% of DI
Gr-29	SST-125-30-4-2.5	1082	920	31.25	1.40	-
	SST-125-30-5-2.5	1310	1114	25	1.46	+4%
Gr-30	SST-125-30-4-0	1011	859	31.25	1.32	-
	SST-125-30-5-0	1180	1003	25	1.34	+1.5%

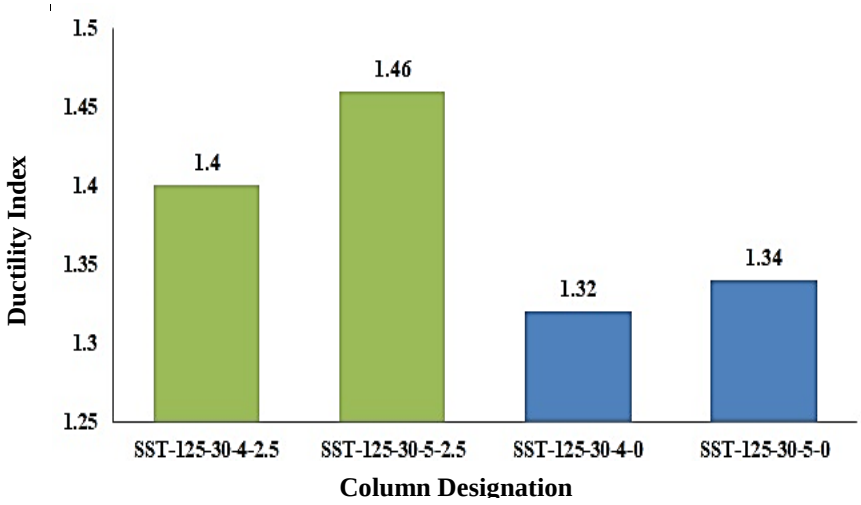

Figure 4.14 Effect of fiber on slenderness ratio by ductility index

4.5 Analysis of Failure Modes

The inclusion of GI fiber, steel tube slenderness ratio (B/t), global slenderness ratio (L/D), loading eccentricity (e/B), infilled concrete properties have a significant effect on the failure mode of the CFST column subjected to concentric and eccentric loading. Various types of failure mode of the CFST column are shown in the Figure 4.15. The failure mode of the tested columns is given in Table 4.13 and Table 4.14.

Table 4.13 Failure modes of tested long columns

Ser	Column designation	Cross sectional slenderness	Global slenderness	Eccentricity ratio	Failure mode
		B/t	L/B	e/B	
1	SST-100-20-5-2.5	20	10	0	Global buckling
2	SST-100-30-5-2.5	20	10	0	Global buckling
3	SST-125-20-5-2.5	25	8	0	Global buckling
4	SST-125-30-4-2.5	31.25	8	0	Global buckling
5	SST-125-30-5-2.5	25	8	0	Global buckling
6	SST-150-20-4-2.5	37.5	6.67	0	Global buckling and Local buckling at the end
7	SST-150-30-4-2.5	37.5	6.67	0	Local buckling at middle
8	SST-150-40-4-2.5	37.5	6.67	0	Global, Local buckling at middle and Welding
9	SSTE-125-40-5-2.5	25	8	0.3	Global buckling
10	SSTE-125-40-4-2.5	31.25	8	0.3	Global buckling
11	SSTE-150-40-4-2.5	37.5	6.67	0.3	Global buckling
12	SSTE-150-20-4-2.5	37.5	6.67	0.3	Global buckling
13	SSTE-100-30-5-0	20	10	0.3	Global buckling
14	SSTE-125-40-4-0	31.25	8	0.3	Global buckling
15	SST-100-30-5-0	20	10	0	Global buckling
16	SST-125-20-4-0	31.25	8	0	Global buckling
17	SST-125-40-4-0	31.25	8	0	Global buckling and Local buckling at the end

Table 4.14 Failure modes of tested stub columns

Ser	Column designation	Cross sectional slenderness	Global slenderness	Eccentricity ratio	Failure mode
		B/t	L/B	e/B	
1	SC-100-20-4-2.5	25	3	0	Local buckling at middle
2	SC-100-20-5-2.5	20	3	0	Local buckling at middle and end
3	SC-100-30-5-2.5	20	3	0	Local buckling at middle
4	SC-100-40-5-2.5	20	3	0	Local buckling at middle and Welding
5	SC-125-20-4-2.5	31.25	3	0	Local buckling at end
6	SC-125-20-5-2.5	25	3	0	Local buckling at middle and end
7	SC-100-20-4-0	25	3	0	Local buckling at end
8	SC-100-30-4-0	25	3	0	Local buckling at middle
9	SC-100-30-5-0	20	3	0	Local buckling at middle
10	SC-125-20-5-0	25	3	0	Local buckling at middle and end
11	SC-125-20-4-0	31.25	3	0	Local buckling at middle
12	SC -125-30-5-0	25	3	0	Local buckling at middle

During applying the load, there is no significant deformation at the beginning of the loading for all the columns. During applying the load near the ultimate load, cracking sounds were audible and then buckling on the columns appeared. There were six types of failure occurred after testing of all the CFST columns described in below section.

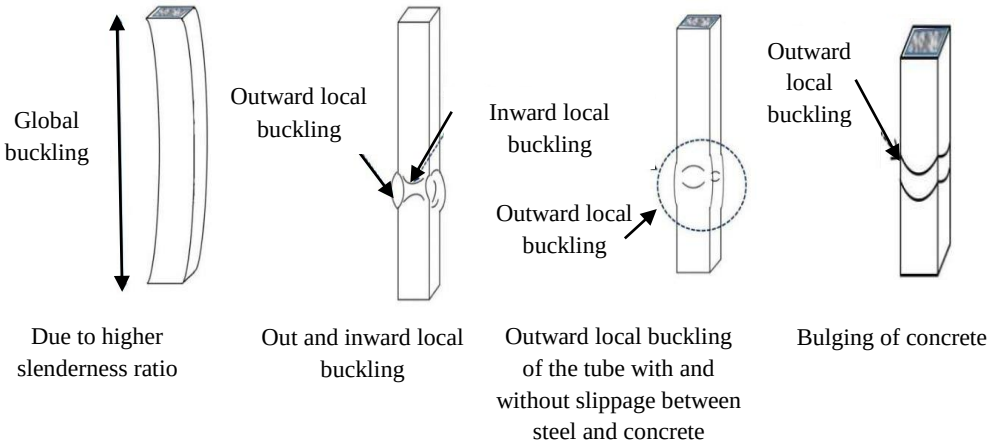

Figure 4.15 Different types of failure pattern

4.5.1 Global buckling

In this form of buckling, the whole column body was buckled in a single curved shape both in concentric and eccentric loading (Figure 4.16). The CFST column deforms with no deformation in its cross-sectional shape, consistent with classical beam theory.

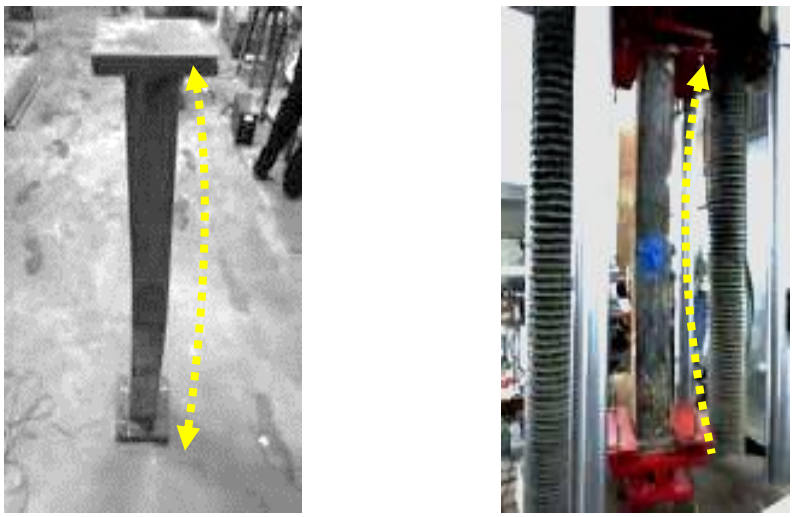

Figure 4.16 Global buckling

4.5.2 Global and local buckling at middle

Some of the columns were buckled both globally and locally. The local buckling can be expressed as the buckling occurred at a particular portion of the section either at the end of

the CFST column or at any specific single place. It involves plate-like deformations alone, without the translation of the intersection lines of adjacent plate elements. In this type of failure, it occurred at the middle of the column (Figure 4.17).

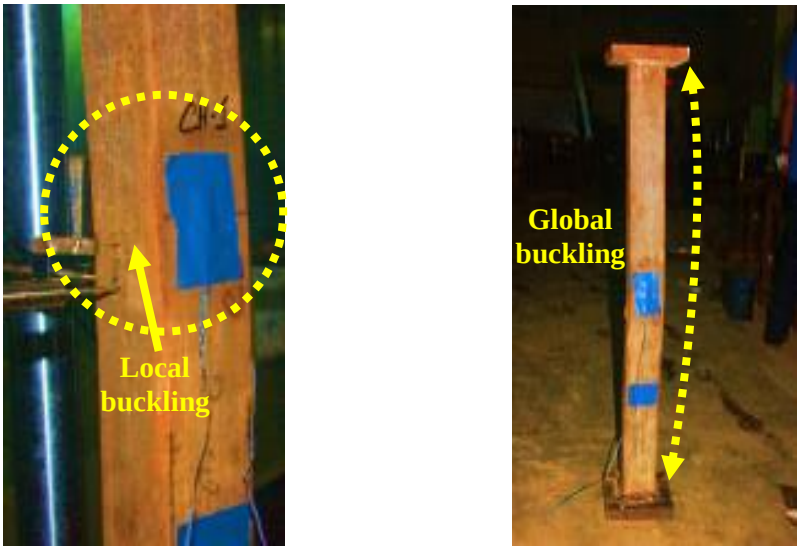

Figure 4.17 Global and local buckling at mid-section

4.5.3 Local buckling at end

There were some columns having only local failure (Figure 4.18). The vertical alignment of these columns remained unchanged but only the local failure happened at the end potion near the joint of plate and the column section.

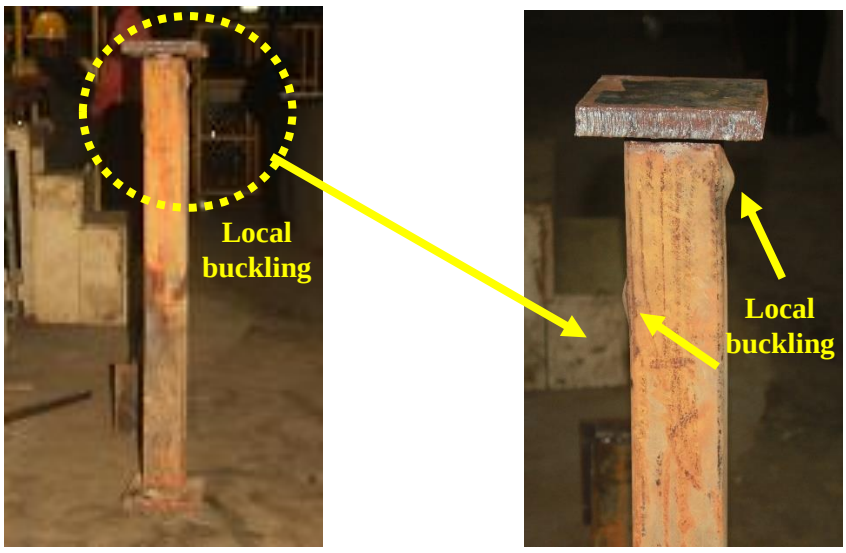

Figure 4.18 Local buckling at end

4.5.4 Global and local buckling at end

This type of failure happened of the columns that were failed both globally and locally as shown Figure 4.19 (a) and 4.19 (b).

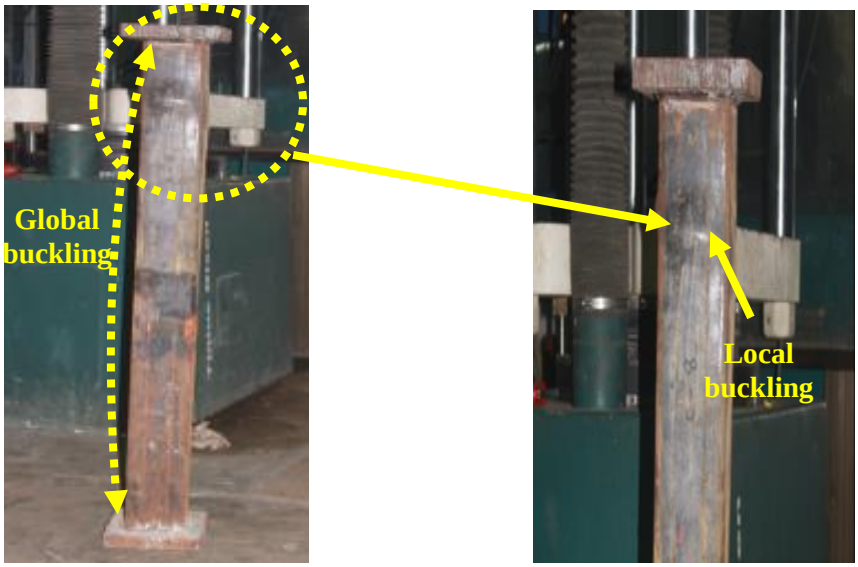

(a) (b)

Figure 4.19 (a) Global buckling (b) Local buckling at end

4.5.5 Local buckling at middle

This failure also happened only at the middle section of the column and also the other potion remained unchanged (Figure 4.20).

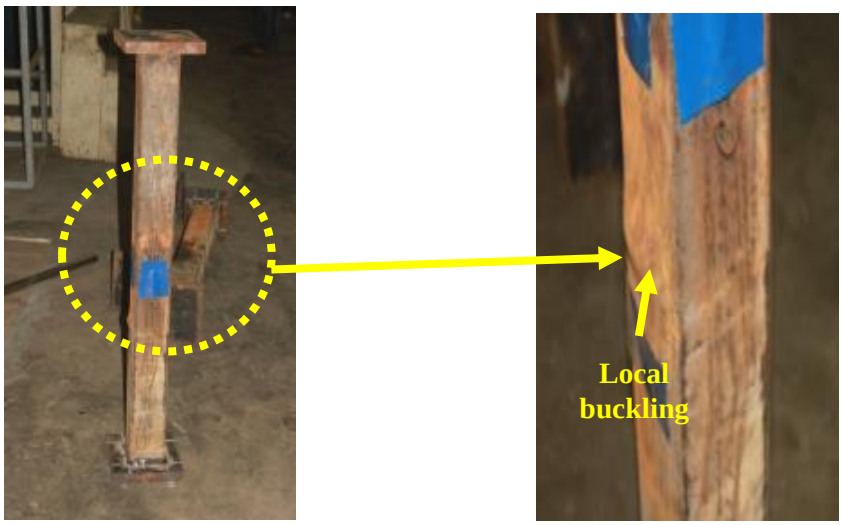

Figure 4.20 Local buckling at middle

4.5.6 Welding failure at middle

This type of failure occurred due to tear-off the welding joint. The CFST columns were buildup section welded through the longitudinal direction at the opposite side of the columns (Figure 4.21).

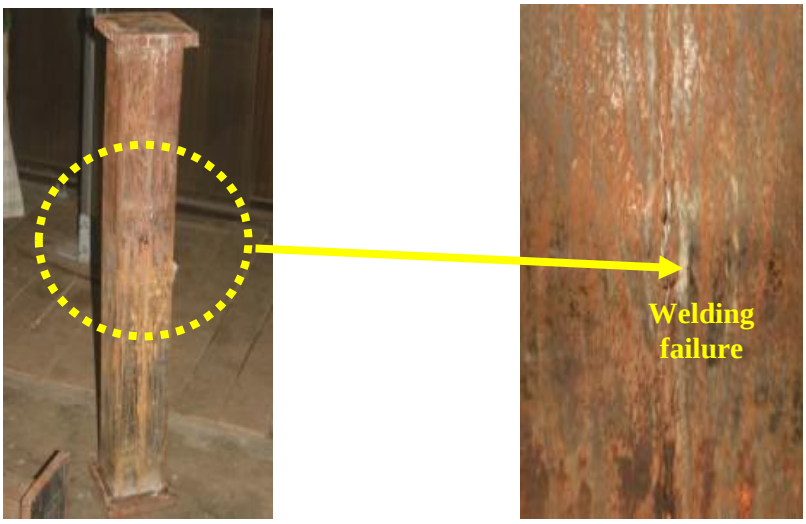

Figure 4.21 Welding failure at middle

4.6 Findings from Result of Failure Pattern

Six types of failure modes were found from this experiment. All the columns were failed due to steel yielding followed by concrete The findings from the experiment of the tested CFST columns are listed below.

(i) From the Figure 4.22 it was observed that column specimen with GI wire delayed the local buckling of composite columns.

(a) (b)

Figure 4.22 After test of CFST column (a) without fiber (b) with fiber

This phenomenon happened because of the confinement from GI wire fibers provided shear and frictional resistance to slide and allowed the transfer of shear forces across the cracked planes.

(ii) For columns with higher L/B ratio, failure was initiated by global buckling followed by crushing of concrete. Because the columns with higher slenderness ratio had greater flexibility which resulted in larger mid-height lateral displacement.

(iii) Columns with higher B/t ratio failed by outward local buckling followed by crushing of concrete. Outward local buckling of the tube may be initiated with or without presence of slippage between steel and concrete. Slippage indicates the bulging formation of the specimen without internal work of the concrete infill.

(iv) The stub column specimens showed local buckling and concrete crushing at failure. Besides the local buckling in the tube, fracture was observed due to three aspects; large axial deformation, welding quality and outstanding stress produced from the welding process. Tensile stresses are prompted in the welded area and compression stresses are developed in the area far from the weld section. The developed tensile stresses usually provide the energetic force to the crack generation.

(v) Columns with geometric imperfection, imperfect welding during making of buildup section failed due to welding failure. This occurred by tearing off the section at longitudinal direction.

4.7 Relation Between Axial Load and Mid-Height Deflection

The CFST composite columns were tested in the UTM both concentrically and eccentrically. Only the mid-height deflection data of the eccentrically loaded columns were considered for the experimental result. The eccentrically loaded columns developed lateral defection due to the generation of secondary moment. The lateral deflection at mid-height started to increase significantly when the load reached about 60-70% of the maximum load. Two no. of Linear Variable Displacement Transducer (LVDT) were installed and mid-height at the alternate side of the columns to measure the lateral deflection. The effect of concrete compressive strength ($f_c^{/}$) and cross sectional slenderness ratio (B/t) on the experimental axial capacity versus mid-height deflection curves are shown in Table 4.15. In the Figure 4.23, it can be observed that the axial loads applied and calculated by UTM and lateral displacement were found from the LVDTs. The values of the mid-height deflections of the specimens are shown in the Table 4.15.

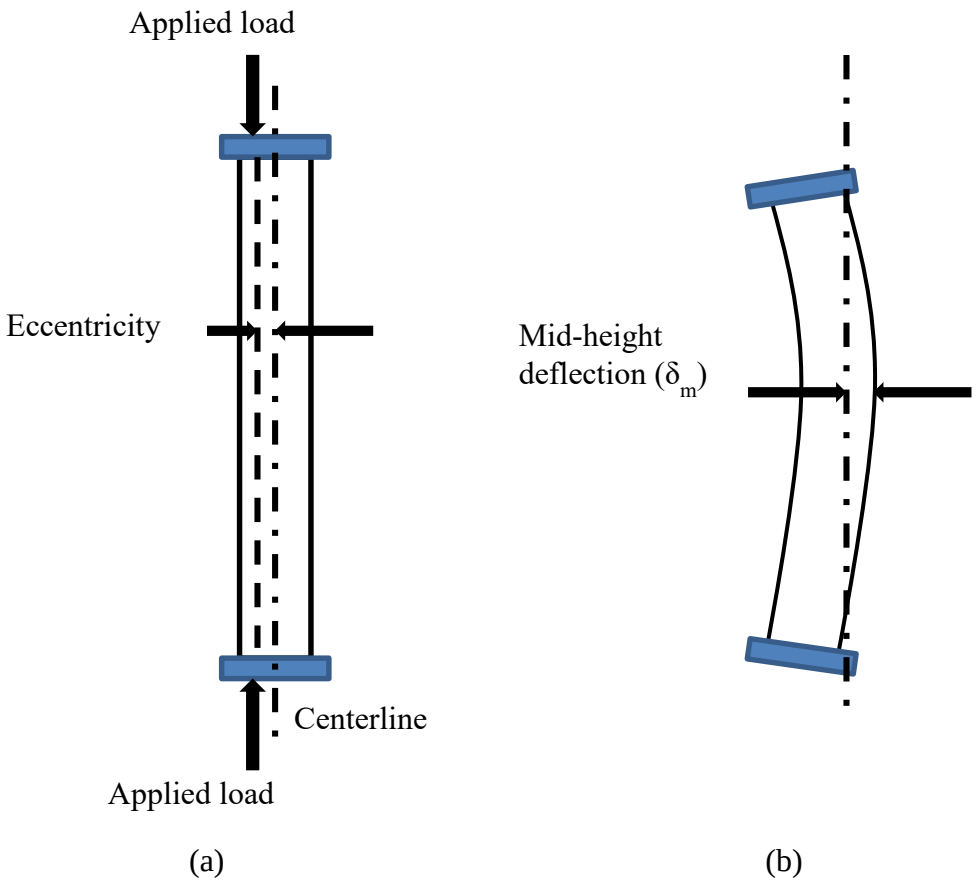

Figure 4.23 (a) Before applying eccentric load (b) mid-height deflection after applying load

Table 4.15 Mid-height deflection at peak load of test specimens

Column designation	Size of the columns			f_c'	Cross sectional slenderness	Overall slenderness	e/B	Mid-height deflection at peak load	% of variation
	B	t	L		B/t	L/B		δ_m	$\Delta\%$ δ_m
	(mm)	(mm)	(mm)	(MPa)				(mm)	
E1 (100-20-4-0) (Ali 2019)	100	4	1000	20	25	10	0.30	4.80	-
E2 (100-30-4-0) (Ali 2019)	100	4	1000	30	25	10	0.30	2.21	-54%
E3 (100-40-4-0) (Ali 2019)	100	4	1000	40	25	10	0.30	2.04	-58%
SSTE-100-20-4-2.5	100	4	1000	20	25	10	0.30	4.22	-
SSTE-100-30-4-2.5	100	4	1000	30	25	10	0.30	2.48	-41%
SSTE-100-40-4-2.5	100	4	1000	40	25	10	0.30	2.32	-45%
E6 (125-40-4-0) (Ali 2019)	125	5	1000	40	25	8	0.30	2.72	-
E5(125-40-4-0) (Ali 2019)	125	4	1000	40	31.25	8	0.30	3.26	+20%
SSTE-125-40-5-2.5	125	5	1000	40	25	8	0.30	2.33	-
SSTE-125-40-4-2.5	125	4	1000	40	31.25	8	0.30	2.72	+18%

4.7.1 Effect of Concrete Compressive Strength (f_c')

The actual effect of concrete compressive strength which varies from 20 MPa to 40 MPa on the mid-height deflection of eccentrically loaded CFST columns is showed in Figure 4.24. It observed from Figure 4.24 that, mid-height deflection of CFST columns increases with the decrease of concrete compressive strength. Generally low strength concrete shows much quicker volumetric expansion than high strength concrete. From the Table 4.15, mid-height deflections of columns of plain concrete were found 4.80, 2.21 and 2.04 with increasing concrete compressive strength of 20 MPa, 30 MPa and 40 MPa, respectively. Similarly, for fibered concrete, the values were found 4.22, 2.48 and 2.32, respectively with increasing concrete compressive strength. It was found that for fibered concrete the variation of mid-height deflections lower rate at 41% and 45% for 20 MPa to 30 and 20 to 40 MPa, respectively than plain concrete. The infilled fiber and concrete strength jointly resist the lateral deflection of the CFST columns generated by the applied load.

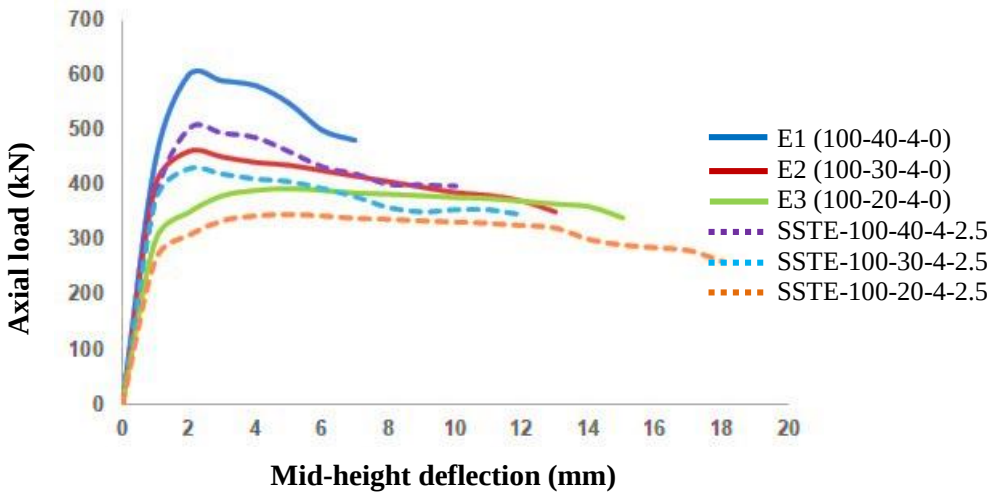

Figure 4.24 Effect of concrete compressive strength on mid-height deflection

4.7.2 Effect of Cross Sectional Slenderness Ratio (B/t)

The relationship between mid-height deflection and cross sectional slenderness ratios (B/t) are verified in Figure 4.25. From the Table 4.15, mid-height deflections of columns of plain concrete were found 2.72 and 3.26 with increasing (B/t) ratios from 25 to 31.25. It can be observed from Table 4.15 that mid-height deflection increases by 20 % when B/t ratio increases from 25 to 31 for plain concrete. On the contrary, the increment was 18% when B/t ratio increases from 25 to 31 for fibered concrete. The deflection is less in the fibered CFST columns compared to the plain CFST columns. This is due to the thicker steel tube restricts the lateral deflection of concrete. The deflection rate of CFST with fiber was lower

than plain concrete because the infilled fiber also helps to restrict the lateral deflection of the specimen.

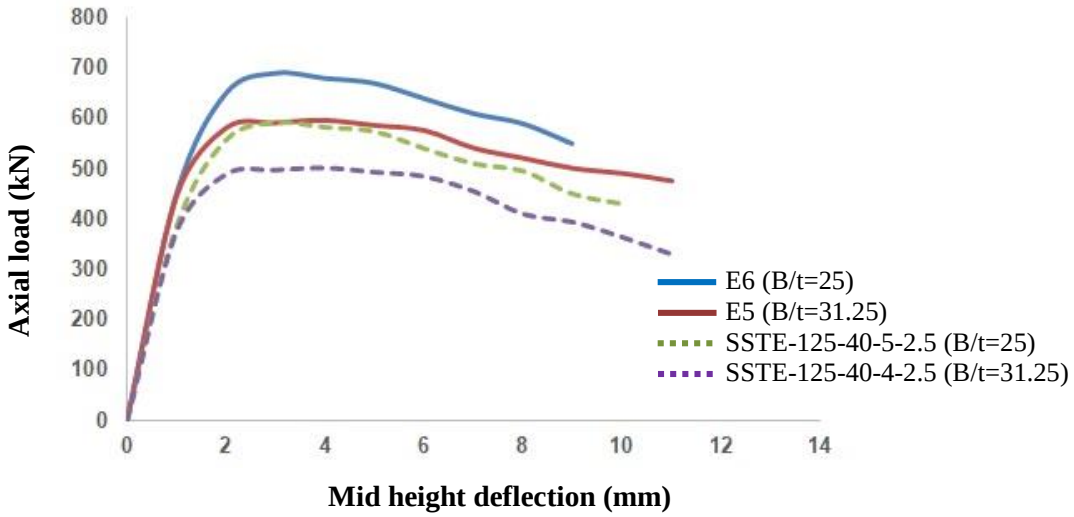

Figure 4.25 Effect of cross sectional slenderness ratio on mid-height deflection

4.8 Comparison of Results with Code Predicted Capacity

In this study, the different design codes (AISC-LRFD 2010, Eurocode 4 and AS4100) were applied to predict the ultimate strength of the tested specimens. Afterwards, the predicted capacities were compared with the experimented results. Design codes present different expression for predicting ultimate strength. However, these strength predictors express the steel and concrete contribution of the CFST column. In design calculations, reduction factors or material safety factors are set to unit. In order to determine the accuracy of the experimental capacity, the predicted results were divided by the experimental results.

4.8.1 AISC-LRFD (2010)

AISC-LRFD (2010) composite column design presents different equations for the cross-sectional strength depending on the ratio maximum dimension to thickness and the shape of the column. Besides, the expression for the nominal axial capacity of stub columns incorporates the effect of slenderness. AISC (2010) presented best prediction with a mean of 1.02 and Standard deviation of 0.07 for long columns and 1.01 and 0.04 for stub columns. The predictions given by this method are shown in Table 4.16 and 4.17.

Table 4.16: Comparison of the results according to AISC-LRFD (2010) – long column

Column Designation	Dimension B,D (mm)	Thickness t (mm)	% of Fiber	e/D (mm)	P_{Exp} (kN)	P_{AISC} (kN)	P_{AISC}/P_{Exp}
SST-100-20-5-2.5	100	5	2.5	0	**890**	**924**	1.04
SST-100-30-5-2.5	100	5	2.5	0	**951**	**943**	0.99
SST-125-20-5-2.5	125	5	2.5	0	**1209**	**1202**	0.99
SST-125-30-4-2.5	125	4	2.5	0	**1082**	**1180**	1.09
SST-125-30-5-2.5	125	5	2.5	0	**1310**	**1293**	0.99
SST-150-20-4-2.5	150	4	2.5	0	**1290**	**1207**	0.94
SST-150-30-4-2.5	150	4	2.5	0	**1359**	**1382**	1.02
SST-150-40-4-2.5	150	4	2.5	0	**1481**	**1557**	1.05
SSTE-125-40-5-2.5	125	5	2.5	0.3	**857**	**891**	1.04
SSTE-125-40-4-2.5	125	4	2.5	0.3	**734**	**777**	1.06
SSTE-150-40-4-2.5	150	4	2.5	0.3	**893**	**937**	1.05
SSTE-150-20-4-2.5	150	4	2.5	0.3	**710**	**760**	1.07
SSTE-100-30-5-0	100	5	0	0.3	**602**	**541**	0.90
SSTE-125-40-4-0	125	4	0	0.3	**614**	**680**	1.11
SST-100-30-5-0	100	5	0	0	**865**	**896**	1.04
SST-125-20-4-0	125	4	0	0	**1009**	**980**	0.97
SST-125-40-4-0	125	4	0	0	**1058**	**1140**	1.08
						Mean	**1.02**
						Standard deviation	**0.07**

Table 4.17: Comparison of the results according to AISC-LRFD (2010) – stub column

Column Designation	Dimension B,D (mm)	Thickness t (mm)	% of Fiber	e/D (mm)	P_{Exp} (kN)	P_{AISC} (kN)	P_{AISC}/P_{Exp}
SC-100-20-5-2.5	100	5	2.5	0	**960**	**1020**	1.06
SC-100-30-5-2.5	100	5	2.5	0	**1051**	**1097**	1.04
SC-100-40-5-2.5	100	5	2.5	0	**1152**	**1200**	1.04
SC-125-20-4-2.5	125	4	2.5	0	**1071**	**1163**	1.08
SC-125-20-5-2.5	125	5	2.5	0	**1392**	**1409**	1.01
SC-125-30-5-2.5	125	5	0	0	**1523**	**1460**	0.96
SC-100-20-4-0	100	4	0	0	**727**	**698**	0.96
SC-100-30-4-0	100	4	0	0	**785**	**854**	1.08
SC-100-30-5-0	100	5	0	0	**945**	**944**	0.99
SC-125-20-5-0	125	5	0	0	**1276**	**1314**	1.03
SC-125-20-4-0	125	4	0	0	**1005**	**975**	0.97
SC-125-30-5-0	125	5	0	0	**1360**	**1400**	1.03
						Mean	**1.01**
						Standard deviation	**0.04**

4.8.2 Eurocode 4 (2005)

According to the design method proposed by Eurocode 4 (2005) for composite members, the experimental ultimate loads were compared to the maximum loads calculated theoretically. Eurocode 4 (2005) uses a different model in function of the cross-sectional shape. For rectangular sections, the capacity of the column is obtained as the sum of the contributions of each material. The results obtained by this method are summarized in Table 4.18 and Table 4.19 of mean (0.98 and 1.00) and standard deviation (0.08 and 0.07) with respect to the experimental values for long and stub columns, respectively.

Table 4.18: Comparison of the results according to Eurocode 4 (2005) – long column

Column Designation	Dimension	Thickness	% of Fiber	e/D	P_{Exp}	P_{EC4}	P_{EC4}/P_{Exp}
	B,D	t					
	(mm)	(mm)		(mm)	(kN)	(kN)	
SST-100-20-5-2.5	100	5	2.5	0	**890**	**877**	0.99
SST-100-30-5-2.5	100	5	2.5	0	**951**	**920**	0.97
SST-125-20-5-2.5	125	5	2.5	0	**1209**	**1178**	0.97
SST-125-30-4-2.5	125	4	2.5	0	**1082**	**1056**	0.98
SST-125-30-5-2.5	125	5	2.5	0	**1310**	**1357**	1.04
SST-150-20-4-2.5	150	4	2.5	0	**1290**	**1228**	0.95
SST-150-30-4-2.5	150	4	2.5	0	**1359**	**1320**	0.97
SST-150-40-4-2.5	150	4	2.5	0	**1481**	**1474**	1.00
SSTE-125-40-5-2.5	125	5	2.5	0.3	**857**	**842**	0.98
SSTE-125-40-4-2.5	125	4	2.5	0.3	**734**	**783**	1.07
SSTE-150-40-4-2.5	150	4	2.5	0.3	**893**	**924**	1.03
SSTE-150-20-4-2.5	150	4	2.5	0.3	**710**	**732**	1.03
SSTE-100-30-5-0	100	5	0	0.3	**602**	**506**	0.84
SSTE-125-40-4-0	125	4	0	0.3	**614**	**594**	0.97
SST-100-30-5-0	100	5	0	0	**865**	**902**	1.04
SST-125-20-4-0	125	4	0	0	**1009**	**946**	0.94
SST-125-40-4-0	125	4	0	0	**1058**	**1022**	0.97
						Mean	**0.98**
						Standard deviation	**0.08**

Table 4.19: Comparison of the results according to Eurocode 4 (2005) – stub column

Column Designation	Dimension B,D (mm)	Thickness t (mm)	% of Fiber	e/D (mm)	P_{Exp} (kN)	P_{EC4} (kN)	P_{EC4}/P_{Exp}
SC-100-20-5-2.5	100	5	2.5	0	**960**	**965**	1.01
SC-100-30-5-2.5	100	5	2.5	0	**1051**	**1123**	1.07
SC-100-40-5-2.5	100	5	2.5	0	**1152**	**1160**	1.01
SC-125-20-4-2.5	125	4	2.5	0	**1071**	**1153**	1.07
SC-125-20-5-2.5	125	5	2.5	0	**1392**	**1339**	0.96
SC-125-30-5-2.5	125	5	0	0	**1523**	**1475**	0.97
SC-100-20-4-0	100	4	0	0	**727**	**681**	0.93
SC-100-30-4-0	100	4	0	0	**785**	**822**	1.04
SC-100-30-5-0	100	5	0	0	**945**	**982**	1.04
SC-125-20-5-0	125	5	0	0	**1276**	**1200**	0.94
SC-125-20-4-0	125	4	0	0	**1005**	**965**	0.96
SC-125-30-5-0	125	5	0	0	**1360**	**1320**	0.97
						Mean	**1.00**
						Standard deviation	**0.07**

4.8.3 Australian Standard (AS4100) Code

In general, Australian Standard 4100 predicts the ultimate strength with good prediction accuracy. The predicted axial strength for each specimen is given in Table 4.20 and Table 4.21. From the table, it is observed that the average P_{AS} / P_{exp} ratio is 1.03 with a standard deviation of 0.09 for long columns. In addition, the prediction accuracy of the AS4100 is very close to the AISC-LRFD (2010), where the average P_{AISC} / P_{exp} ratio is 1.01. the AS appeared to be very conservative, due to the fact that concrete confinement is ignored in their estimation of axial load capacity.

Table 4.20: Comparison of the results according to AS4100 Code – long column

Column Designation	Dimension B,D (mm)	Thickness t (mm)	% of Fiber	e/D (mm)	P_{Exp} (kN)	P_{AS} (kN)	P_{AS}/P_{Exp}
SST-100-20-5-2.5	100	5	2.5	0	**890**	**918**	1.03
SST-100-30-5-2.5	100	5	2.5	0	**951**	**991**	1.04
SST-125-20-5-2.5	125	5	2.5	0	**1209**	**1233**	1.02
SST-125-30-4-2.5	125	4	2.5	0	**1082**	**1103**	1.02
SST-125-30-5-2.5	125	5	2.5	0	**1310**	**1323**	1.01
SST-150-20-4-2.5	150	4	2.5	0	**1290**	**1228**	0.95
SST-150-30-4-2.5	150	4	2.5	0	**1359**	**1412**	1.04
SST-150-40-4-2.5	150	4	2.5	0	**1481**	**1510**	1.02
SSTE-125-40-5-2.5	125	5	2.5	0.3	**857**	**867**	1.01
SSTE-125-40-4-2.5	125	4	2.5	0.3	**734**	**805**	1.10
SSTE-150-40-4-2.5	150	4	2.5	0.3	**893**	**940**	1.05
SSTE-150-20-4-2.5	150	4	2.5	0.3	**710**	**723**	1.02
SSTE-100-30-5-0	100	5	0	0.3	**602**	**598**	0.99
SSTE-125-40-4-0	125	4	0	0.3	**614**	**656**	1.07
SST-100-30-5-0	100	5	0	0	**865**	**937**	1.08
SST-125-20-4-0	125	4	0	0	**1009**	**1002**	0.99
SST-125-40-4-0	125	4	0	0	**1058**	**1107**	1.05
						Mean	**1.03**
						Standard deviation	**0.09**

Table 4.21: Comparison of the results according to AS4100 Code – stub column

Column Designation	Dimension B,D (mm)	Thickness t (mm)	% of Fiber	e/D (mm)	P_{Exp} (kN)	P_{AS} (kN)	P_{AS}/P_{Exp}
SC-100-20-5-2.5	100	5	2.5	0	**960**	**943**	0.98
SC-100-30-5-2.5	100	5	2.5	0	**1051**	**1048**	0.99
SC-100-40-5-2.5	100	5	2.5	0	**1152**	**1132**	0.98
SC-125-20-4-2.5	125	4	2.5	0	**1071**	**1137**	1.06
SC-125-20-5-2.5	125	5	2.5	0	**1392**	**1414**	1.02
SC-125-30-5-2.5	125	5	0	0	**1523**	**1597**	1.05
SC-100-20-4-0	100	4	0	0	**727**	**705**	0.97
SC-100-30-4-0	100	4	0	0	**785**	**808**	1.02
SC-100-30-5-0	100	5	0	0	**945**	**987**	1.03
SC-125-20-5-0	125	5	0	0	**1276**	**1205**	0.94
SC-125-20-4-0	125	4	0	0	**1005**	**1065**	1.06
SC-125-30-5-0	125	5	0	0	**1360**	**1428**	1.05
						Mean	**1.02**
						Standard deviation	**0.04**

4.9 Conclusions

A comprehensive experimental investigation was performed to study the behavior of CFST columns with and without GI wire fiber of 2.5% in weight basis. The geometric and material properties were varied and their effect with respect to ultimate load, failure modes, mid-height defection and ductility index of plain and fibered CFST columns. It was determined from the result that inclusion of fiber in concrete has significant effect on the fundamental behavior of CFST columns as compressive strength, cross sectional slenderness ratio, global slenderness ratio, column cross section and loading eccentricity.

(i) From the result, the load carrying capacity was increased by 10-11% and average deformation capacity was increased about 30% for addition of 2.5% of GI fiber in the concrete. The ductility indexes were also increased about 25-30% due to increase in toughness only for the GI fiber within concrete.

(ii) The axial load capacity was increased by 10% and 19% for fibered concrete and 5% and 15% for plain concrete when compressive strength increased from 20 MPa to 30 MPa and 20 MPa to 40 MPa respectively. But ductility was decreased by average 4% and 10%, respectively for plain and fibred concrete with increasing of compressive strength.

(iii) For fibered concrete, the axial load and deformation capacity were increased by 21% and 19% whilst for the plain concrete 19% and 18%, respectively when cross sectional slenderness ratio decreased from 31.25 to 25. The DI increment was 4% for the fibred concrete and 1.5% for the plain concrete.

(iv) For the fibered concrete, due to the eccentricity, the axial load and deformation capacity were decreased by 40% and 25%, respectively. On the contrary, the decrement rates were 31% and 35%, respectively for plain concrete. But ductility was increased about 16% more than plain concrete which was due to the indirect concrete and fiber could be considered as a continuous support, provides extra provision in eccentricity of fibered concrete.

(v) Based on the result, for fibered concrete, the variation of mid-height deflections were lower rate at 41% and 45% for 38 MPa to 47 and 38 to 53 MPa, respectively compared to plain concrete (54% and 58%). mid-height deflection increased by 20 % for plain concrete and 18% for fibered concrete when B/t ratio increased from 25 to 31.

(vi) The axial load and deformation capacity of fibered concrete was increased greater than plain concrete and the values are 7% and 5%, respectively for the decrement of

global slenderness. The decrement of ductility of fibered columns was 4% lower than the plain concrete column for increment of global slenderness ratio.

(vii) By adding GI wire fiber into concrete had effect on the failure mode and delayed the local buckling of composite columns. For columns with higher L/B ratio, failure was initiated by global buckling followed by crushing of concrete. Columns with higher B/t ratio failed by outward local buckling. Outward local buckling of the tube may be initiated with or without presence of slippage between steel and concrete.

(viii) The code predicted results were compared with the experimental results individually. AISC-LRFD (2010) code predicted result shows only average 1% of higher load bearing capacity with respect to the experimental result. Another AS4100 and EC4 (2005) presented best prediction with a mean of 1.03 and 1.01 standard deviation 0.09 and 0.04 respectively for long column and mean of 0.98 and 0.99 standard deviation 0.08 and 0.07, respectively for stub columns.

CHAPTER 5
CONCLUSIONS AND RECOMMENDATIONS

5.1 General

This experimental investigation was carried out to observe the effect of steel wire fiber on compressive strength of concrete filled steel tubular columns with normal strength plain concrete. Total seventeen (17) numbers of long CFST column having length 1000 mm and twelve (12) numbers of CFST stub column with length 300 and 375 mm were tested experimentally. Out of these twelve (12) long columns and six stub columns were made with 2.5 % of GI wire (weight basis). These columns were three different in cross-sectional sizes (100 mm × 100 mm, 125 mm × 125 mm, 150 mm × 150 mm) with a steel tube thickness of 4 mm and 5 mm. These columns were constructed with three different types of concrete strength 20, 30 and 40 MPa. Yield strength of structural steel of these columns was 345 MPa. These columns were tested for concentric and eccentric axial loads. Knife edge arrangement was placed at the top and bottom of the columns to apply eccentric axial loads. The loads were applied until the specimens failed. LVDT (Linear Variable Displacement Transducer) was used to measure the load-displacement of CFST columns under axial compression.

The influence of GI fiber on the global slenderness, cross sectional slenderness ratio, eccentricity ratio, infilled concrete compressive strength, failure modes, ductility index and lateral deflection of the CFST columns were investigated through this study. The failure occurred by crushing of the concrete combined with global and local buckling of the steel tube confined with crushed concrete and GI fiber influence in the failure pattern. Finally, the design codes adopted in AISC-LRFD (2010), Eurocode 4 and Australian Standard (4100) were reviewed and applied to estimate the ultimate strength of the tests columns. Afterward, the predicted values were compared with the experimental results obtained from this experiment.

5.2 Conclusions

Within the scope, following conclusions can be summarized according to the objective of this study:

(i) From the result, the load carrying capacity was increased by 10-11% and average deformation capacity was increased about 30% for addition of 2.5% of GI fiber in the

concrete. The ductility indexes were also increased about 25-30% due to increase in toughness only for the GI fiber within concrete.

(ii) The axial load capacity was increased by 10% and 19% for fibered concrete and 5% and 15% for plain concrete when compressive strength increased from 20 MPa to 30 MPa and 20 MPa to 40 MPa respectively. But ductility was decreased by average 4% and 10%, respectively for plain and fibred concrete with increasing of compressive strength.

(iii) For fibered concrete, the axial load and deformation capacity were increased by 21% and 19% whilst for the plain concrete 19% and 18%, respectively when cross sectional slenderness ratio decreased from 31.25 to 25. The DI increment was 4% for the fibred concrete and 1.5% for the plain concrete.

(iv) For the fibered concrete, due to the eccentricity, the axial load and deformation capacity were decreased by 40% and 25%, respectively. On the contrary, the decrement rates were 31% and 35%, respectively for plain concrete. But ductility was increased about 16% more than plain concrete which is due to the indirect concrete and fiber can be considered as a continues support, provides extra provision in eccentricity of fibered concrete.

(v) Based on the result, for fibered concrete, the variation of mid-height deflections lower rate at 41% and 45% for 38 MPa to 47 and 38 to 53 MPa, respectively compared to plain concrete (54% and 58%). Mid-height deflection increased by 20 %for plain concrete and 18% for fibered concrete when B/t ratio was increased from 25 to 31.

(vi) The axial load and deformation capacity of fibered concrete was increased greater than plain concrete and the values were 11% and 5%, respectively for the increment of global slenderness. The decrement of ductility of fibered columns was 5% lower than the plain concrete column.

(vii) By adding GI wire fiber into concrete had effect on the failure mode and delayed the local buckling of composite columns. For columns with higher L/B ratio, failure was initiated by global buckling followed by crushing of concrete. Columns with higher B/t ratio failed by outward local buckling. Outward local buckling of the tube might be initiated with or without presence of slippage between steel and concrete.

(viii) Ultimate load carrying capacity matched with the AISC-LRFD (2010), Australian Standard and Eurocode 4 code predicted capacity with good accuracy. On the other hand, AISC-LRFD (2010) taken more conservation approach (Mean 0.99 and

standard deviation 0.07) on determining the ultimate load carrying capacity of CFST columns.

5.3 Recommendations for the Future Study

The following recommendations are made for future investigation:

(i) Study can be carried varying percentages (%) of GI wire fiber.

(ii) Study can be carried out using stainless steel as structural steel.

(iii) The numerical simulation can be carried out to compare the experimental results.

REFERENCES

AS4100 (1998), “Bridge Design-steel and Composite Construction”. Australian Standard.

AIJ (2008). “Recommendations for design and construction of concrete filled steel tubular structures”. Architectural Institute of Japan, Tokyo, Japan.

American Institute of Steel Construction. (2010). “Specification for structural steel buildings.” *American National Standard, ANSI/AISC 360-10*, Chicago.

Abed, F., Alhamaydeh, M., andAbdalla, S. (2013). “Experimental and numerical investigations of the compressive behavior of concrete filled steel tubes (CFSTs)”, *Journey of Constructional Steel Research,* 80, 429-439.

American Concrete Institute. (2014). “Building code requirements for structural concrete and commentary.” *ACI 318-14*, Farmington Hills, MI.

Ali, R. B. (2019). “Strength and deformation behabiour of eccentrically loaded square concrete-filled steel tubular columns”, M.Sc. in Civil Engineering, *BUET,* Dhaka, Bangladesh.

Bangladesh National Building Code (2017). *BNBC*, Dhaka, Bangladesh.

European Committee for Standardization (1994), “Eurocode 4: Design of Composite Steel and Concrete Structures”. CEN.

Emon, M. A. B. (2014). “Study of strength and ductility of galvanized iron wire reinforced concrete”, M.Sc. in Civil Engineering, *BUET,* Dhaka, Bangladesh.

Emon, M. A. B., Manzur, T., and Yazdani, N. (2016). “Improving performance of light weight concrete with brick chips using low cost steel wire fiber”, *Construction and Building Materials,* 106, 575-583.

Fujimoto, T., Mukai, A., Nishiyama, I., and Sakino, K. (2004). “Behavior of eccentrically loaded concrete-filled steel tubular columns”, *Journal of Structural Engineering,* ASCE, 130(2), 203-212.

Gibbons C., and David Scott, D. (1996). “Composite hollow steel tubular columns filled using high strength concrete”, Report by *Ove Arup and Partners Reseacrh and Development.*

Giakoumelis, G., and Lam, D. (2004). “Axially capacity of circular concrete-filled tube columns”, *Journey of Constructional Steel Research,* 60, 1049-1068.

Gardener, L., and Nethercot, D. (2004), “Experiments on stainless steel hollow sections-part 2: Member behavior of columns and beams”, *Journal of Constructional Steel Research,* 60, 1319-1332.

Ghannam, S., Al-Rawi, O., and El-Khatieb, M. (2011). “Experimental study on light weight concrete-filled steel tubes”, *Jordan Journal of Civil Engineering,* 5(4), 521-529.

Han, L.H., Yang, Y. (2001). “Influence of concrete compaction on the behavior of concretefilled steel tubes with rectangular sections”, *Advances in Structural Engineering,* 4(2), 93-108.

Islam, M. (2019). “Experimantal investigation on concentricall loaded square concrete-filled steel tubular columns”, M.Sc. in Civil Engineering, *BUET,* Dhaka, Bangladesh.

Kumar, H., Muthu, K., and Kumar, N. (2017), “Study on predicting axial load capacity of CFST columns”, *Journal of Institution of Engineers (India),* 66-80.

Lam, D.,and Gardner, L. (2008).“Structural design of stainless steel concrete filled columns”, *Journal of Constructional Steel Research,* 64, 1275-1282.

Lam, D., Gardener, L., and Burdett, M. (2010), “Behavior of axially loaded concrete-filled stainless steel elliptical stub columns”, *Advances in Structural Engineering*, 13(3), 493-500.

Li, G., Yang Z., and Lang, Yan. (2010), “Experimental behavior of high strength concrete filled square steel tube under biaxial eccentric loading”, *Advanced Steel Construction,* 6(4), 963-975.

Lu, Y., Li, N., Li, S.,and Liang, H. (2015). “Behavior of steel fiber reinforced concrete-filled steel tube columns under axial compression”, *Construction and Building Materials,* 95, 74-85.

Long, Y., Li, W., Dai, J., and Gardner, L. (2017). “Experimental study of concrete-filled CHS stub columns with inner FRP tubes”, *Thin-Walled Structures,* 122, 606-621.

Muktadir, G., Islam, M., Reza, R. (2017). “Axial capacity enhancement of CFRP confined columns made of steel fiber reinforced concrete”, *IOSR Journal of Mechanical and Civil Engineering*, 14(1), 28-33.

Nardin, S., and Debs, A. (2007), “Axial load behavior of concrete filled steel tubular columns,” *Journal of Structures and Building*, 160.

O’Shea, M. D., and Bridge, R.(2000). “Design of circular thin-walled concrete filled steel tubes”, *Journal of Structural Engineering*, 126(11), 1295-1303.

Petrus, C., Hamid, H. A., Azmi Ibrahim, A., and Nyuin, J.D. (2011). “Bond strength in concrete filled built up steel tube columns with tab stiffeners”, *Journey of Civil Engineering*, 38,627-637.

Qui, W. (2017). “Beam-Column Behavior of Concrete-Filled Elliptical Hollow Sections”, Thesis of PhD, Imperial College, London.

Ravindran, S., Aafia, and Hameed, S. (2016). “An experimental study on hybrid fiber reinforced concrete filled steel tube column”, *International Journal of Innovative Research in Technology*, 3, 180-187.

Ren, Q.-X., Zhou, K., Hou, C., Tao, Z., and Han, L.-H. (2018). “Dune sand concrete-filled steel tubular (CFST) stub columns under axial compression: Experiments.” *Thin-Walled Structures*, 124, 291–302.

Stephen P. Schneider. (1998). “Axially loaded concrete-filled steel tubes”, *Journal of Structural Engineering*, 124, 1125-1138.

Shanmugam,N.E., and Lakshmi, B.(2001). “State of the art report on steel-concrete composite columns”, *Journey of Constructional Steel Research*, 57, 1041-1080.

Sakino, K., Nakahara, H., Morino, S., and Nishiyama, I. (2004). “Behavior of centrally loaded concrete-filled steel-tube short columns,” *Journal of Structural Engineering*, ASCE, 130(2), 180-188.

Tao, Z., Han, L.H., and Wang, D.Y. (2007). “Experimental behavior of concrete-filled stiffened thin-walled steel tubular columns,” *Thin-Walled Structures*, 45, 517-527.

Tokgoz, S., and Dundar, C. (2010). “Experimental study on steel tubular columns in-filled with plain and steel fiber reinforced concrete”, *Thin- Walled Structures*, 48, 414-422.

Uy, B. (2001). “Axial compressive strength of short steel and composite columns fabricate with high strength steel plate”, *Steel and Composite Structures*, 1(2), 171-185.

Varma, A. H., Ricles, J.M., Sause, R., and Lu, L. W. (2002). “Experimental behavior of high strength square concrete-filled steel tube beam-columns”, *Journal of Structural Engineering*, 128(3), 309-318.

Wang, Z. B., Tao, Z., and Yu, Q. (2017). “Axial compressive behavior of concrete-filled double-tube stub columns with stiffeners”, *Thin-Walled Structures*, 120, 91-104.

Xiamuxi, A., and Hasegawa, A. (2012). “A study on axial compressive behaviors of reinforced concrete filled tubular steel columns.” *Journal of Constructional Steel Research*, 76, 144–154.

Xiong, D. X. (2012). “Structural behavior of concrete filled steel tubes with high strength materials”. *PhD thesis*, National University of Singapore.

Young, B. and Ellobody, E. (2006). “Experimental investigation of concrete-filled cold-formed high strength stainless steel tube columns.” *Journal of Constructional Steel Research*, 62(5), 484–492.

Yang, Y. F. and Han, L. H. (2006). “Experimental behavior of recycled aggregate concrete filled steel tubular columns.” *Journal of Constructional Steel Research*, 62(12), 1310–1324.

Yu, Q., Tao, Z. and Wu, Y. X. (2008). “ Experimental behaviour of high performance concrete-filled steel tubular columns. ” *Thin-Walled Structures*, 46(4), 362–370.

Yiyan, L., Ma, L., and Shan, L. (2014), “Behavior of FRP-confined concrete- filled steel tube columns”, *Journal on Polymers*, 6, 1333-1349.

Yang, J., Sheehan, T., Dai, X.H., and Lam, D. (2015). “Experimental study of beam to concrete-filled elliptical steel tubular column connections”, *Thin-Walled Structures*, 95, 16-23.

Yi-yan, L., Na, L., Shan, L., and Hong-jun, L. (2015).“Experimental investigation of axially loaded steel fiber reinforced high strength concrete-filled steel tube columns”, *Central South University Press and Springer-Verlag Berlin Heidelberg*, 22, 2287-2296.

Zhong, S.-T. and Miao, R.-Y. (1988). “Stress-Strain Relationship and Strength of Concrete Filled Tubes”, Composite Construction in Steel and Concrete, Proceedings of the Engineering Foundation Conference, 773-785.

Zhang, S. and Zhou, M. (2000). “Stress-Strain Behavior of Concrete-Filled Square Steel Tubes”, Composite and Hybrid Structures, Proceedings of the Sixth ASCCS International Conference on Steel-Concrete Composite Structures, 403-409.

Zhao, X. L. and Grzebieta, R. (2002). “Strength and ductility of concrete filled double skin (SHS inner and SHS outer) tubes”. *Thin-Walled Structures*, 40(2), 199–213.

Zeghiche, J., and Chaoui, K. (2005). “An experimental behaviour of concrete-filled steel tubular columns.” *Journal of Constructional Steel Research*, 61(1), 53–66.

Zhu, M., Liu, J., Wang, Q., and Feng, X. (2010). “Experimental research on square steel tubular columns filled with steel-reinforced self-consolidating high-strength concrete under axial load.” *Engineering Structures*, 32(8), 2278–2286.

Zhao, XL, Han, LH and Lu, H (2010). “Concrete-filled tubular members and connections”, Spon Press London.

ANNEXURE – A

Test Specimens from the Published Literature

Experimental results of thirteen CFST column specimens from published literature (Islam (2019) and Ali (2019), M.Sc. in Civil Engineering, BUET, Dhaka, Bangladesh) were considered for comparing the results in this study. These test specimens represented a variety of geometric as well as material properties. These specimens varied in inclusion of fiber, compressive strength of concrete, size of columns and eccentricity.

Islam (2019)

The author conducted experimental investigation on CFST columns under concentric load. Six test specimens as shown on the table from the data were selected for comparative study of results of this study. The description of the test specimens is given in the below Table A-1.

Table A-1: Experimental capacity and geometric properties of columns

Specimen	Cross-section	Concrete compressive strength	Yield stress	Cross-sectional slenderness	Overall slenderness	Ultimate load
	B x t x L	$f_c^{/}$	f_y	B/t	L/B	P_u
C1	100 x 4 x 1000	27	350	25	10	697
C2	100 x 4 x 1000	35	350	25	10	729
C3	100 x 4 x 1000	44	350	25	10	804
C6	125 x 5 x 1000	35	350	25	8	1169
C5	125 x 4 x 1000	35	350	31	8	1011
C8	100 x 4 x 300	44	350	25	3	810

Ali (2019)

The author conducted experimental investigation on CFST columns under eccentric load. Seven test specimens as shown on the table from the data were selected for comparative study of results found from the mid-height deflection of this study. The description of the test specimens is given in the below Table A-2.

Table A-2: Experimental capacity and geometric properties of columns

Specimen	Cross-section	Concrete compressive strength	Yield stress	Cross-sectional slenderness	Load eccentricity	Ultimate load	Mid-height deflection at peak load
	B x t x L	$f_c^{/}$	f_y	B/t	e/B	P_u	δ_m
E1	100 x 4 x 1000	27	350	25	0.30	377	4.80
E2	100 x 4 x 1000	35	350	25	0.30	466	2.21
E3	100 x 4 x 1000	44	350	25	0.30	595	2.04
E6	125 x 5 x 1000	35	350	25	0.30	693	2.72
E5	125 x 4 x 1000	35	350	31.25	0.30	586	3.26
E9	150 x 5 x 1000	44	350	30	0	1474	3.11
E10	150 x 5 x 1000	44	350	30	0.30	968	3.34